AN ABSTRACT OF THE THESIS OF

GEORGE OTTO MARMORINO for the MASTER OF SCIENCE

in OCEANOGRAPHY presented on April 23, 1974

Title: EQUILIBRIUM HEAT AND SALT TRANSPORT THROUGH A DIFFUSIVE, THERMOHALINE INTERFACE

Abstract approved: Redacted for privacy

Douglas R. Caldwell

An experimental investigation of the thermohaline, diffusive interface between convecting layers, with heat fluxes more similar to natural fluxes than in previous studies, shows that the formula suggested by Huppert (1971) for the dependence of heat flux on interface stability cannot be extrapolated to stability numbers higher than seven and a new formula is proposed. The non-dimensional ratio of salt to heat flux is observed to increase from the value 0.15, found by Turner (1965), as the heat flux is lowered through almost three orders of magnitude. Migration of the interface is found even in experiments with anti-symmetric temperature boundary conditions; Huppert's (1971) analysis of the stability of a pair of diffusive interfaces was based on the assumption of stationary interfaces. For oceanic values of the heat flux, the thickness of the interface was in the range observed for the layered system of microstructure in the Arctic Ocean.

Equilibrium Heat and Salt Transport through a Diffusive, Thermohaline Interface

by

George Otto Marmorino

A THESIS

submitted to

Oregon State University

in partial fulfillment of
the requirements for the
degree of

Master of Science

June 1974

APPROVED:

Redacted for privacy

Associate Professor of Oceanography
in charge of major

Redacted for privacy

Dean of School of Oceanography

Redacted for privacy

Dean of Graduate School

Thesis presented on April 23, 1974

Typed by Suelynn Williams for George Otto Marmorino

ACKNOWLEDGMENTS

I wish to thank:

Dr. A. D. Kirwan who stimulated my curiosity about mixing and stirring processes in geophysical fluids;

Dr. Steve Neshyba for inviting me to accompany him to Ice Island T-3 where I first became interested in layered microstructure;

Dr. G. Bodvarsson for serving on my committee and for his constructive comments especially on Chapter II;

Dr. D. R. Caldwell for accepting the responsibility for my experimental apprenticeship and for his continued guidance and tempered impatience throughout this project;

Salmo gairdnerii and the four white walls for making the rainy winter months completely enjoyable.

During my studies, I have been supported by the National Science Foundation Graduate Fellowship Program.

TABLE OF CONTENTS

TABLE OF CONTENTS CONTINUED

LIST OF TABLES

LIST OF FIGURES

LIST OF FIGURES CONTINUED

EQUILIBRIUM HEAT AND SALT TRANSPORT THROUGH A DIFFUSIVE, THERMOHALINE INTERFACE

I. INTRODUCTION

Oceanographers have long been interested in mixing processes. Much work has been devoted to attempts at parameterizations of the Reynolds mixing terms. Use of the so-called Austauch or eddy coefficients has been partially successful in explaining the observed distributions of temperature, salinity, oxygen, and phosphate.

A specific mixing problem is that of the density interface. Study of this problem is useful in several related contexts: (1) extension of layered models of ocean dynamics by including mixing between layers, (2) erosion of a stratified fluid by mixing from above or from below, e.g. the seasonal thermocline and developing wind-mixed layer in the oceans; mixing at and below an atmospheric inversion (the trade wind subsidence inversion, for example).

Momentum transfer dominates in the above applications but heat and solute transport through density interfaces has, in the last ten years, received much attention because of observations in the ocean and atmosphere of what is now commonly called fine-structure or microstructure. Recent laboratory investigations of thermohaline convection have discovered new forms of convective systems which have features in common with the ocean observations. The difference

between the molecular diffusivities of heat and salt has been found to be responsible for two new types of convection collectively called double diffusive convection.

Double diffusive convection was discovered about a decade ago, theoretically by Stommel, Arons, and Blanchard (1956), Stern (1960), and Stommel (1962) and experimentally by Stommel and Faller (Stern, 1960) and Turner and Stommel (1964). Two forms of convection were distinguished; salt finger convection (a direct or monotonic convective mode) and diffusive convection (an overstable mode). For a demonstration of the difference between the two the reader is referred to a recent article by Gregg (1973).

We know now that there are two requirements for double diffusive convection. The first is that the fluid be binary (at least) in the sense that it have two (or more) components (solutes) or properties having different diffusivities. The second is that the components contribute to the vertical density distribution in opposing manners such that the fluid is gravitationally stable. That convection can take place at all when the fluid is stably stratified is the remarkable aspect of double diffusive convection.

When the density gradient is vertical[1], double diffusive

---

[1] The essence of the case of a horizontal gradient is considered in Turner (1973) and need not be mentioned here.

convection has produced a stepped density distribution in the laboratory: thin regions through which transports are controlled by a double diffusive process separated by deep layers in which the dynamics are dominated by density differences alone. The relatively thin regions are called salt-finger or diffusive interfaces. The diffusive interface can exist when component distributions are such that heat is destabilizing and salt is stabilizing. Both the salt-finger and diffusive interface are more complex than a simple density interface (formed, for example, with salt alone) in the sense that each has an internal structure. In the case of the diffusive interface, this takes the form of a double boundary layer.

Examples of specific natural situations in which double diffusive effects could be especially prevalent follow. One situation, a sediment-laden river flowing into a large body of water, is discussed by Houk and Green (1973). Another occurs in fjord-type estuarine circulation as described by Pickard (1966) where, during the summer, salt is transported upwards through a large salt gradient (10 to 20‰ m^{-1}).

Although first investigated with the ocean in mind, it has been recognized that double diffusive convection can occur in gases (Veronis, 1965), in a fluid with two solutes and no property variation (Stern and Turner, 1969), in solidifying metal alloys, and in astrophysical situations (Spiegel, 1972).

Our concern with diffusive convection is twofold. On the one

hand, we wish to extend our knowledge of convective processes. This is a natural extension of laboratory work performed here, most recently that of Caldwell (1974a). On the other hand, we have the best documented case of layered (possibly diffusive) convection yet available in the work of Drs. Steve Neshyba and Victor Neal in the Arctic Ocean. Enough should be learned not only to be able to recognize diffusive convection in such natural situations but to determine the extent of correspondence with analogous laboratory work. As an example of potential use, suppose a series of diffusive interfaces forming part of a layered system are discovered in the ocean. They are a signature of some physical process which has occurred in the past. Information can be gained about this process and the behavior of the system by answering the following questions, among others. Are the interfacial fluxes in a steady state or is the system only transient? Are the interfaces in equilibrium with the stirring in the adjoining layers? Are the stability numbers suggestive of a formation similar to that which occurs in the laboratory? If so, are the time scales reasonable? How does the system change in response to interaction with itself, shear, and time dependent boundary conditions? These questions can be investigated in the laboratory.

The most important of the previous experimental investigations are Turner (1965), Broughton (1972), and Shirtcliffe (1973). The latter is peculiar because heat was not used (the effects caused by

temperature were produced by a varying concentration of a second solute). Turner's work is no doubt quite reliable and, though an exploratory work, produced two significant results. However, there are the following points to consider: (a) The range of the heating rate used by Turner is small and an average value is much higher than would normally be encountered in the ocean or in a lake; (b) Greater precision in measurements of heat and salt fluxes could be hoped for; (c) The effect of varying the aspect ratio (layer diameter divided by layer thickness) has not been explored. Turner used a ratio of about 2.5 for each of two layers in every experiment; (d) For the relatively high heating rates used (an average value is 4×10^{-2} cal cm^{-2} sec^{-1}) the interface may have been partially coupled to the heated plate via thermal bursts; (e) Mechanical stirring of the fluid in the upper layer was often necessary for convection to begin in that layer. This stirring is not present in a natural system or in the more usual kind of thermal convection experiment and should be eliminated by a suitable modification of the experimental device; (f) When the density difference across an interface was large, an intermediate layer often formed in the interface. The removal of this layer probably necessitated additional mechanical stirring.

If ΔT and ΔS are the differences in temperature and salinity across a diffusive interface then a dimensionless ratio characterizing the interface is the stability number, $R\rho \equiv \beta \Delta S / \alpha \Delta T$ and three

additional considerations are: (g) A quantitative picture of the variation of the interface thickness with $R\rho$ and the heat flux, H would be helpful in deciding if naturally-occurring interfaces are maintained by diffusive convection; (h) The fluxes when $R\rho > 7$ were not determined by Turner and this region is important observationally; (i) The interesting region in stability, $1 < R\rho < 2$, needs further study. Specifically, the reason for the rapid increase in the fluxes, as measured by Turner, needs to be found.

The desire for measurements while the fluxes remain constant in time (steady) expressed by Turner (1968a) and Veronis (1968) may have prompted Broughton (1972) to attempt a steady-state experiment (as it did us). Though Broughton sets up several layers bounded by permeable boundaries, we feel his experiments were not steady state for two reasons. First, the interfacial values of ΔS are extremely large, typically 50‰. Since the layers are formed by artificial means (not by the layering mechanism itself) a large salt gradient is established over an interface of some arbitrary thickness (dependent on the method used to fill the tank). Though the interfaces may appear stable in time for this reason, their thickness may not be at equilibrium with the convective stirring in the layers on either side. If this the case, the transports are not uniquely determined by ΔT and ΔS. Second, if one assumes that a particular experiment is steady-state the heat flux should of course be the same through each interface; under

this circumstance, if $R\rho$ and ΔT vary from one interface to another, they must both increase or decrease. However, we find that every kind of pairwise variation occurs in Broughton's results.

Using previous work as a base, the "ideal" experiment can be formulated. One in a series of identical layers should be studied under steady state conditions. Small, controlled changes in the boundary conditions will allow the system to be studied over a range of stabilities. It should be possible to come close to the oceanic flux ranges. Provision is to be made for profiling temperature, salinity, and turbulent velocities. Visual techniques will allow study of the interface, mechanisms of transport from the interface, and turbulent intensities near and far from the interface. We have attempted steady state experiments with some of the above features but a technical problem thwarted us (see Appendix D); a compromise was made.

The diffusive experiments were conducted so that the heat flux through the system was approximately constant and fixed from below; the mean temperature of the system was held approximately constant by an upper plate held at a fixed temperature. The varying salt flux caused the interfaces to move slowly through equilibrium states over a continuous range of $R\rho$. The states are equilibrium states in the sense that changes occur slow enough (at least for $R\rho > 2$) to allow the interface to adjust its thickness in response to the mixing in the layers. The equilibrium state is assumed to be identical to a steady state in

which permeable boundaries would allow steady salt fluxes.

In the next chapter, some pertinent theoretical work on thermal and thermohaline convection is reviewed together with previous observations. The power law relating heat flux and temperature difference is given; this law is used in Chapter III to non-dimensionalize both the interfacial heat and salt fluxes. The mechanism of heat transfer from a solid boundary is introduced as this will be compared with experimental results on the thermal burst phenomenon in Chapter V. Results of the stability analysis of the "thermohaline Rayleigh-Bénard" problem are outlined, explained, and, in Chapter III, shown not to explain the increased efficiency of the interfacial heat transport at low stability.

Chapter III reviews previous dimensional analysis and energy arguments for diffusive convection in detail not found in previous papers, and summarizes previous published and unpublished work on the diffusive interface. It is shown that salt transport due to thermal diffusion is always less than 10% of Fickian transport. An upper bound of one is derived for the non-dimensional ratio of salt to heat flux, Rf. Since Rf is positive, a negative mass flux produces an interfacial migration of the order of 1 mm day^{-1}. Entrainment can provide a transfer mechanism which is unaccounted for in any analytical development to date.

Chapter IV contains experimental details and a summary of the diffusive experiments. The results of these experiments are compared

with the thermal burst phenomenon in Chapter V. It is concluded that bursts may originate from the transition layer of the interface but are less effective as a transport mechanism than in the non-layered experiments. Bodily oscillations of the interface increase markedly as the stability decreases.

Further experimental results are given in Chapters VI and VII. Small bumps in the temperature profile are sometimes found at the edge of the interface and are compared with those seen by Elder (1969) and by Linden (1971). The interfacial heat flux for stability numbers greater than three is given by

$$H = A(\Delta T)^{4/3}(0.35)(R\rho - 2)^{-0.6}$$

where A depends only on fluid properties, and $R\rho$ is the stability number. The flux ratio is found to increase slowly as the heat flux decreases. Interface thickness is contoured on the heat flux-stability number plane and for heat fluxes approaching oceanic values the interface is observed to thicken to 4 cm. The double boundary layer structure is measured but the salinity layer is never less than half the thickness of the thermal layer. Entrainment of interfacial fluid is present in all the experiments; interface migrations as large as 3.7×10^{-2} cm sec^{-1} were measured.

II. REVIEW OF THERMOHALINE CONVECTION

Thermal convection between parallel plates

During the past seventy years a large amount of theoretical and experimental work (see Whitehead, 1971 and Turner, 1973 for summaries) has been devoted to the problem of thermally-driven convection in a layer of pure fluid bounded above and below. In most of the theoretical treatments the fluid is horizontally infinite; experimentally, one must be aware of the effects of lateral boundaries. This situation was first studied experimentally by Bénard in 1901 and theoretically by Rayleigh in 1916.

Rayleigh-Bénard convection in a pure fluid

When a destabilizing temperature difference, ΔT, is imposed across a depth of fluid of thickness L, heat flows through the fluid by molecular conduction. Convection will start only if buoyant forces overcome the viscous forces; that is, when a dimensionless group called the Rayleigh number becomes "critical"[2]. We define[3] the

---

[2] The critical Rayleigh number for a pure fluid depends only on boundary conditions and aspect ratio (see for example Stommel, 1947). When the fluid is rotating the Taylor number becomes important (Chandrasekhar, 1957; Rossby, 1969).

[3] Notation is defined in detail in Appendix A.

thermal Rayleigh number in the usual way as

$$R \equiv g \alpha \Delta T L^3/(\kappa\nu) \qquad (1)$$

Notice that R is a ratio of a driving force (a temperature difference) to two dissipative diffusive processes (thermal conduction and viscosity).

When R becomes critical, infinitesimal temperature and velocity perturbations in the fluid (damped in the conductive mode) are amplified. The range 1708 (the critical value of R for rigid boundaries) $< R < 240,000$ has been thoroughly studied experimentally (Krishnamurti, 1970 or Busse and Whitehead, 1971). As R is increased above its critical value the convecting fluid passes through transitions at which instabilities cause changes in the type of motion, for example, from two-dimensional laminar roll cells to a three dimensional flow. The flow patterns can be detected visually or deduced by changes in slope on a plot of heat flux vs. temperature gradient. Each mode of motion transfers heat at a different rate. It is thought that the discrete transitions represent an approach to turbulence by allowing the fluid to amplify different modes of instabilities. Another interpretation is that some of the transitions represent new interactions among already existing modes. This latter view emphasizes the need for steady state measurements in work of this type.

The transition to turbulent flow from a time dependent three dimensional flow occurs at $R \approx 14,000\ Pr^a$ where $a \approx 0.6$ for $Pr \gg 1$

(Rossby, 1969; Khrishnamurti, 1970; Turner, 1973). Hence, for water at room temperature, the turbulent regime exists for $R > 45,000$. All the experiments reported in Chapter V are well into the turbulent regime.

Though naturally occurring flows have extremely high Rayleigh numbers (10^{18} not being unusual in the ocean) the Rayleigh-Bénard experiments are still significant. For example, convection alone or coupled with shear is responsible for certain cloud formations; cellular solar (granular) convection has been photographed; and Rayleigh-Bénard convection is used to explain convection in the earth's mantle.

High Rayleigh number convection

Studies of turbulent convection result in a functional relationship between the non-dimensional heat flux (the Nusselt number), the Rayleigh number, and a number which reflects the properties of the particular fluid being used (usually the Prandtl number):

$$Nu = f(R, Pr) \tag{2}$$

Most often one assumes a correlation of the form

$$Nu = a R^m Pr^n \tag{3}$$

where a and m can, in general, depend on Pr. Experimentally, n is found to be small and the dependence on Pr can be absorbed in a new

constant. When m = 1/3, Eq. (3) can be written as

$$H = c\, k_T \left(\frac{g\alpha}{\kappa\nu}\right)^{1/3} \Delta T^{4/3} = A\Delta T^{4/3} \tag{4}$$

where

$$A = c\, k_T \left(\frac{g\alpha}{\kappa\nu}\right)^{1/3}$$

Notice that A depends only on fluid properties and the constant c.

Equation (4) is known as the $R^{1/3}$ or $\Delta T^{4/3}$ power law. Notice that the length L does not appear. When m = 1/3, the plate spacing does not matter; the heat transport must be controlled by boundary layers near the plates. Equation (4) in a more general form is

$$H = 2^{4/3} A\Delta T_{(1/2)}^{4/3} \tag{5}$$

where $\Delta T_{(1/2)}$ is the positive temperature difference between one plate and the well mixed interior (for the case with two plates, $\Delta T_{(1/2)} = \frac{\Delta T}{2}$). The experiments of Thomas and Townsend (1957) and Townsend (1959) have verified Equation (5) in air.

The results of various investigations on turbulent convection are summarized in Tables I and II. The variation between the experimental results (Table II) are large considering the precision cited in the individual papers. This is due to several factors: variation and uncertainty of values for fluid properties; variation in thickness and

Table I. Nusselt and Rayleigh number correlations from theoretical investigations (partly after Lindberg, 1970).

Investigator	$Nu = bR^x$	c (Eq. 4)	Comments
Herring (1963, 1964)	$Nu = 0.115\ R^{1/3}$	0.115	Mean field stability
	$Nu = 0.135\ R^{1/3}$	0.135	Maximum heat transfer
Howard (1963)	$Nu \leq 0.123\ R^{3/8}$	0.242	Maximum heat transfer
Howard (1969)	$Nu = 0.198\ R^{3/8} + 1$	0.390	Power law theory
Kraichnan (1962)	$Nu = 0.089\ R^{1/3}$	0.089	Valid for high Pr
Lindberg (1970)	$Nu = 0.1\ R^{1/3}$	0.1	Thermal burst model
	$Nu \leq 1 + 0.152\ R^{3/8}$		Power law model
Musman (1968)	$Nu \backsim R^{1/3}$		Lower boundary rigid. Upper boundary is a density interface.
O'Toole and Silveston (1961)	$Nu = 0.123\ N^{0.305}$	0.068 to 0.088	Valid for $10^5 < R < 10^9$. Review of published and unpublished work.

Note: When $x = 1/3$, an $R^{1/3}$ dependence is forced on the correlation by matching Nu, as given by $Nu=bR^x$, with $Nu=cR^{1/3}$ at the limits of the domain of R. When no domain is given, the match is made at $R=10^6$. This is done to allow comparison of values of c between experiments.

Table II. Nusselt and Rayleigh number correlations from high Rayleigh number experiments.

Investigator	Domain of R	$Nu = bR^x$	c (Eq. 4)	Fluid	Comments on Boundary Conditions
Boger and Westwater (1967)	10^3 to 10^7	$Nu \doteq 0.12\ R^{1/3}$	0.12	Water	Freezing and melting
Chu and Goldstein (1973)	2.8×10^5 to 1.0×10^8	$Nu = 0.183\ R^{0.278}$	0.066 to 0.091	Water	
Federico and Foraboschi (1966)	2.2×10^4 to 1.2×10^7	$Nu = 0.092\ R^{1/3}$	0.092	Water	Top surface free and evaporating
Globe and Dropkin (1959)	7×10^6 to 3×10^8	$Nu = 0.08\ R^{1/3}$	0.08	Water Silicone oils Mercury	
Malkus (1954)	10^5 to 10^9	$Nu = 0.05\ R^{0.32}$	0.045	Water	
Mull and Reiher (1930)	$.7 \times 10^4$ to 2.7×10^5	$Nu = 0.22\ R^{1/4}$	0.08 to 0.1	Air	
(from Rossby, 1969)	$R > 2.8 \times 10^5$	$Nu = 0.075\ R^{1/3}$	0.08		
Rossby (1969)	$R > 7000$	$Nu = 0.131\ R^{0.30 \pm 0.005}$	0.098	Water	
Schmidt and Silveston (1959)	10^5 to 10^7	$Nu = 0.110 R^{0.310}$	0.076 to 0.084	Five liquids	
Somerscales and Gazda (1969)	10^5 to 10^8	$Nu = 0.196\ R^{0.283}$	0.078 to 0.11		
Thomas and Townsend (1957)		$Nu = 0.08\ R^{1/3}(\Delta T_{1/2})$	0.08	Air	Lower boundary heated

Note: (1) When a Pr dependence is given by the investigator, it is incorporated into the constant b by using Pr=7.2, the value for water at 20 C;
(2) The values of R studied by Krishnamurti (1970) and Schmidt and Saunders (1938) are too low to warrant inclusion; also, see the note for Table I.

material of the plates; failure to account for all heat paths through the walls of the experimental device; and unsteadiness of the imposed heat flux. In order to achieve high Rayleigh numbers, the length L must be increased. This lowers the aspect ratio and increases the volume of fluid in the device. The system, as a result, is thermally sluggish because of the large thermal capacity and the approach to equilibrium is long; in addition, interaction with the side walls becomes increasingly possible. The experiments reported in this thesis suffer from these two effects.

No doubt, some of the scatter in Table II is produced by our method of comparison (see the caption for Table II); but much results from the use of Eq. (3) by different workers to report their results. Theoretical work suggests Eq. (3) has a sound basis in certain domains of R but if data, covering more than one domain, is fit by Eq. (3) the results may be misleading (Eq. (3) is, in fact, used in Chapter V to summarize our findings for high Rayleigh number thermal convection). It is suggested that in work of this type, the "raw" observables be reported, especially when many fluids are used to increase the range in Pr. Even at this late date, then, there is still need for more data in the highly turbulent regime: for oceanic use at high Pr (c. 10) and at extremely low Pr for astrophysical application (Spiegel, 1971).

Mechanics of heat transfer from a solid boundary

It is useful at this point to derive a simple result pertaining to the mechanisms of heat transport through a system with boundaries. The turbulent heat transport equation for a pure fluid reduces to

$$\kappa \frac{d^2\overline{T}}{dz^2} = \frac{d}{dz}\left(\overline{w'T'}\right)$$

where w' and T' are fluctuating vertical velocity and temperature and we assume a statistical steady state ($\partial_t = 0$) and horizontal homogeneity (T, u, v, w, and derivatives are functions only of z and t). Integrating once between a conductive boundary layer at z_o, say, and z:

$$H = -k_T \frac{d\overline{T}}{dz} + \rho c_p \overline{w'T'} \qquad (6)$$

where the heat flux is given by

$$H = -k_T \left.\frac{d\overline{T}}{dz}\right|_{z_o} .$$

The temperature records and profiles of Thomas and Townsend (1957) are the first demonstration of the two modes of transport represented in Eq. (6). Very close to the boundary the heat transport is molecular. At the outer edge of the boundary layer, turbulent temperature fluctuations are high and turbulent kinetic energy is

produced.[4] Experimentally, at a point above the lower boundary layer one sees quiet periods in the temperature records interrupted by periods in which T' is large and positive and rapidly varying. The physical interpretation is that buoyant elements or thermals (see Chu and Goldstein, 1973 for visual evidence) are released from the boundary layer in bursts. Away from the boundary layer the second term on the right hand side of Eq. (6) dominates.

The interaction of the buoyant elements with the fluid environment is discussed by Turner (1973). Probably no theory will be successful at explaining turbulent convection unless it accounts for thermal bursts. Krishnamurti (1973) finds that all periodicities observed at a fixed point in the high Rayleigh number, time-dependent flow are due to hot or cold thermals or plumes One may think of the thermals as a microstructure of vorticity and buoyancy which give the fluid an internal structure. Theories which take account of the generation of thermals at boundaries have been developed by Lindberg (1970) for thermosolutal convection. Lindberg's (theoretical) boundaries are

---

[4] The turbulent temperature fluctuations, $\frac{1}{2}\partial_t\overline{T'^2}$ are produced by the interaction of a Reynolds flux with the gradient of the mean temperature field, e.g., a term like $\overline{T'w'}\,\frac{d\overline{T}}{dz}$. Buoyancy production is then produced by a term $\alpha\overline{T'w'}\overline{\rho}g$ in the kinetic energy equation which causes $\frac{1}{2}\partial_t\overline{w'^2}>0$. This production of buoyancy is responsible for the salt transfer in diffusive convection.

maintained at constant concentration. The interior is well mixed, the convection is very similar to (pure) thermal convection, and his results do in fact reduce to explain thermal convection (see Table I). More complex dynamics become possible in a binary fluid when there are initial gradients of solute concentration.

Thermohaline convection between free boundaries: the linear, stability analysis of the thermohaline Rayleigh-Bénard problem

Prior to stating the problem it is necessary to discuss what is meant by stability. Let A(t) be the amplitude of the perturbed part of a signal, temperature, for example. In general, A(t) might be represented by

$$A(t) = \sum_{n=0}^{N} \mathrm{Re}\{A_o^{(n)} e^{p^{(n)} t}\},$$

where $p^{(n)} = p_r^{(n)} + i p_i^{(n)}$ and Re means "the real part of". Each "n" corresponds to a different temperature perturbation ("mode"). In a free convection problem, a knowledge of $p^{(n)}$, $n = 1, 2, \ldots, N$, is equivalent to knowing the response of the convection system to various temperature perturbations. The response of the system is (linearly) stable when $p_r^{(n)} < 0$ for $n = 1, 2, \ldots, N$; and unstable when $p_r^{(n)} > 0$ for any n. If some of the $p_r^{(n)} = 0$ while the others are negative, the system is neutrally or marginally stable. As $p_r^{(n)}$ passes through zero, instabilities can arise in one of two forms: if

$p_i^{(n)} = 0$, the marginal state is stationary for the nth perturbation ($p_r^{(n)} = 0$ is then called the point of exchange of stabilities); if $p_i^{(n)} \neq 0$, the marginal state is oscillatory and a sine-like perturbation will look like an oscillating standing wave. As $p_r^{(n)}$ is increased beyond zero, we have convection in the former case and overstability in the latter.

Ordinary Rayleigh-Bénard convection always begins as an instability governed by the principle of exchange of stabilities (Pellow and Southwell, 1940). For rigid boundaries, the point of exchange of stabilities corresponds to the critical Rayleigh number, 1708. If constraints, such as rotation in a pure fluid, a solute gradient in an inhomogeneous fluid, or a vertical magnetic field in a conducting fluid are present, the initial instability may be time-dependent or oscillatory in nature. As pointed out by Veronis (1965), a time-dependent motion may be able to take advantage of potential energy sources which are not available to a steady motion. It is also possible for growing, overstable modes to become direct, growing modes if their frequency goes to zero while $p_r > 0$. Thus, convective instability can be initiated by transient overstability at a Rayleigh number lower than that corresponding to the exchange of stability point (Spiegel, 1972).

The full set of non-linear equations governing heat and salt transport will not be examined for stability but will be linearized according to the following assumptions:

(1) the motion is initiated by infinitesimal perturbations and therefore only linear terms in the governing equation are important, (2) a linear equation of state is used, i.e., $\Delta\rho/\rho = \alpha\,\Delta T + \beta\,\Delta S$ where α and β are constants, (3) concentrations at the boundaries of the fluid are maintained at constant values, and (4) density fluctuations are important only in generating buoyant forces (Boussinesq approximation).

The stability problem has been extended by Vertgeim (1955), Lieber and Rintel (1963), Weinberger (1963), Walin (1964), Sani (1965), Veronis (1965), Nield (1966)[5], Veronis (1968), and Baines and Gill (1969). We follow below in the fashion of Veronis and Baines and Gill.

Consider a layer of fluid of depth d:

$z = d$ ——— Tm - ΔT, Sm - ΔS ——— free

fluid

$z = 0$ ——— Tm, Sm ——— free

The boundaries are dynamically free or slippery ($\partial_z u = 0$) and are maintained at constant values of temperature and salinity. In

---

[5] The many boundary conditions treated by Nield may make his work particularly useful in interpreting results from experiments which usually have rigid boundaries (for example, see Shirtcliffe, 1969a).

addition, no flux of fluid is allowed through the boundaries

($\int_{-\infty}^{\infty} \rho \; w dx = 0$). The analysis is spatially two-dimensional: $V = (u, w)$. Temperature and salinity are broken up as

$$T_{total} = Tm - \Delta T \; z/d + T(x, z, t) \tag{7a}$$

$$S_{total} = Sm - \Delta S \; z/d + S(x, z, t) \tag{7b}$$

Then the governing equation of motion to the Boussinesq approximation and the equation of continuity of mass flow are:

$$\partial_t V + V \cdot \nabla V = - \frac{1}{\rho_m} \nabla p' + g(\alpha T - \beta S)\hat{k} + \nu \nabla^2 V \tag{8}$$

$$\partial_x u + \partial_z w = 0 \tag{9}$$

where p' is the deviation of the pressure from hydrostatic equilibrium ($\partial_z p_o = - \rho_m g$) and where the equation of state, $\rho = \rho_m (1 - \alpha T + \beta S)$ has been used. The equations of heat and salt conservation are

$$\partial_t T + V \cdot \nabla T - w \; \Delta T/d = \kappa \nabla^2 T \tag{10}$$

$$\partial_t S + V \cdot \nabla S - w \; \Delta S/d = \kappa_s \nabla^2 S \tag{11}$$

The non-dimensionalization is straightforward but of course it is nice to know the answer beforehand. Equation (9) is satisfied by introducing a stream function, ψ. Equation (8) is converted into a vorticity equation by taking the curl; neglecting the non-linear terms we have

$$\left(\frac{1}{Pr}\partial_t - \nabla^2\right)\nabla^2\psi = -R\,\partial_x T + Rs\,\partial_x S \tag{12}$$

Equations (10) and (11) become

$$(\partial_t - \nabla^2)T + \partial_x\psi = 0 \tag{13}$$

$$(\partial_t - \tau\nabla^2)S + \partial_x\psi = 0 \tag{14}$$

The boundary conditions can be written

$$\psi = \partial_{zz}\psi = T = S = 0 \quad \text{at } z = 0, 1. \tag{15}$$

The form of the perturbations are selected to satisfy Eq. (15) immediately:

$$\psi \sim e^{pt}\sin(a\pi x)\sin(n\pi z),$$

$$T, S \sim e^{pt}\cos(a\pi x)\sin(n\pi z),$$

where the wave number is $k \equiv (a^2 + n^2)^{1/2}\pi$. After substituting for ψ, T, and S a characteristic equation in p is obtained.

The characteristic equation is found to be

$$p^3 + (Pr+\tau+1)k^2p^2 + [(Pr+\tau Pr+\tau)k^4 - (R-Rs)Pr\,\pi^2a^2/k^2]p$$

$$+ \tau Pr\,k^6 + (Rs-\tau R)Pr\,\pi^2a^2 = 0\,. \tag{16}$$

Equation (16) has been examined for loci of marginal stability in the (R, Rs) plane (see Fig. 1). Primary interest is in the possibility of

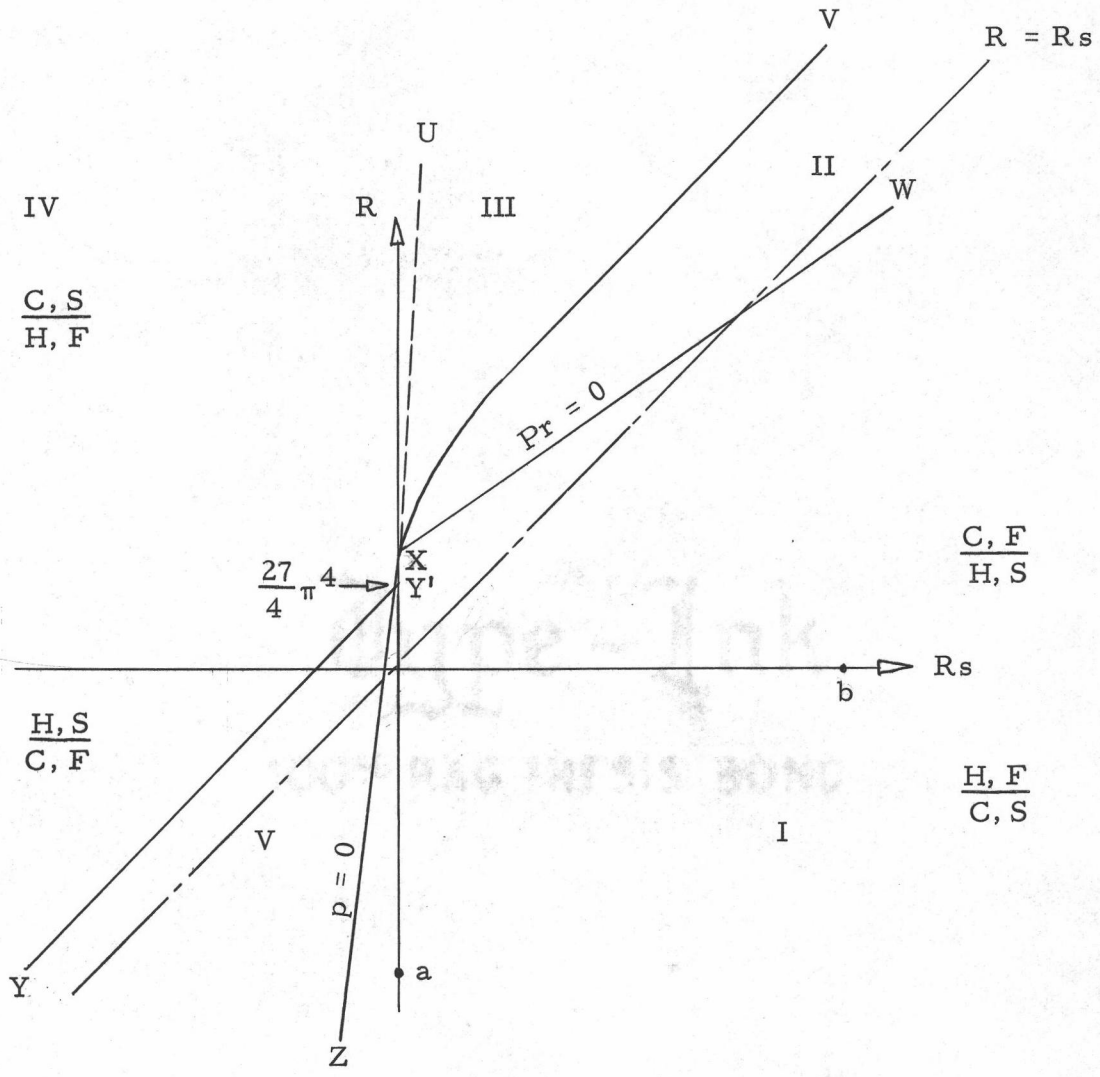

Figure 1. Mapping of thermohaline convective regimes made by varying R and Rs while holding other parameters fixed in Eq. (16). The wavenumber corresponding to the fastest growing mode is used: $a^2 = 1/2$, $n = 1$. Recall that $R < 0$ and $Rs > 0$ are stabilizing (after Baines and Gill, 1969).

steady convection, efficiency of transport, rate of growth of a mode of convection, and the type of mode. We take only a qualitative look at these questions partly because of deficiencies in the theoretical model (discussed later).

Since Eq. (16) is cubic in p we can expect one real root and two complex conjugate roots, or three real roots, each root representing a convective mode. A graphical interpretation is a pole-zero map as used by Huppert (1972). Using this device, infinitesimal motion in five[6] regimes on the (R, Rs) plane can be discussed.

Referring to Fig. 1, the equations of the curves shown are

$$\overline{XU}: \quad R \doteq \frac{Pr}{(Pr+1)\tau^2} Rs$$

$$\overline{XV}: \quad R \doteq Rs + 0(Rs^{2/3})$$

$$\overline{XW}: \quad R \doteq \frac{Pr}{Pr+1} Rs + \frac{27}{4}\pi^4$$

$$\overline{XZ}: \quad R = \frac{1}{\tau} Rs + \frac{27}{4}\pi^4$$

$$\overline{YY'}: \quad R = Rs + \frac{27}{4}\pi^4$$

The five convective regimes are denoted by Roman numerals. Each quadrant is concisely labeled (after Huppert, 1972) as to conditions

---

[6] Turner and Stommel (1964) and Neshyba, Neal, and Denner (1969) divide the (R, Rs) plane into six regions in a simpler fashion.

in an experiment using heat and salt. For example, to study convection in the first quadrant one would set up Hot, Salty water below Cold, Fresh water. It is by controlling the contributions of temperature and salt concentration to the density gradient that one can explore convective regimes I, II, or III in the first quadrant. Notice that as R and Rs go to infinity, double diffusive convection operates over a large part of the area below the line of neutral gravitational stability. The point X is a kind of triple point.

Region I is the region of complete stability: no root of Eq. (16) has $p_r > 0$ and so all perturbations are damped and all modes are stable. By manipulation of the experimental variables instability can be induced. Beginning at the point marked "a" on the negative R-axis, hold R constant and gradually destabilize the fluid by moving to the left. While in I there can be no convection. Convection via direct instability (salt-fingers) starts after passing the line $\overline{XZ}$ on which $p = 0$. Hence, salt-finger convection is similar to Rayleigh-Bénard convection in that it passes through neutral stability. Near marginal conditions the horizontal wavelength of the disturbance is of the order of the depth of the fluid layer. Further into V, the wavelength decreases which means the convection cells become tall and thin, hence the name salt-fingers. This was first indicated by Stern (1960) and then confirmed by Baines and Gill. The pole-zero plot of salt-finger convection is shown as one (direct) convective mode (mode 1) with the overstable

modes (modes 2 and 3) suppressed:

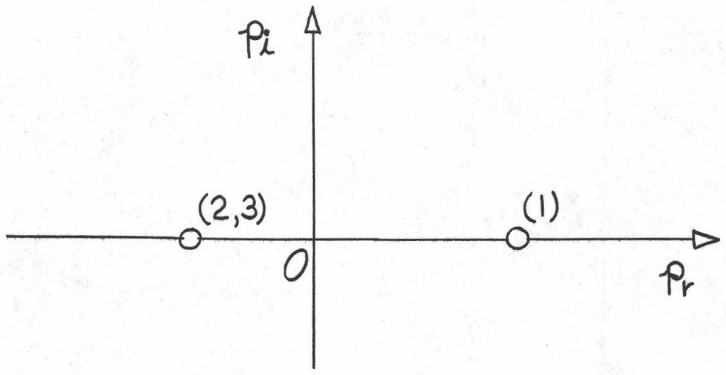

The salt-finger instability is similar to the thermal burst of thermal convection or the salt plume in purely haline convection, in the sense that all three are direct modes.

To examine overstability, hold Rs fixed at a positive value (a stable salt gradient) and increase R by heating the fluid from below or cooling from above thereby moving vertically from the point labelled "b". When the line $\overline{XW}$ is crossed, instability sets in in the form of two conjugate overstable modes and a damped direct mode:

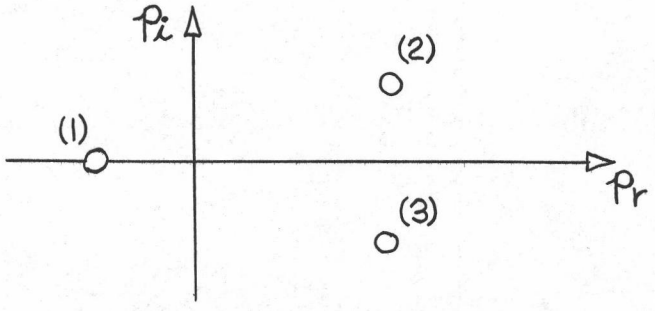

Since $p_r > 0$, the two oscillatory modes grow in amplitude. The horizontal cell size is $2^{1/2}$ d, where d is the depth of the fluid layer. Regime II coincides with the realm of diffusive convection. As $\overline{XV}$ is approached, the instability becomes more and more direct. In Chater III, regime II is examined further.

The situation for higher R consists of two unstable direct modes of unequal growth rates in III. In IV it is possible to have three direct modes. The most efficient transport of heat and salt should occur in regime IV. Notice that Rayleigh-Bénard convection in a pure fluid coincides with the R-axis; for free-free boundaries, convection sets in through the mechanism of exchange of stabilities at $R = 27\pi^4/4$.

The difficulties in applying the results of the theoretical analysis directly to laboratory experiments include: (1) experimentally, the boundaries are commonly rigid-rigid or rigid-free and not free-free, (2) the motions to be expected are three, not two, dimensional, (3) non-linear terms may be important, (4) Soret or thermal diffusion effects have been neglected[7], (5) the condition of no flux through the

---

[7] Caldwell (1970) and Hurle and Jakeman (1971) have found that the onset of convection is affected by salt fluxes caused by Soret diffusion. Hurle and Jakeman have included this effect into the governing equations and have found the critical parameters and mode of instability to be changed. Caldwell (1974a), however, has shown that the Soret transport does not appreciably affect the dynamics of onset of instability. He also shows that the nature of the boundaries does not much matter when the fluid is a salt solution.

boundaries may be unrealistic for our application, and (6) the possible existence of finite-amplitude instabilities. Points (5) and (6) will be discussed again in Chapter III.

III. PREVIOUS WORK ON THE DIFFUSIVE INTERFACE

Theoretical considerations

In the first half of this chapter, we use energy and dimensional arguments to anticipate some of the experimental results. Expressions developed are used in a summary of previous work and in reporting the results of our own experiments. Part of the material discussed and much of the notation has its base in the paper by Turner (1965).

Non-dimensionalization of the interfacial heat flux

Following Turner, the heat flux through a diffusive interface is non-dimensionalized by dividing by the flux given in Eq. (5). Physically, imagine a thin solid plane to take the place of a diffusive interface (Fig. 2). Above and below the plane, which is fixed in space, are symmetric boundary layers in which $\left|\frac{dT}{dz}\right|$ and $\left|\frac{dS}{dz}\right|$ are large. The boundary layers separate well-mixed layers of concentrations T, S (upper layer) and $T + \Delta T$, $S + \Delta S$ (lower layer) where ΔT, $\Delta S > 0$. Define the heat flux through the conductor as H_{sp} where "sp" stands for "solid plane". Using Eq. (5)

$$H_{sp} = 2^{4/3} A \left(\frac{\Delta T}{2}\right)^{4/3} = A \Delta T^{4/3} .$$

Non-dimensionalize the interfacial heat flux, H, with H_{sp} to obtain an

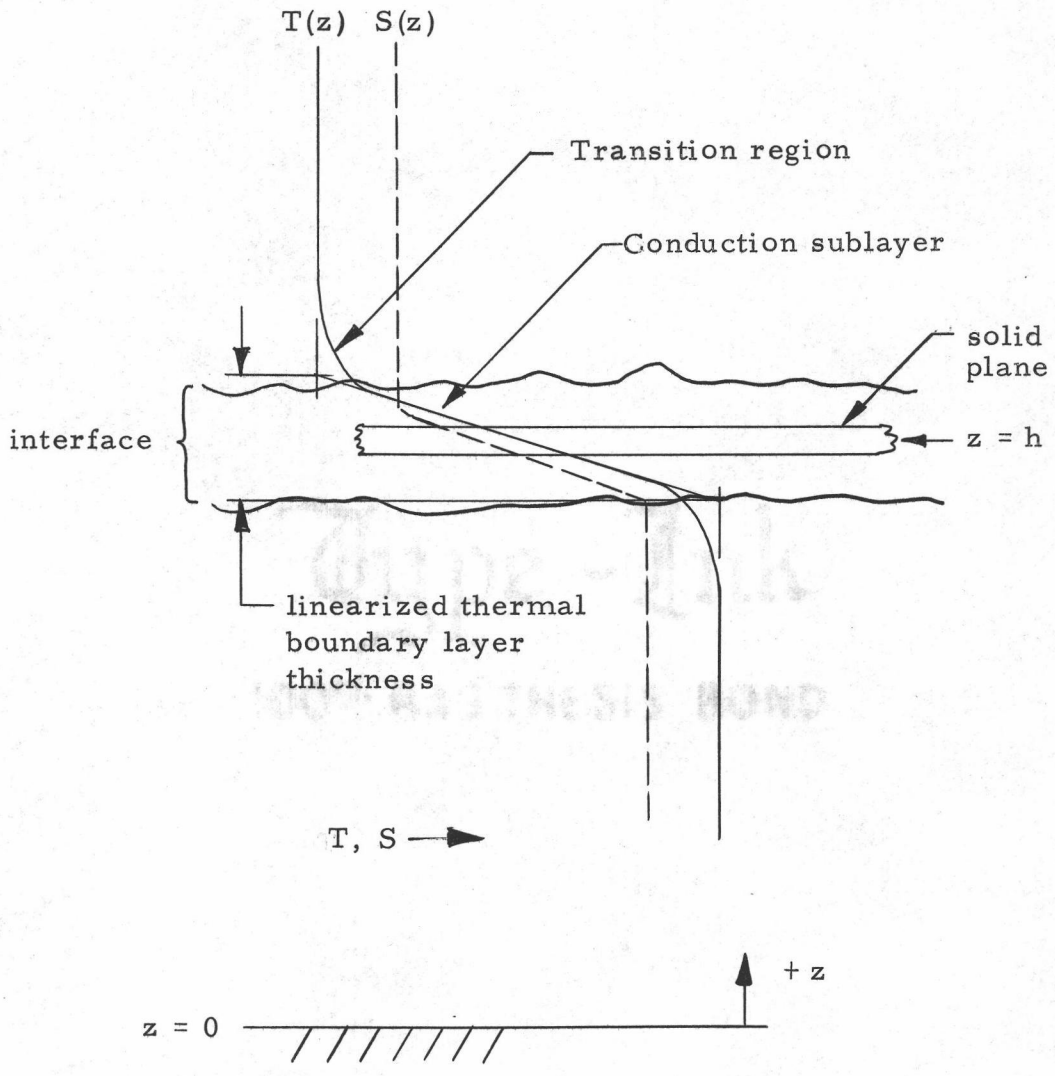

Figure 2. A working model of a diffusive interface.

interfacial Nusselt number, viz.,

$$Nu_i \equiv \frac{H}{H_{sp}} = \frac{H}{A\,\Delta T^{4/3}} \tag{17}$$

where A is still given by

$$A = ck_T\left(\frac{g\alpha}{\kappa\nu}\right)^{1/3}$$

Let c = 0.085 after Turner, a good choice for rigid-rigid boundaries (see Tables I and II). The boundaries of the interface are physically closer to free-free and perhaps another value should be used for c but the only change would be a constant fractional change in the non-dimensionalized flux[8]. The scaling will result in a universal heat flux relationship if the $R^{1/3}$ law holds for the diffusive heat flux and if salt gradient influences on H are either constant or can be neglected.

A more obvious way perhaps to non-dimensionalize H is

$$\frac{H}{-k_T \left.\frac{dT}{dz}\right|_{z=h}}$$

where the denominator is evaluated at the center of the interface, z=h, where the transport mechanism is solely conduction. The quantity $\left.\frac{dT}{dz}\right|_{z=h}$ can be approximated by $\frac{\Delta T}{d_T}$ where d_T is the linearized

---

[8] The physical significance of the change is the weaker constraint of free boundaries on the velocity.

thermal thickness of the interface (see Fig. 2). Then, the interfacial Nusselt number becomes

$$Nu' \equiv \frac{H}{k_T \frac{\Delta T}{d_T}} \tag{18}$$

This definition, Eq. (18), is implied by the non-dimensionalization used in the stability analysis for which $d_T = d$, the spacing of the boundaries, and ΔT is the imposed temperature difference. Notice that

$$\frac{Nu'}{Nu_i} = \frac{A\,\Delta T^{1/3}\,d_T}{k_T} = cR^{1/3}(d_T) \tag{19}$$

Though it is difficult to use Nu' in the experimental analysis, it facilitates the derivation of a relationship between the Nusselt number and the other non-dimensional variables of the problem. The procedure is to use physical arguments and the governing equations of the problem, Eqs. (12)-(14). From the equations, it is clear that the temperature is a function of certain variables and parameters, viz.,

$$T = f_4(x, z, t, Pr, \tau, R\ Rs).$$

The vertical heat flux, Q, can be obtained as follows:

$$Q = -k_T \partial_z T_{total} = -k_T(-\frac{\Delta T}{d} + \partial_z T)$$

where Eq. (7a) has been used. Equivalently,

$$Nu' = 1 - \frac{d}{\Delta T} \partial_z T = f_3(T) .$$

To simplify further, average over time to obtain a steady state Nusselt number, average horizontally to eliminate x, let Pr be a constant, and eliminate Rs by defining a new variable, $R\rho \equiv Rs/R$. These steps allow one to write

$$Nu' = f_2(\tau, R\rho)\bar{f}_2(R) .$$

Furthermore, choose f_2 so that the heat transfer is independent of any length scale; then

$$Nu' = f_2(\tau, R\rho)cR^{1/3} .$$

Eliminate τ arguing that it is roughly constant for experiments using the same set of components. Hence,

$$Nu' = cf_1(R\rho)R^{1/3} . \tag{20}$$

Using Eq. (19), we have finally that

$$Nu_i = f_1(R\rho) \tag{21}$$

or that the interfacial Nusselt number depends only on the stability ratio. Apparently, the density difference across the interface, $\Delta\rho$, is unimportant. The reason for this can be seen from the linear equation of state:

$$\Delta\rho = \rho_o(\beta\Delta S - \alpha\Delta T) = \rho_o\alpha\Delta T(R\rho - 1) \tag{22}$$

Clearly, $\Delta\rho$ is specified once ΔT (or R) and $R\rho$ are given and since both the latter have been accounted for in the above analysis, $\Delta\rho$ loses independent importance. The density difference can enter into the problem in another role however and this will be discussed later.

Keep in mind that Eq. (21) holds rigorously only when the conditions of the linear stability analysis are met, the convection is steady, and the salt distribution has negligible effects on the heat transfer. Furthermore, Eq. (21) holds for only particular values of Pr and τ.

Non-dimensionalization of the interfacial salt flux

Turner points out that it is reasonable to expect the non-dimensional salt flux to depend on the thermal Rayleigh number since it is the temperature difference which is destabilizing and thus responsible for the salt transport. If a solutal Nusselt number or Sherwood number is defined as

$$Sh' \equiv \frac{Fs}{k_S \frac{\Delta S}{d_S}}$$

where d_S is the linearized thickness of the solutal interface across which ΔS exists then the following relationship should hold:

$$Sh' = cg_1(R\rho)R^{1/3}, \tag{23}$$

where c is included for symmetry with Eq. (20). This can be written alternatively as

$$Sh_i = g_1(R\rho).$$

Notice the existence of two length scales, d_T and d_S.

Can the Soret effect (salt transport due to a temperature gradient) account for a significant portion of the observed salt flux through a diffusive interface? Caldwell (1973a) shows that the ratio of salt flux due to the Soret effect to that due to ordinary Fickian diffusion is

$$\frac{J_C(\text{Soret})}{J_C(\text{Fickian})} = \frac{s_T \nabla T}{\frac{1}{C}\nabla C}$$

where s_T is the Soret coefficient (typically $10^{-3}\ ^\circ C^{-1}$). For the case $d_T = d_S$, the above ratio reduces to $S\beta s_T/(\alpha R\rho)$ which for typical conditions is about $1/10R\rho$. Transport ascribable to Soret or thermal diffusion then is small and can be neglected in the present investigation.

Derivation of the flux ratio, Rf

We will proceed to derive a quantity called the flux ratio, Rf, which for salt water solutions is approximately equal to $\beta Fs/\alpha H$. It will be shown that Rf is a ratio of potential energy changes and that it has an upper bound.

Imagine the upper layer of a simple two-layer diffusive experiment to be as shown in Fig. 3. At time t=0, let $T=T(0)=T_o$ and

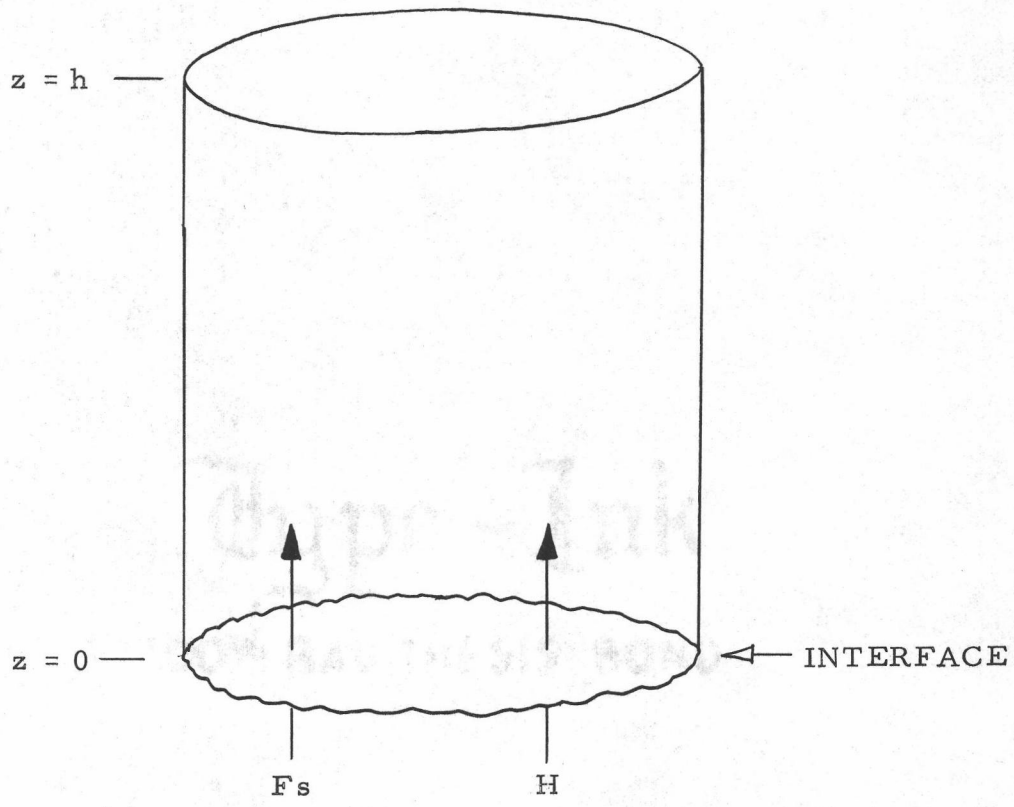

Figure 3. The interface and upper layer of a transient, two-layer, diffusive experiment. For convenience, the interface is considered to be a plane at z = 0. The heat flux through the top and sides of the layer is assumed to be zero.

$S=S(0)=S_o$ where $S[=]$ gm cm^{-3} for convenience. Let the density be given by

$$\rho(T,S) = \rho_o[1 + \beta(S - S_o) - \alpha(T - T_o)] \tag{24}$$

where $\rho_o = \rho(T_o, S_o)$.

As time proceeds, T will increase and the potential energy change in the layer due to the changing temperature will be negative, i.e., $(\Delta PE)_T < 0$. On the other hand, $(\Delta PE)_S > 0$. We want to find the ratio $(\Delta PE)_S/(\Delta PE)_T$.

The initial potential energy is given by

$$(PE)_o = Ag\int_0^h \rho(z)z\,dz = Ag\rho_o h^2/2 .$$

At some later time, t,

$$T(t) = T_o + \frac{Ht}{h\rho c_p}$$

$$S(t) = S_o + \frac{Fs\,t}{h}$$

$$\rho(t) = \rho_o\left(1 + \frac{\beta Fs\,t}{h} - \frac{\alpha Ht}{h\rho c_p}\right) \tag{25}$$

from which it follows that

$$(PE)_t = Ag\rho_o \frac{h^2}{2}(1 + \beta Fs\,t/h - \alpha Ht/h\rho c_p). \tag{26}$$

Therefore,

$$\frac{(\Delta PE)_S}{(\Delta PE)_T} = -\rho c_p \beta Fs/\alpha H$$

and by definition

$$Rf \equiv \left| \frac{(\Delta PE)_S}{(\Delta PE)_T} \right| = \rho c_p \beta Fs/\alpha H \quad . \tag{27}$$

Since for salt water $\rho c_p \approx 1$, Rf is sometimes written in dimensional form as

$$Rf \doteq \frac{\beta Fs}{\alpha H} \quad .$$

If the lower layer had been analyzed, we would have found that $(\Delta PE)_S < 0$ and $(\Delta PE)_T > 0$ but again that $Rf = \beta Fs/\alpha H$. If both layers are analyzed with an energy reference level at the tank bottom,

$$(\Delta PE)_t = Ag\rho_o ht(\beta Fs - \alpha H/ c_p) \, . \tag{28}$$

Assuming $\Delta PE = 0$, a limiting energetic case, Eq. (28) shows that the upper bound for the flux ratio is one. Strictly, then,

$$Rf < 1$$

and

$$\beta Fs - \alpha H/\rho c_p < 0. \tag{29}$$

Equations (28) and (29) imply that the rate of change of PE/unit mass is negative. Finally, note that the ratio

$$\left(\frac{\Delta IE}{\Delta PE}\right)_{\text{unit mass}} = \frac{c_v J}{\alpha g(Rf - 1)h} >> 1$$

where $J = 4.186 \times 10^7$ ergs cal^{-1}, showing potential energy changes are miniscule compared to increases in heat content.

Introduction of turbulent transfer coefficients

It is customary in transport problems to present the transport or flux in terms of transfer coefficients for heat and salt for a diffusive experiment as follows:

$$H = K_T \Delta T \tag{30a}$$

$$Fs = K_S \Delta S \, . \tag{30b}$$

The coefficients incorporate all the physics of the interface and its interaction with the well-mixed layers. When the convection is steady, K_T and K_S have meaning even if there is no interface.

The ratio of transfer coefficients gives

$$\frac{K_S}{K_T} = \frac{Fs \, \Delta T}{H \, \Delta S} \, .$$

Using Eqs. (20) and (23) and the definitions of Nu' and Sh' this can be rewritten as

$$\frac{K_S}{K_T} = \frac{1}{\rho c_p} \tau \frac{d_T}{d_S} h(R\rho) \tag{31}$$

where $h(R\rho) \equiv g_1(R\rho)/f_1(R\rho)$. The ratio d_T/d_S may also be a function of $R\rho$. The quantity $\frac{1}{\rho c_p} \frac{d_T}{d_S} h(R\rho)$ measures the deviation of the ratio of turbulent coefficients from the ratio of molecular coefficients, $\frac{\kappa_s}{\kappa}$. Equation (31) holds for all $R\rho$ by definition.

By studying the transfer of a parcel of fluid from one layer into

the other it can be shown that complete mixing can occur only when $Rf = R\rho$. Equation (22) shows this is possible only when $R\rho = 1$. Furthermore, when $R\rho = 1$, $\rho c_p K_S/K_T = 1$ and salt and heat are mixed equally well between layers, that is, both components are transferred by the same turbulent mechanism and are completely diffused (this is equivalent to saying $(\Delta PE)_T = (\Delta PE)_S$).

Near $R\rho = 1$, Rf is close to one and Eqs. (27) and (30) combine to give the condition:

$$\frac{K_S}{K_T} \leqq \frac{1}{\rho c_p R\rho}$$

with equality only when $R\rho = 1$. When this result is compared with Eq. (31) it is seen that a reasonable form for the unknown function h is

$$h(R\rho) \sim \frac{1}{R\rho} \ .$$

The exact form of h cannot be determined without knowing the dependence of d_T/d_S on $R\rho$. At this point we can only guess that

$$\text{for } R\rho \text{ large, } \frac{d_T}{d_S} \to n, \quad \text{where } 1 < n < 10 \ ; \tag{32a}$$

$$\text{for } R\rho \to 1 \ , \ \frac{d_T}{d_S} \to 1 \ . \tag{32b}$$

In the above, the range of n is chosen on the basis of work done by Elder (1969) and Lindberg (1970), which deals with d_T/d_S for a free boundary layer and one attached to a solid boundary, respectively. At

low stabilities, $\Delta\rho$ is small and the mixing in the layers will decrease the thickness of the interface. Asymptotically, as $R\rho \to 1$ and $\Delta\rho \to 0$, both d_T and $d_S \to 0$; and if they do so at the same rate, $d_T/d_S \to 1$.

Calculation of the interfacial mass flux

Recall from Fig. 3 that the interface is fixed at z = 0 and compute the mass between the interface and z = h at time t. Using Eq. (25)

$$\text{mass } (t) = \rho_o Ah + A\rho_o(\beta Fs - \alpha H/\rho c_p)t \; . \tag{33}$$

Since $\beta Fs - \alpha H/\rho c_p < 0$, the mass in the upper layer decreases linearly with time: there is a downwards mass flux or as some researchers put it, a positive (upwards) buoyancy flux[9]. The positive buoyancy flux drives convective mixing in the upper layer. The quantity $F\rho \equiv \beta Fs - \alpha H/\rho c_p$ has the dimensions of a velocity and is, in fact, the speed at which the interface would have to move to balance the mass flux (c.f. the entrainment velocity which appears in thermocline models, e.g., Turner and Kraus, 1967, and in laboratory work, Turner, 1968b). Substituting typical experimental values, one calculates the velocity to be less than +1 mm day^{-1} ($+1 \times 10^{-6}$ cm sec^{-1}).

---

[9] The buoyancy flux is defined as $B \equiv -g\rho'w'/\rho$. In thermal convection, B is positive when hot buoyant fluid ($\rho' < 0$) moves upwards tending to locally increase the stability. In this sense, the lifting of salt is a negative buoyancy flux.

From Eq. (33) it can be seen that ρF_ρ is a mass flux; therefore, F_ρ is a flux of specific volume or inverse density. The idea of a density flux and a density diffusion coefficient, κ_ρ, for a two-component system was introduced by Veronis (1968). He shows that one should expect $\kappa_\rho = -(\kappa\kappa_s)^{1/2}$. The negative sign reflects the interesting part of double diffusive convection: convection in the presence of a stable density gradient.

Though the movement of the interface due to a mass flux is small, entrainment of fluid from a layer or erosion of the interface might lead to larger motion. The very name, diffusive interface, has so far suggested transport by molecular processes. Entrainment would of course enhance heat and salt transport. We now consider under what conditions this is possible.

Consideration of entrainment

If the turbulent intensity or level of convective mixing are equal on both sides of an interface, one expects the interface to remain at a constant height. If, on the other hand, there is some asymmetry, the interface will move away from the layer in which the mixing is more vigorous. These ideas have been verified by Turner (1968b) who studied mixing rates of salt and heat (independently) across an interface with mechanical mixing in the adjoining layers. Turner shows that for fixed turbulent intensities in the layers, heat is more easily

entrained across a strong (large Richardson number[10]) density interface than is salt. As $\Delta\rho \rightarrow 0$ (smaller Ri), effects of buoyancy become negligible, and both salt and heat are transferred equally well. Can we use these results to anticipate the behavior of the diffusive interface with changes in $R\rho$?

As Turner (1973, p. 292) points out: "Superficially, the two layer system with stirring on both sides of an interface has much in common with the double diffusive interfaces...since in both cases the interface is kept sharp by turbulence in the layers on each side. The latter are complicated, however, by the double boundary layer structure and by the fact that the stirring is through convection driven by the interfacial flux; no theoretical framework which can include both of these has yet been suggested."

It may help to look at an electrical analog of the interface, two layers, and a supply of heat:

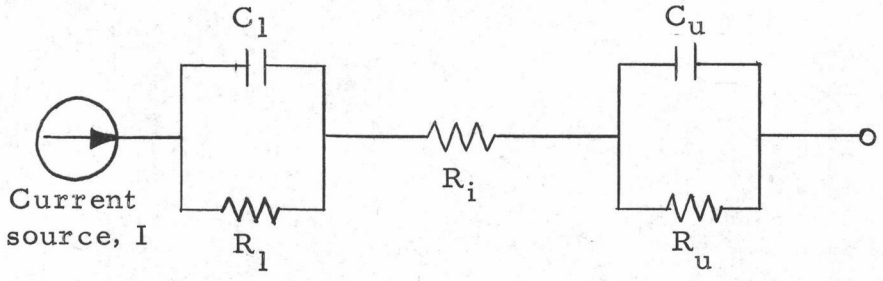

[10] The Richardson number, Ri, is the ratio of buoyancy to inertial terms, $g\Delta\rho\, L/\rho u^2$.

The analogs of heat, temperature, thermal capacitance, and d_T/k_T are current (I), potential (V), capacitance (C), and resistance (R). The capacitance of the interface is assumed to be negligible; its resistance (and the resulting voltage drop) is controlled by the layer circuit elements. Physically, the interface thickness is controlled by the mixing in the layers which sweeps away interfacial fluid and keeps the thickness at an appropriate value. The parameters which characterize the mixing intensity are u', an rms horizontal velocity and l, the diameter of the energy-containing eddies. They combine with $\Delta\rho$ to form the Richardson number. Now Eq. (22) shows that $\Delta\rho$ depends on $R\rho$ and ΔT. The conclusion is that $\Delta\rho$ (or ΔT) can exert an effect on the interface independent of $R\rho$ via mixing and entrainment. This can be interpreted, in the electrical analog, as a kind of voltage feedback mechanism.

Historical survey and discussion

The experimental verification of salt-fingers (regime V in Fig. 1) came in 1960. Two years later it was anticipated (Stommel, 1962) that convection in regime II would occur as a mode different from the monotonic mode of salt fingers and that "finite amplitude convection" might produce horizontal layering.

Turner and Stommel (1964)

Turner and Stommel (1964) demonstrated that layering can indeed occur when a smoothly stratified salt solution is heated from below. A rather strong heating rate was used in this preliminary work so that lateral losses, conduction up the side walls of the container, and evaporative cooling could be dismissed as being important influences[11]. The layering begins at the bottom of the fluid with the formation of a single convecting layer. Other layers form above the first sequentially, separated from one another by thin interfaces. One can think of this as a thermal front propagating upwards leaving behind, in its wake, semi-permanent structures or patterns in the fluid. The layers slowly increase in thickness and merge when the density difference across an interface becomes sufficiently small. Therefore, the layers are only a transient feature in this particular experiment.

---

[11] Side wall heating can, independent of a vertical heat flux, cause layering. Turner and Stommel point out that a difference in flow patterns distinguishes layering caused by a vertical flux from a horizontal heat flux. Nevertheless, Veronis (1965) allows for the possibility that the layering observed in this experiment might be due to side wall effects. The phenomenon of layered convection in a stratified fluid due to side wall heating, first studied by Mendenhall and Mason (1923), has, since 1964, been further studied by Blumsack (1967), Thorpe, Hutt, and Soulsby (1969), Chen, Briggs, and Wirtz (1971), and Wirtz, Briggs, and Chen (1972). This work shows in great detail that distinction can be made on the basis of layer depth and convection patterns.

The experimental conditions of this investigation and other work on diffusive convection are given in Table III.

Turner and Stommel make certain observations which, considering the impact of this initial work, are important enough to list here. These are: (1) there are no observable horizontal motions with length scales comparable to a tank diameter. This seems to reaffirm the assumption that the side walls do not drive the motion in the interior, (2) the formation of the layers depends on κ being greater than κ_S, (3) layers can be formed from very large salinity gradients when a large enough heat flux is applied; the layer depth increases with increased heat flux and decreases with increased initial salinity gradient, (4) each layer is in "vigorous turbulent convective motion", (5) the convective elements in the layers are small in scale, about as wide as the depth of the layer and random in position, (6) the motions in adjacent layers tend to be in opposing directions near the interface, that is, a shear exists across the interface, (7) the motions are thermally, not frictionally, driven across the interface, and (8) though the temperature field is driving the motion, salt is transferred across the interface at a rate greater than can be explained by molecular diffusion alone.

Turner (1965)

Recognizing that independent of how the interface is created,

Table III. Previous experimental work on diffusive convection.

Author	T component	S component	H cal $cm^{-2} sec^{-1}$	Stability	Container	Bottom Plate	Observation
Turner & Stommel (1964)	heat	salt	3.3×10^{-2}	0.6‰ cm^{-1} initial linear gradient	square 25 cm depth	not given	layering
Turner (1965)	heat	salt	1.8 to 5.5 $\times 10^{-2}$	$1.3 < R\rho < 7$	30 cm dia. 25 cm depth Perspex	metal 1/4 to 1/2"	one diffusive interface
Turner (1968a)	heat	salt	2 to 20 $\times 10^{-2}$	1/2 to 5‰ cm^{-1}	29 cm dia. 25 cm depth	aluminum 0.25 in.	layering
Shirtcliffe (1969a)	heat	sucrose	$\|R\|$, $\|Rs\| \approx$	1 to 3×10^4	25x6.4 cm 9.7 cm depth	brass 0.5 in. plate glass and Tufnol	over-stability
Broughton (1972)	heat	salt	1.3 to 8 $\times 10^{-3}$	$1 \leq R\rho < 13$	cube 2 ft/side acrylic	thin permeable membrane	diffusive interfaces
Shirtcliffe (1973)	sugar	salt	*	$1.1 < R\rho < 3.2$	Perspex 20 cm and 6 cm of fluid	no external heating	flux measure-ments & profiles

* Shirtcliffe gives the range of mass flux for sugar, J_s (gm $cm^{-2} sec^{-1}$), as $3 \times 10^{-8} < J_s < 7 \times 10^{-7}$. We convert this into an equivalent heat flux, H (cal $cm^{-2} sec^{-1}$), by equating J_s and $\alpha H / c_p$. This procedure gives the range $1.5 \times 10^{-4} < H < 3.5 \times 10^{-3}$.

fluxes through a system of layers and interfaces will be controlled by each interface and its interaction with the layers, the next step experimentally was to quantitatively study the transfer processes at a single (diffusive) interface. Turner (1965) used the boundary between two artificially-created layers to produce an interface. Heating from below with the top of the tank insulated produced two convection layers and a sharp diffusive interface (some mechanical stirring was often necessary in the upper layer before it would convect). Turner then studied the transport of salt and heat across the interface as a function of R_ρ. The position of the interface was found to change slowly or not at all before low stabilities were reached at which time the interface lost its identity and the layers mixed completely. Turner used heating rates known to about 30% and covering a range of three (2.8 to 5.5 x 10^{-2} cal cm^{-2} sec^{-1}). Turner arrived at three fundamental conclusions:

(a) the heat flux through the diffusive interface varies systematically with the stability of the interface,

(b) the ratio of the salt flux to the heat flux is a constant for $R_\rho > 2$, the so-called constant regime, and approaches one as the interface collapses, the variable regime, and

(c) the ratio of turbulent transfer coefficients for salt and heat varies with stability.

These three results will be discussed further.

(a) Interfacial heat flux

Instead of examining a plot of the experimental results of Turner (1965) we look at an analytical expression developed by Huppert (1971) which fits Turner's measurements to within experimental error over the cited range of $R\rho$. The expression is

$$Nu_i = \psi R\rho^{\phi} \tag{34}$$

where $\psi = 3.8$ and $\phi = -2$. The equation

$$Nu_i = 3.8 R\rho^{-2} \tag{35}$$

is plotted in Fig. 4.

Using the definitions of Nu_i and $R\rho$, Eq. (35) can be written alternatively as

$$H = \frac{3.8 A\alpha^2}{\beta^2 \Delta S^2} \Delta T^{10/3} \tag{36}$$

from which it is clear that the heat flux is proportional to $\Delta T^{10/3}$. This enhancement over the $R^{1/3}$ relationship is due to the weaker constraint of free boundaries (c.f. footnote 8).

An examination of Fig. 4 shows that the heat transport is much more efficient at low stability numbers than at high stability numbers. In fact, it seems there are two distinct regimes of transfer separated by a transition region.

In an attempt to explain the shape of the curve in Fig. 4 once

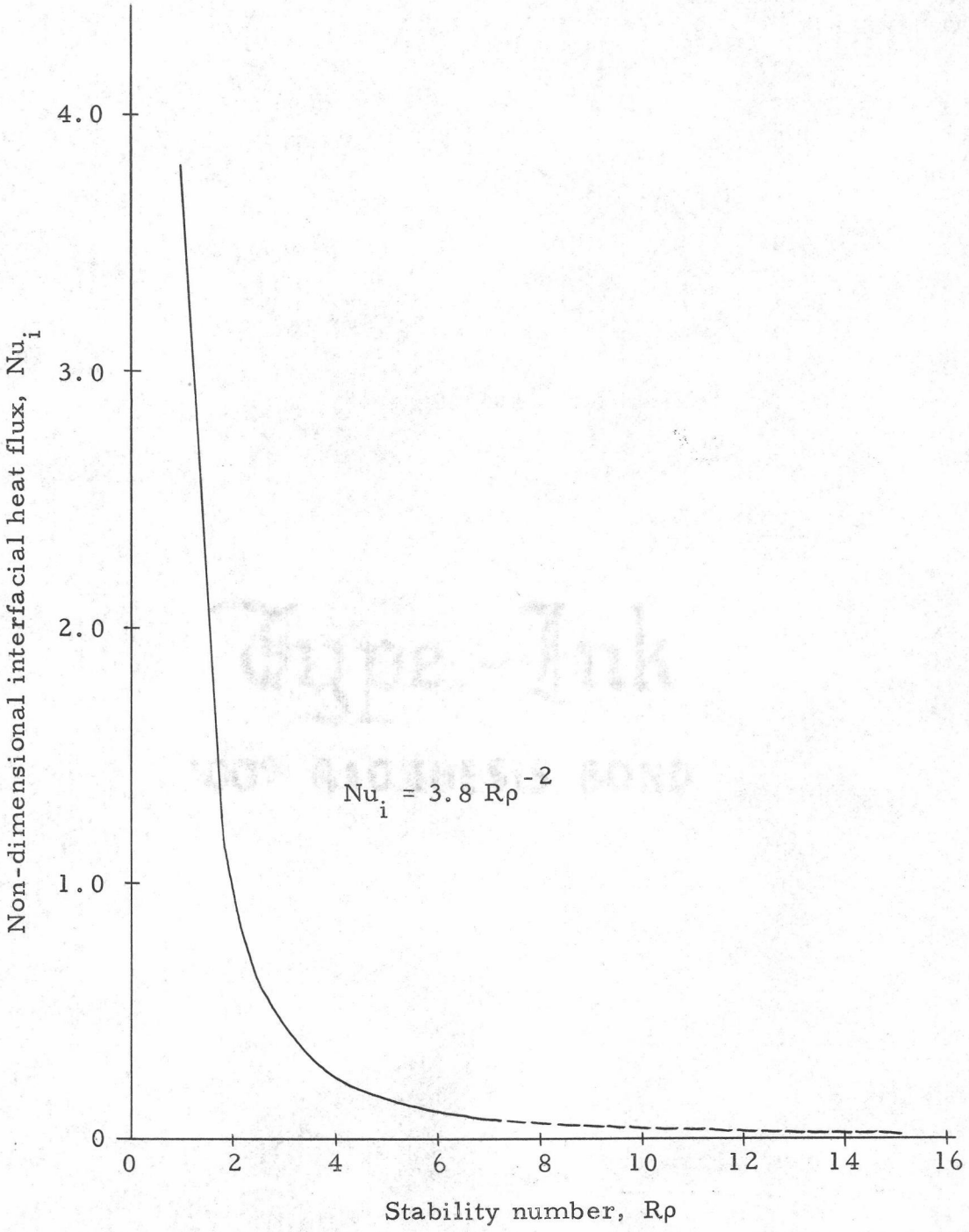

Figure 4. Plot of interfacial Nusselt number against stability number (Equation 35).

again let the linear stability model apply to the interface. Can we predict the value of the heat flux in the stable regime? The answer is no because the stability model tells us nothing about the thickness of the interface when it is in equilibrium between two convecting layers. This is not the fault of the stability theory but points to the need for a more complete theoretical model. Can we then at least account for the transition region in terms of gradual growth of oscillatory convection? To answer this question we must look at the path of an experiment through the R-Rs plane. For convenience, a part of quadrant I of Fig. 1 is reproduced as Fig. 5.

In the construction of Fig. 5 it is assumed that $d_S = d_T = d$. We have hypothesized this condition to be true already (see Eq. (32b)) at small $R\rho$. In the stable regime it is probably true that $d_T = d$ and $d_S < d_T$. If the difference in thicknesses is accounted for the lines $R\rho$ = constant for constant > 6 move further away from the line $R\rho = 1$ than is shown in Fig. 5. Recall that the equation for the line $\overline{XW}$ is

$$R = \frac{Pr}{Pr + 1} Rs + \frac{27}{4} \pi^4$$

Two lines, $\overline{XW}_1$ and $\overline{XW}_2$ are shown. For $\overline{XW}_1$ Pr = 7 (roughly corresponding to an interfacial mean temperature of 20 C) and for $\overline{XW}_2$ Pr = 4.3 (40 C). The starting point for the experimental path and its assumed curved shape are somewhat arbitrary.

From Fig. 5 notice that the experimental path approaches an

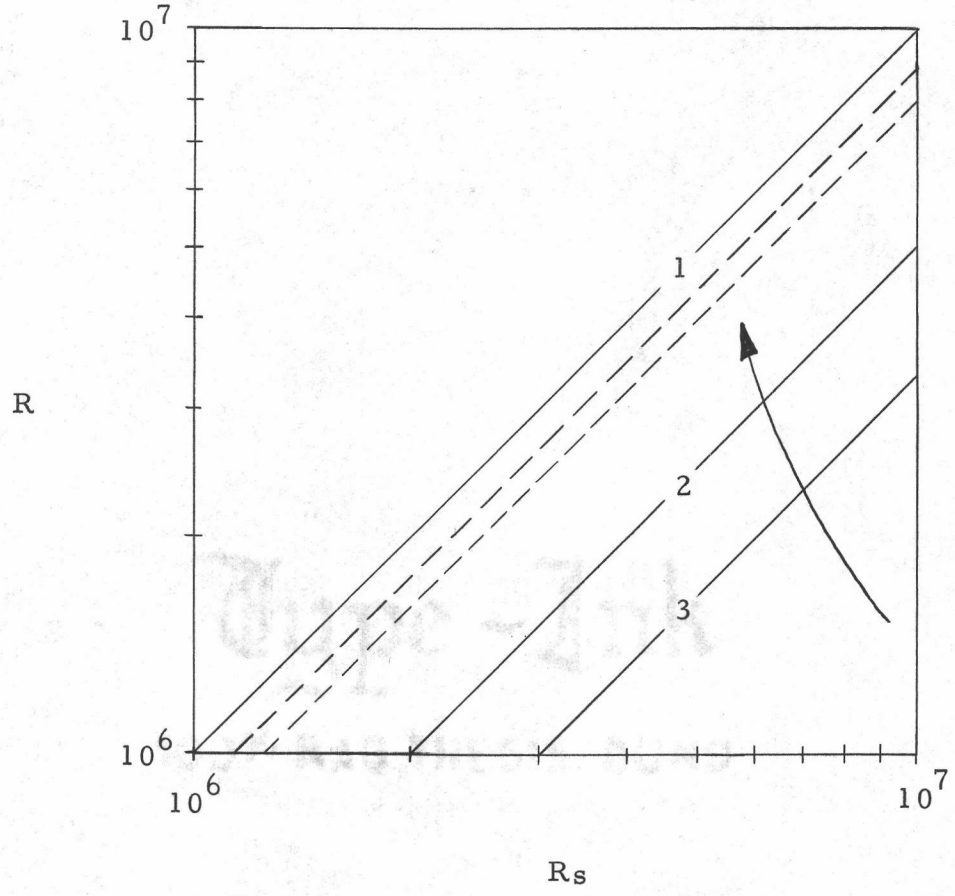

Figure 5. Part of quadrant I of Fig. 1 reproduced as log R vs log Rs. The solid lines are lines on which $R\rho$ = constant. The two dashed lines enclose the range of the line $\overline{XW}$ for typical experimental conditions. The arrow represents a hypothetical experimental path.

intersection with $\overline{XW}$ only well after passing through the line $R\rho = 2$. Therefore, the interface is stable, for almost the entire experiment, in the sense that infinitesimal oscillations in the interfacial temperature and salinity fields are damped, on the basis of the linear analysis. The rapid increase in the heat transport beginning at $R\rho \approx 3$, then, cannot be explained by the growth of small oscillations. As possible answers to our question, we are left with the existence of a subcritical (occurring well before the intersection of the path with $\overline{XW}$) finite amplitude instability; or some other mechanism which is not hinted at by the stability analysis.

The possibility of a finite amplitude convective mode has been investigated theoretically by Veronis (1965, 1968). For the case of $\tau = 1$ and $Pr > 1$ there is no possibility that finite modes will set in before smaller overstable motions. The case for salt water, $\tau = 0.01$, has not been studied analytically; but finite amplitude effects are responsible, according to Veronis (1965), for the layer creation observed by Turner and Stommel (1964). If not finite amplitude instability, what else? In response to pressure fluctuations caused by convective elements, it is possible that the interface can become irregular and effectively allow the heat flux to "see" a larger area.

(b) Ratio of salt flux to heat flux

Probably Turner's most interesting result is the variation of Rf

with R_ρ shown in his Fig. 7 and our Fig. 23. The equations describing this variation are:

$$R_f = 1.85 - 0.85\, R_\rho \text{ , for } R_\rho \leq 2 \qquad (37a)$$

$$R_f = 0.15 \text{ , for } R \geq 2 \qquad (37b)$$

His interpretation of this result is that for the constant regime, a "self-limiting mechanism" bounds the heat flux and causes a fraction (0.15) of the potential energy released by the temperature field to be used to lift the salt.

Veronis (1968) gives a discussion of why Rf may assume the value $\sqrt{\tau}$ [12] when $R_\rho = 1$ (see also Turner, 1973). Other evidence (Turner, 1967; Shirtcliffe, 1973) supports this value for Rf in double diffusive convection. Therefore, one suspects that the rapid change in the variable regime reflects the onset of direct buoyant convection as the dominant transfer mechanism through the interface.

Finally, note as an aside, that when R_ρ is very large (say 15) there can be no layers and $R_f \doteq \tau R_\rho$. Therefore, Rf will begin to increase with R_ρ.

(c) Ratio of turbulent transfer coefficients

The results of Turner's study of the ratio of transfer coefficients

---

[12] For $\bar{S} = 28.5‰$, $\bar{T} = 22$ C, Caldwell (1973a) gives $\kappa_S = 1.37 \pm 0.12 \times 10^{-5}$ cm^2 sec^{-1}. Combining this with the best estimate of κ_T (Fabuss and Korosi, 1968 and Caldwell, 1974b), $\sqrt{\tau} = 0.98$.

are sketched in Fig. 6. Implicit in this single curve are changes between experiments and within any experiment in heating rate, Richardson number, interface thickness, and initial conditions (mainly initial ΔS). In view of Eqs. (35) and (37a, b), a plot of K_S/K_T really presents no new information since it is easy to show that $K_S/K_T = Rf/R\rho$; therefore,

$$\frac{K_S}{K_T} = \begin{cases} \dfrac{1.85}{R\rho} - 0.85, & \text{for } R\rho \leq 2 \\ \dfrac{0.15}{R\rho}, & \text{for } R\rho \geq 2. \end{cases} \tag{38}$$

It is interesting to explore the consequences of the assumption that transport by molecular processes can fully account for the observed fluxes through a horizontal[13] interface. Assuming identical boundary layer thicknesses,

$$K_S \Delta S = k_S \Delta S/d_S \tag{39a}$$

and

$$K_T \Delta T = k_T \Delta T/d_T \tag{39b}$$

which can be combined to give

$$\frac{K_S}{K_T} = \frac{k_S}{k_T} \approx 0.01.$$

From Eq. (38), then, molecular transports exist when $R\rho \approx 15$ (c.f.

---

[13] This constraint assures that the same area is used for both sides of Eqs. (39a, b).

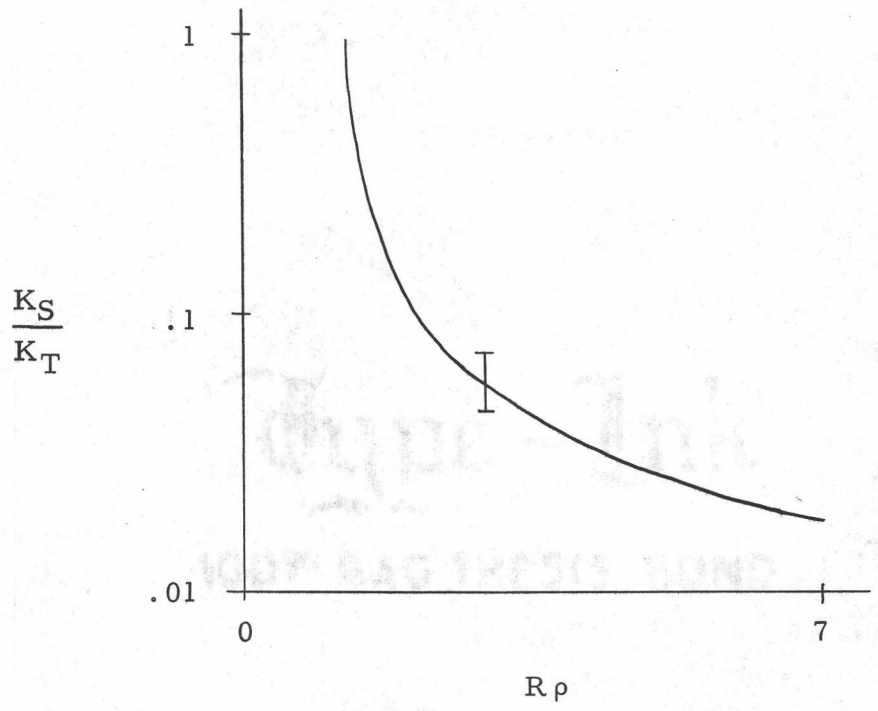

Figure 6. Ratio of turbulent transfer coefficients vs. stability number (from Turner, 1965). The error bar gives a rough indication of the spread of the data in the vertical about the sketched curve.

Neshyba, Neal, and Denner, 1971; Osborn, 1973).

Finally, notice from Fig. 6 that as $R\rho \rightarrow 1$, $K_S/K_T \rightarrow 1$ which implies, as mentioned before, that salt and heat are transported equally well presumably by the same turbulent motions.

Turner (1968a) and Shirtcliffe (1967; 1969a)

Turner (1968a) quantitatively studied the formation of layers from a stable salinity gradient. He found that $R\rho = 1$ at an interface of a growing layer. One can show analytically that for this particular situation $Rf = 1/3$ but since the fluxes were not measured, no verification of this value is possible. The condition $R\rho = 1$ implies the interface has marginal (neutral) gravitational stability and that entrainment or growth should be at a maximum. Turner also develops and tests an analytical expression which gives the (critical) thickness of a layer when another first forms above it.

Turner (1968a) and Shirtcliffe (1967, 1969a) have experimentally observed overstable motions while heating a stable gradient from below. These observations support the theoretical prediction that instability will first occur as an oscillatory mode.

Shirtcliffe (1969a) has made the following observations from Schlieren photography of the nature of the convective elements or cells in the first layer: (1) near the top of each cell there is a "build-up of solute" tending to make the cell top heavy, (2) the cells

were "continually appearing and disappearing", (3) the cells migrated sideways (cf. Krishnamurti, 1973 and Chu and Goldstein, 1973), (4) in general, the cell arrangement was much different than might be expected from analogous work in pure thermal convection. Shirtcliffe was able to draw a stability diagram for the overstable motions. He found the critical thermal Rayleigh number to be higher than predicted by the linear theory and hence the stability margin may deviate somewhat from the line $\overline{XW}$ in Fig. 1.

Shirtcliffe (1969b)

Shirtcliffe (1969b) also has performed layering experiments and developed a computational scheme which reproduces the features of his experiment. His computer model uses empirical formulae for the transfer coefficients for solute and heat. The formulae were adjusted slightly to give good fit to the experimental results. It would be interesting to compare these numerical results with laboratory work for which ΔT and ΔS are known across the interfaces. In Shirtcliffe's model, when convection is present, $K_S/K_T \approx 1$ which would imply from Turner's work that $R\rho \approx 1$.

Elder (1969)

Elder has performed numerical experiments with salinity and temperature fixed at the boundaries. In all cases examined an

"active" diffusive interface exists for a long time but ultimately decays. This work indicates that steady state "layered" thermohaline experiments with similar boundary conditions might not be possible.

Turner, Shirtcliffe, and Brewer (1970)

The variation of transport coefficients for salt, sugar[14], potassium, sodium, and calcium chloride across diffusive interfaces was investigated. The transport coefficient for component C, K_C, is defined as the flux of C divided by the difference in the concentration of C across the interface. The K_C's are found to vary systematically with molecular diffusivities as is to be expected if the interfaces are indeed diffusive.

Huppert (1971)

Huppert performed an analysis of the equilibrium positions of a layer sandwiched between two diffusive interfaces and infinite bounding reservoirs of constant concentrations. An equilibrium curve of permitted temperature and salinity perturbations in the central layer is derived. The important conclusions are: (1) if both interfaces in the

---

[14] The reason for the use of sugar in this and other investigations is that its diffusivity in water solutions is one third that of sodium chloride. This is a large difference and hence is useful experimentally.

unperturbed state have $R\rho > 2$ then the system is stable. If perturbations in T or S occur in the central layer (even if one interface is perturbed to the unstable state of $R\rho < 2$) the system will attain a new position on the equilibrium curve. The stability is, therefore, only neutral, (2) if either interface in the unperturbed state has $R\rho < 2$ then the system is unstable, and (3) though all possible positions on the equilibrium curve provide equal fluxes through each interface, only the origin of the curve (an unperturbed state) allows both interfaces to have the same stability number. Observationally, then, one should not expect to see steady-state layers with interfaces each having identical stability numbers. Huppert based his analysis on Turner (1965) and may need modification in view of subsequent laboratory work.

Broughton (1972)

Three reports on work conducted at Colorado State University should be noted at this time: (1) Reinders and Haberstroh (1972) describe a simple model for steady state heat transfer through a system of immiscible fluid layers and report experimental verification. We suggest that any model of the diffusive interface should reduce to their results in the limit of zero solute diffusivity; (2) Broughton and Loehrke (1972) and Broughton (1972) report a first attempt to produce a steady, layered thermohaline convection system. Though we feel

they fell short of the mark, a number of worthwhile observations are made: (a) Through the use of dye and shadowgraph techniques and temperature profiling, it is concluded that conduction is the only mode of transport through the central part of the interface (at least for $R\rho > 2$) and on either side of the conductive core there is a transition zone; (b) heat transport from the edge of the conducting zone (the beginning of the transition zone) takes place by the "thermal-burst" mechanism. Two results determined by the present author by manipulation of Broughton's original data are (c) in a plot of Rf vs. $R\rho$ there is no significant variation with heat flux and the average value of Rf is slightly greater than 0.15; and (d) by reconstructing the original temperature profiles it was possible to obtain the interfacial Nusselt number for each interface and to make the usual plot against stability number. The resulting curve is below that shown in Fig. 4 and will be plotted in Chapter VII.

Some experiments were conducted by Broughton to study layer formation from an initially linear salt gradient. The layers formed in this manner persisted in time for as long as a week. The interfaces were not highly irregular and hence were called stable. Measurements of $R\rho$ were not made and comparison with Turner's 1968 result is therefore not possible. It may be that Turner's result for a growing layer, $R\rho = 1$, may be heating-rate dependent (compare the photographs of Broughton's interfaces with those of Turner and Stommel,

1964); (3) Loehrke, Mancini, and Haberstroh (1973) report that the thickness of the diffusive interface is apparently proportional to $R\rho$. This confirms what has been stated previously, i.e., we expect the interface thickness to decrease with decreasing $R\rho$. It is also quite possible that the thickness depends on the magnitude of the imposed flux for a constant $R\rho$.

Shirtcliffe (1973)

Shirtcliffe has studied the diffusive interface in a transient sugar-salt two layer experiment. He shows that the interfacial fluxes as determined from property changes in the layers are equal to the molecular fluxes one would calculate on the basis of deduced profiles of salt and sugar through the interface. The flux law for the sugar-salt interface is much different from the law for the heat-salt interface. Referring to Eq. (34), he finds that $\psi = 2.6$ and $\phi = -12.6$. Since he finds no variable regime in his experiment, Shirtcliffe compares his data to only the constant-regime data of Turner. His analysis of Turner's data for the constant regime yields $\psi = 2.67$ and $\phi = -1.79$. Apparently, then, ψ is roughly constant between each type of experiment while ϕ depends on τ or perhaps on the different experimental conditions. As Shirtcliffe points out, the two values for ψ, 2.6 and 2.7, are not significantly different from the value 2.3 which Huppert (1971) suggests one should expect for free-free boundaries

(when $R\rho = 1$, $Nu_i = 2.6$ and the heat transport is roughly 2.6 times more effective than for solid boundaries).

Shirtcliffe finds no variable regime for $R\rho$ as low as 1.1 and also that $Rf = \tau^{1/2}$ for $R\rho \geq 1.1$ to within experimental error. These results combined imply that an experiment with heat forcing has a unique quality which leads to a change in Rf as $R\rho$ approaches 1. The interfacial thickness was measured to be about 1 cm.

IV. EXPERIMENTAL METHOD AND SUMMARY OF THE DIFFUSIVE EXPERIMENTS

Convection tank apparatus

The convection tank is constructed from a length of 0.25 in. cylindrical polymethyl methacrylate (acrylic) of 11.5 in. circular cross-section. The convecting fluid is bounded below by a heated aluminum plate and above by a cooled aluminum plate. The effective height between plates is 65 cm.

The tank (Fig. 7) has three sections which join together at positions A and B by means of a cylindrical flange coupling (not shown). A cross-section of the flange coupling is shown in Fig. 8. Any material of thickness up to 0.25 in. and of a diameter slightly larger than the interior diameter of the tank can be supported across the tank at A and B. For example, one of the aluminum plates of the upper heat flux meter (described later) is supported in this way. A 0.0625 in. lip around its circumference is squeezed between the edges of the tank, holding the plate firmly in position.

The tank should be imagined as surrounded by 43 cm of styrofoam insulation constructed in the form of a thick donut which can be slipped over the two lower sections of the tank. Any small space between the donut and the tank were filled with suitable packing. Below the heater at the bottom of the tank is an additional 25 cm of

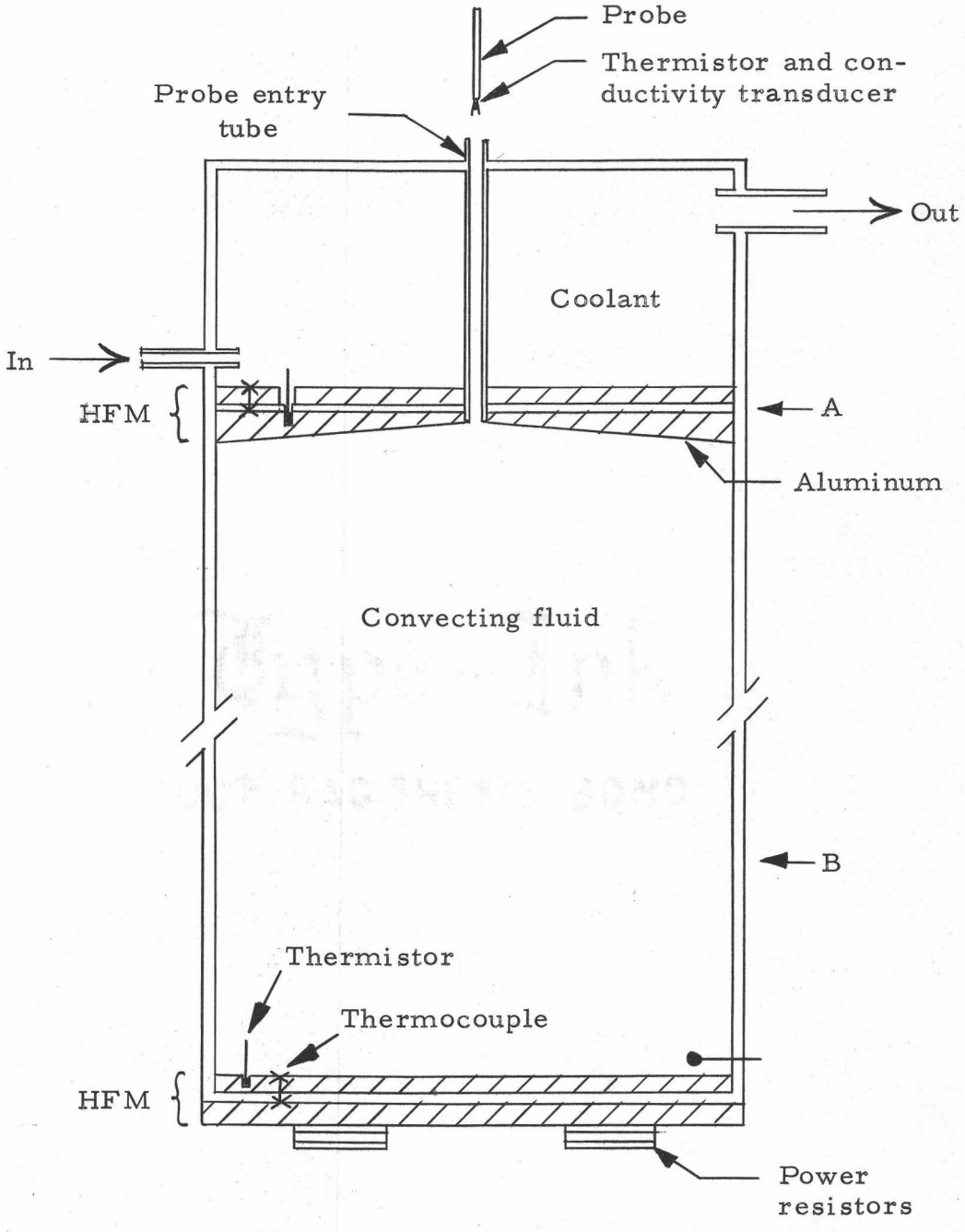

Figure 7. Simplified cross-sectional sketch of convection tank (approximately 1/4 scale). The taper (exaggerated) in one aluminum plate allows the tank to fill properly. Heat flux meter is abbreviated HFM.

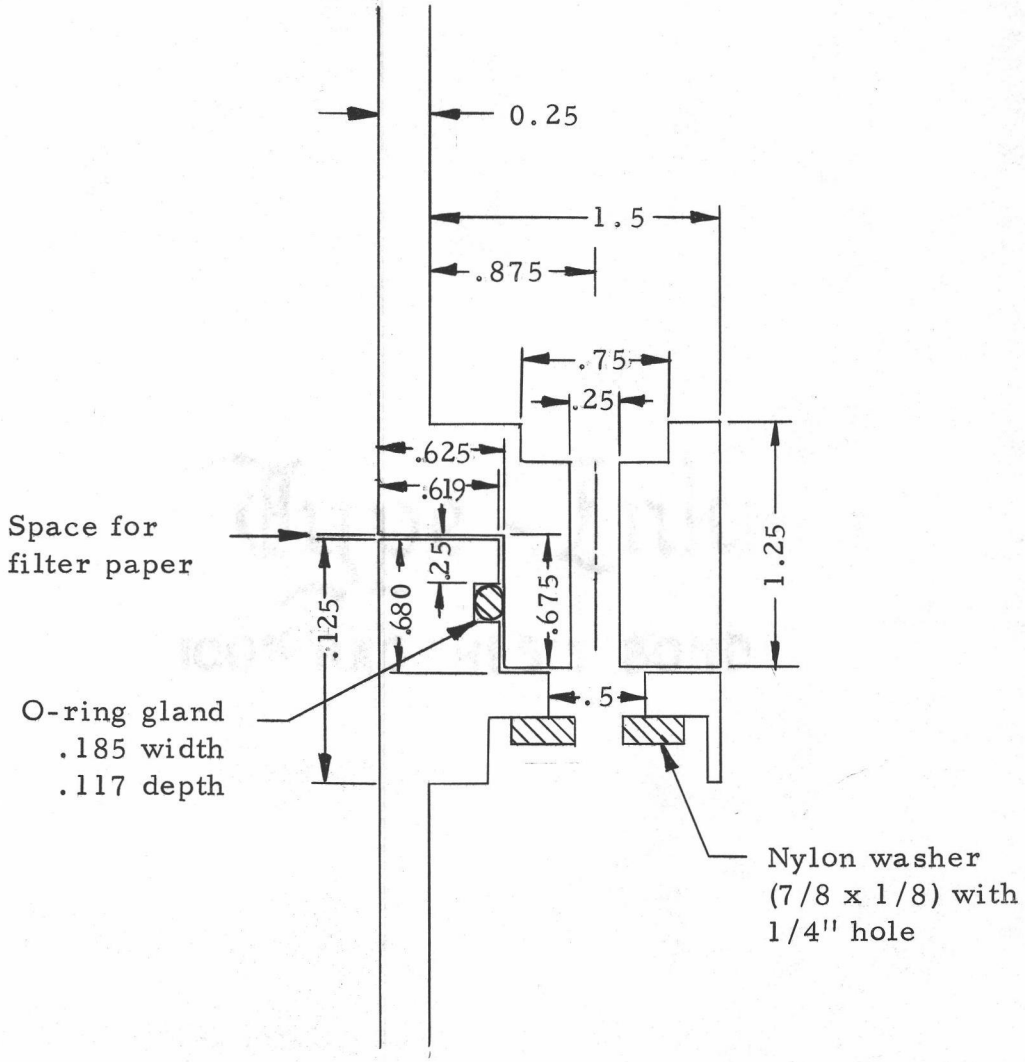

Figure 8. Drawing of the flange coupling.

insulation. The heat transfer coefficient describing side wall losses was measured to be 5×10^{-6} cal cm^{-2} sec^{-1} $°C^{-1}$. This value compares well with the insulating quality obtained by Miller (1968) who used a vacuated annulus as an insulator. By recording the temperature in the laboratory (generally between 20.5 and 22.5 °C), the thermal losses through the side walls could be computed. These losses were minimized by constraining the mean temperature of the convecting fluid to be near 21°C. Maximum losses were about 10% the amount of the heat convected vertically by the fluid. The insulated tank sits on a plywood base supported by three levelling bolts.

Heat is provided by dissipating current from regulated 60 cps 115 vac in 10 precision power resistors radially mounted flush to the underside of the lower heat flux meter. The voltage to the resistors is controlled by an auto-transformer and measured to ± 1% on an oscilloscope. It is calculated that less than 0.1% of the heat goes up the walls of the tank as opposed to going directly into the fluid. Heat loss out the leads to the heater is negligible.

Distilled water from a chilled thermostated temperature bath serves as coolant and enters the top section of the tank at 2.7 liters per minute through a constricted tube to enhance mixing, extracts heat from the upper plate of the heat flux meter, and returns to the bath. Water hoses to and from the bath are of 0.25 in. vacuum tubing thickly wrapped with neoprene and covered with aluminum foil. The

top section of the tank is insulated with one inch thick neoprene sheet. The temperature of the bath water is constant within ±0.03 C.

Filling the tank with fluid requires some care in the case of diffusive experiments. A foam float covered with cheese cloth is placed on the free surface of the lower, saltier layer already in the tank; a controlled flow of the lighter solution onto the float completes the fill. The upper heat flux meter with the probe entry tube attached is then put into position and the upper section of the tank is screwed into place. Additional fluid is then used to "top up" the tank. Partially degassed distilled water is used in all the experiments; sodium chloride (C. P. grade) is used as solute.

Sensors and electronics

In the most comprehensive experiments the measurables include temperature, electrical conductivity, thermocouple voltages, and sensor height above the tank bottom.

Temperature is sensed in the two aluminum plates which bound the fluid, at 0.5 cm from the bottom plate, and at various heights in the fluid by VECO glass-encased bead thermistors of 5000 ohm nominal resistance and 0.060 in. diameter. To take a reading, a thermistor is switched into a bridge circuit and the out-of-balance voltage is amplified and nulled. Each thermistor was calibrated in this circuit against a crystal thermometer at 1 C intervals over its

expected working range. The precision of the temperature measurements is ± 0.005 C.

For experiments prior to No. 19 a combined thermistor-conductivity probe was used to profile the temperature and conductivity fields in the fluid. The conductivity transducer is discussed in detail in Appendix B. The probe had an effective sampling length of about 3 mm and a sampling volume of less than 0.04 ml.

In experiments subsequent to No. 18, salinity was determined by withdrawing samples of fluid from the tank and measuring the electrical conductivity in specially designed cells[15] immersed in a 25 C thermostatically-controlled bath. Generally, two samples, one from each side of the diffusive interface, are withdrawn and placed in the matched cells. The sample size of a cell is 2.5 ml but about 8 ml are needed per sampling. The additional fluid is used for rinsing the sampling tube, syringe, and cell. All fluid is returned to the tank by slow injection at the appropriate height. Transport of heat and salt caused by mechanical mixing due to the sampling procedure can be safely neglected.

---

[15] The cells were made from acrylic stock and are cylindrical (0.25 in inside diameter; 3.0 in long) with platinized platinum electrodes at both ends. The measured cell constants are 23.922 ± 0.006 and 24.153 ± 0.002. Measurements were made at a frequency of 10 KHz.

Thermocouples are used in conjunction with high thermal impedances (devices which we call heat flux meters, hfm) to measure the heat flux into the bottom and out the top of the convecting fluid. A pair of junctions of 0.005 in copper-constantan wire are firmly attached to each meter so that a junction is on either side of the acrylic spacer plate (see Fig. 7). The thermocouple output voltage is measured using a microvolt potentiometer. The voltage, along with the mean temperature of the thermocouple pair, is converted to a temperature difference, ΔT. Then, ideally, the heat flux through the meter is given by $k_a \Delta T/d_a$ where k_a is the thermal conductivity of the acrylic spacer and d_a is its thickness. Calibrations[16] yielded an average value for k_a of 4.12×10^{-4} cal (cm °C sec)$^{-1}$ for the top and 4.43×10^{-4} cal (cm °C sec)$^{-1}$ for the bottom. A good value for k_a is 4.10×10^{-4} (Pears, Engelke, and Thornburgh, 1964). Hence, the hfms work as expected.

The height of the profiling transducer was measured with a meter stick; the height was known to ± 0.5 mm.

---

[16] The calibration of the top hfm is easily done by cooling a warmer-than-room-temperature tank of water and recording the mean temperature. When the mean temperature is the same as room temperature, all heat fluxes except that out the top can be assumed to be zero. A large heating rate is used to assure a well-mixed tank.

Data analysis

An experiment might take from three days to two weeks to run down, i.e., for the interface to break down and for the fluid to become well mixed, depending on the heat flux and the initial salt difference. By a "run" we will mean that the measurements discussed in the previous section are taken. The number of runs in an experiment varied from 8 to about 25. As the experiment proceeds it is essential to analyze the data as a guide to the spacing of future measurements. The analysis takes into account interface movement, heat losses, and variation of fluid properties with temperature and salinity. Calculation of interfacial fluxes is based on equations expressing the conservation of salt and the balance of heat.

It should be noted that unidirectional, vertical migration of the interface is present in all experiments. Its effects in the calculations are easily seen by values of transports which are much larger than expected. For example, suppose the lower layer is increasing in thickness at the expense of the upper, i.e., the interface is moving upwards. A certain amount of cold, fresher water is incorporated and mixed into the lower layer by some means. If the depth of the interface were not measured directly, the change of temperature and salinity in the layers would lead one to falsely ascribe large values to the diffusive transports, H and Fs. We compensate for this by

subtracting the amounts $\rho c_p \overline{T}_h \Delta h/\Delta t$ and $\overline{S}_h \Delta h/\Delta t$ from the calculated fluxes where $\overline{T}_h$ and $\overline{S}_h$ are mean values of temperature and salt concentration (gms/cm^3) evaluated at the interface, Δh is the change in height of the interface between runs, Δt (sec).

Often, at high $R\rho$, the movement of the interface is small enough for a sufficient number of runs to allow a good estimate of $\frac{dS}{dt}$ in each layer. In such cases the salt flux is evaluated by using finite difference forms of

$$F_s^{\,u}(t) = (H-d)\frac{dS^u}{dt}$$

and

$$F_s^{\,l}(t) = d\frac{dS^l}{dt}$$

where the superscripts refer to the upper and lower layers, d is the height of the center of the interface, and H is the fluid depth.

When using the combined temperature-conductivity probe, many number pairs were generated during a run. For computational convenience, the calibration curve for the thermistor used in the probe was fit exactly with a numerical spline; the conductivity and temperature were then converted to salinity by using an approximate relation between the specific conductivities of seawater and sodium chloride solution for a given salinity and then by solving numerically a transcendental formula due to Accerboni and Mossetti (1967). The discrete water samples were analyzed at 25.00 C to take advantage of the data of Chiu and Fuoss (1968).

The properties α and β were obtained from the formulae developed by Fisher, Williams, and Dial (1970); values of c_p, ρ, k_T and ν can be calculated from computer programs and formulae developed by Korosi and Fabuss and Korosi (1968).

Diffusive convection experiments

Summary

A total of 21 experiments (Numbers 4 to 24) were conducted to study the diffusive interface. Those which receive some analysis are listed and described briefly in Table IV. A descriptive summary follows. Experiments 4 and 5 were attempts at achieving steady state salt fluxes with filter-paper boundaries (see Appendix D). After replacing the boundaries with thin cellulose acetate, Exps. 6-9 were conducted. Experiments 10-18 were designed to be similar to those of Turner (1965) in an attempt to reproduce his results. The upper boundary for these experiments is a thick styrofoam lid. Experiments 19-24 use the massive side insulation previously described to allow attainment of low, steady heat fluxes. Experiments 21 and 22 were set up initially with four layers. The central interface was thus decoupled from the metal boundaries; also, the Rayleigh number was decreased because of the smaller layer depths. The Rayleigh numbers, based on the distance between layer centers,

Table IV. Summary of the diffusive experiments.

Exp. No.	Symbol	$H \times 10^3$ cal/cm^{2}sec	$Fs \times 10^7$ gm/cm^{2}sec	Constant regime Rf	Range of ΔS (‰)	$\overline{T}$ (°C)
4	◭	1.07	.62	0.155±.005	10	25
7	◑	1.38-2.15	1.30-2.49	.25 ± .07	0.3-4.7	≈ 14
9	○	3.76-5.65	1.95-4.22	.18 ± .05	0.7-7.8	≈ 15
10	✳	16.0	25	.27 ± .14	8.2-11.0	≈ 35
12	◐	14.8-18.9	12.2-24.2	.26 ± .12	6.3-13.0	≈ 35
15	+	39.2-44.1	39.6	.21 ± .09	28-61	≈ 30
18	×	1.73-2.89	----	----	15-19	≈ 35
19	◇	8.27-9.15	7.2	.22 ± .06	7.5-14	25
20	□	8.81-17.2	3-20	.16 (min)	.8-30	20
22	▽	8.5-10.0	not measured	not measured	8-20	22
23	△	.54-.77	.42	0.24 ± .01	≈0-1.5	20.5
24	◨	.08-.1	.153	0.42 ± .05	≈0- .9	20.5

ranged from 7×10^7 at $R\rho = 3.1$ for Exp. 24 to 2.2×10^{10} at $R\rho = 3.1$ for Exp. 15.

Referring to Table IV it can be seen that a range of heat flux is given for many experiments. This reflects the non-steady nature of the experiments; as an experiment proceeds the impedance to heat flow is decreased and the interfacial heat flux will increase. The extent to which this occurs depends of course on the range of the impedance factor ($\sim R\rho$) as can be seen, for example, in Exp. 20. Notice also that for some experiments (e.g., 10 and 12) $\overline{T}$ is quite high. Necessarily, the temperature of the heater plate was well over 55 C and fear of melting the acrylic tank bottom forced the premature termination of these experiments. To avoid this problem, the working fluid was cooled to a low temperature before the start of a transient (foam lid) experiment.

V. THE THERMAL BURST PHENOMENON

Thermal convection experiments

A number of high Rayleigh number, steady state experiments were conducted using distilled water as the working fluid. Their purpose was threefold: (1) to check the operation of the heat flux meters, (2) to determine the transfer law (Nu vs. R correlation) in an apparatus with such a small aspect ratio, and (3) investigate the properties of the thermal boundary layers on the two bounding solid surfaces with a comparison with the diffusive interface in mind.

The experiments are arranged in order of heat flux in Table V. Typical values of α, κ, ν, and k_T are 2.3×10^{-4}, 1.4×10^{-3}, 0.95×10^{-2}, and 1.4×10^{-3} (cgs) respectively. Once the heat flux is chosen, the temperature of the upper plate determines the mean temperature of the convecting water. The temperature of the circulating water was regulated so the mean temperature was at average room temperature.

An average experiment might take several days to reach a steady state heat flux. Of course, the higher the heating rate, the faster the system can "tune" itself. A steady state can be identified by constant readings of voltage of the heat flux meters and by lack of any change in the plate temperature.

The results are most conveniently displayed on a plot of Nu· R

Table V. Summary of the thermal convection experiments.

Exp. No.	$H \times 10^3$ (cal/cm^{2}sec)	Mean T (°C)	ΔT (°C)	Pr	Nu	$Rx10^{-9}$
1	0.223	22.43	0.22	6.65	45.4	1.02
2	0.89	21.89	0.54	6.74	71.1	2.41
3	3.56	20.75	1.44	6.94	109.	5.98
4	3.56	21.02	1.45	6.89	110.	6.13
4a	3.56	20.59	1.51±.14	6.97	105.	6.20
5	6.50	28.64	1.86	5.60	129.	12.5
6	8.02	21.85	2.70	6.75	137.	12.0
8	14.3	23.28	4.05	6.50	155.	19.8
9	14.3	21.33	4.09	6.84	147.	17.6
10a	18.0	21.13	4.93	6.87	145.	21.0
11a	18.0	22.26	4.96	6.68	152.	22.7
12	20.1	22.24	5.64±.58	6.68	140±15.	25.8±2.6

vs. R which is shown in Fig. 9. The straight line is a best fit by eye while constraining the slope to be 4/3. From the plot one finds that

$$Nu = 0.077 \pm 0.002\, R^{0.33 \pm .01} \tag{40}$$

which is in good agreement with a result of Broughton (1972) who found that

$$Nu = 0.072\, R^{0.33} \tag{41}$$

using distilled water in a large tank of aspect ratio 0.9 over a range in R of 12 to 246×10^9.

The proportionality factors in Eqs. (40) and (41) are not vastly different from c = 0.085 which was chosen on the basis of experimental work at low R. The one-third power law seems to have wide validity but keep in mind that we have forced this relationship and over only 1.5 decades of Rayleigh number at that.

What can be said about the nature of the convection in this type of high Rayleigh number experiment? It occurs as thermal bursts. A typical temperature record from a thermistor suspended[17] above

---

[17] Burst records shown or analyzed in this section were made using a thermistor held at only a slight angle to vertical. This causes a disturbance which is only slightly noticeable in the records. For measurements in the thermal boundary layer near the plate and measurements just above, below, and in the diffusive interface, a 90 degree bend in the glass support tubing held the thermistor horizontally in the fluid.

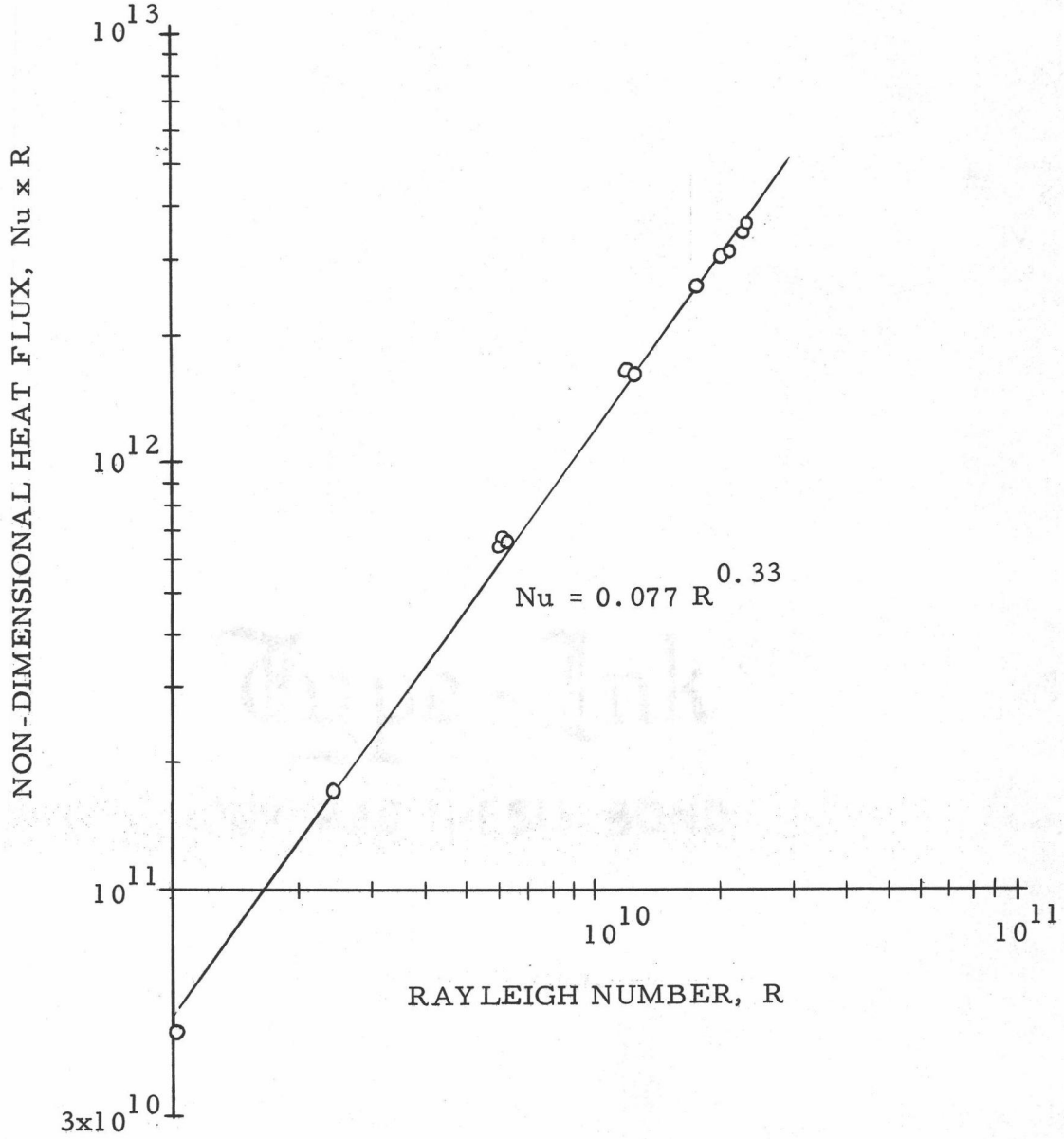

Figure 9. Non-dimensional heat flux vs. Rayleigh number based on the 12 thermal experiments. The line drawn is a best fit by eye while constraining the slope to be 4/3.

the heated plate is shown in Fig. 10. The sudden increases in temperature are clearly evident in the record. These thermals or bursts can be interpreted as small blobs of hot fluid suddenly released or escaping from a thermal boundary layer very close to the plate. The thermals typically grow to only a few times their original diameter. Their ascent is retarded by a drag which arises because of fluid external to the thermal which must be accelerated from rest and either incorporated or entrained into the thermal or displaced around it (Turner, 1973).

The general appearance of the temperature record is quite similar to that observed by other investigators in different physical contexts. For example, our burst records are similar to plots of $(w')^2$ vs. time in a turbulent estuary flow (see Seitz, 1973). There are also obvious similarities to the "burst phenomenon" encountered in turbulent flows at high Reynolds number (see Mollo-Christensen, 1971).

Our records can be compared directly with temperature traces reported by Elder (1967) for thermal turbulence ($R = 1.4 \times 10^8$) in water (depth of 5 cm). His traces from near the hot or cold boundaries show quiescent periods of about 10 sec during which the temperature is close to the mean temperature of the fluid and bursts of hot or cold fluid of 1 sec duration. Near the midplane, $z = 3$ cm, nearly equal numbers of hot and cold bursts are seen but as a

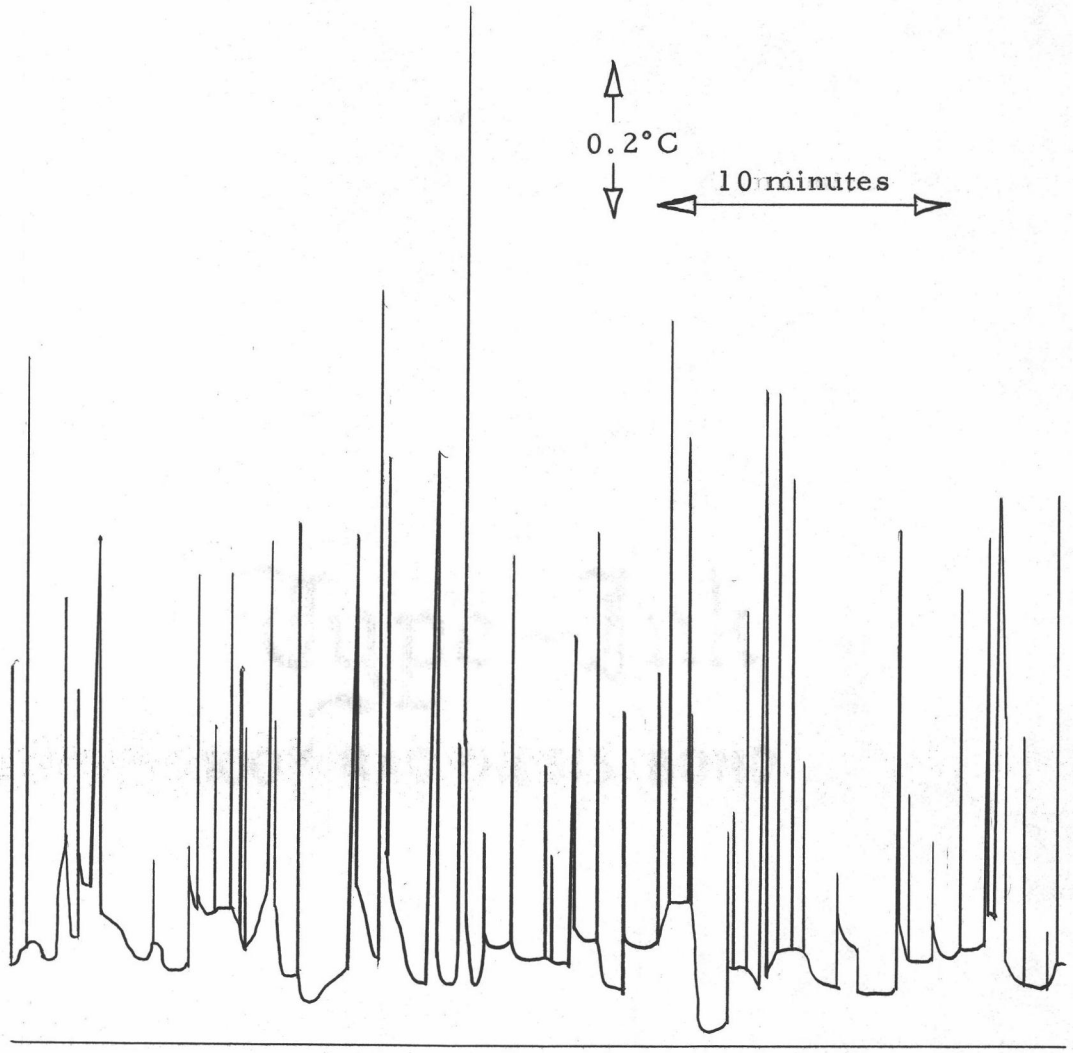

Figure 10. A typical temperature record showing thermal bursts. The thermistor is 0.75 cm from the bottom plate. (From Exp. 12)

boundary is approached, the frequency and amplitude of bursts increase. These observations will be seen to agree with our results. He found that the strongest bursts could completely cross the turbulent interior. It is possible that this occurs in our experiments also.

Very near the plate, there exists a region over which most of the temperature drop occurs. Here, molecular effects can be important and this region or its sublayers are known as viscous and conductive sublayers. We will simply call this region the thermal boundary layer. Ideally, as the plate is approached, temperature fluctuations become small to the extent that $\lim_{z \to 0} T'(z) = 0$. As z increases, $T'(z)$ increases to some maximum value; this marks the edge of the thermal boundary layer. A temperature record from near this edge is shown in Fig. 11. This record has a regular, oscillatory nature not seen in Fig. 10 and has symmetric variation about a mean. Elder (1967) shows traces at z = 0.02, 0.05, 0.1, and 0.2 cm. He reports: "The appearance is now dominated by the hot plumes and there are no longer noticeable periods of quiescence. The inmost trace z = 0.02 is well within the sublayer. Here the fluctuations are more symmetrical and no longer suggest that substantial portions of this fluid are moving out of the layer."

To fully understand the nature of the heat transport from the bottom plate we should like to know the following:

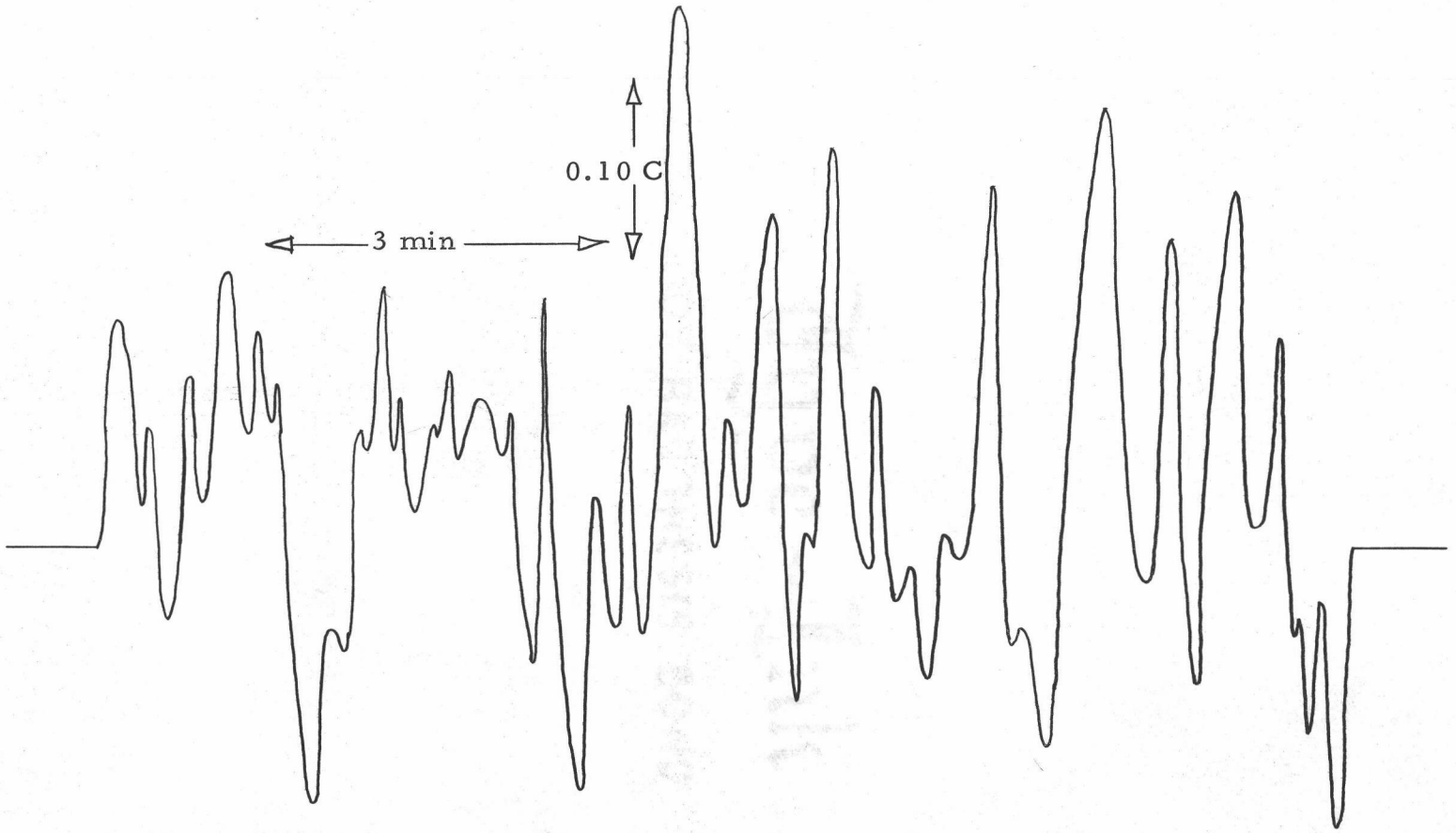

Figure 11. Temperature record from the edge of the thermal boundary layer. The thermistor bead is within 1 mm of the bottom plate. (From diffusive experiment 18)

(i) the thickness of the thermal boundary layer and the dynamics therein including the criterion for release of the buoyant elements,

(ii) the initial mass and buoyancy of a thermal,

(iii) the spacing of thermals in time and space and their magnitude at different heights, i.e., we want probability density functions for the temperature of the burst (T_b), the period between bursts (τ_b), and for the spatial distribution[18],

(iv) the interaction of the burst with the environment (especially if it is solute-stabilized), and

(v) the extent of dependence upon the heat capacity and composition of the bottom plate.

The above points are a major research effort in themselves. Nevertheless, they have a bearing on the diffusive experiments and so some discussion is called for. First, the thermal layer attached to the rigid boundary (of thickness δ_r) is somewhat analogous to the free diffusive boundary layer (thickness δ_f). An understanding of one should complement study of the other.

When the heat flux is large (say 10^{-1} cal cm^{-2} sec^{-1}) δ_r is of the order of δ_f: both are 0 (1-5 mm). Estimates of the thickness δ_r can be obtained in at least two ways. First, assume that in the

---

[18] Some kind of horizontal sensor array is needed here.

thermal boundary layer $\left|\overline{w'T'}\right| << \left|\partial_z \overline{T}\right|$ (see Eq. (6)), then by using the definition of Nu, $-\partial_z \overline{T} = Nu \cdot \Delta T/L$ and

$$\delta_r \sim \frac{1}{2}\frac{L}{Nu} \quad . \tag{42}$$

Second, assuming L to be unimportant in determining δ_r we have (Thompson, 1962)

$$\delta_r \alpha R^{-1/4} L^{3/4} \quad . \tag{43}$$

Assuming the constant of proportionality in Eq. (43) to be 0 (1) and using typical values from Table V, δ_r is about 0.25 cm for these estimates. This agrees with our observations from profiling with a thermistor (diameter 0.15 cm) in the thermal experiments. Notice that Eq. (42) predicts that δ_r becomes thinner as the heat flux increases. Although this could not be validated in the thermal experiments, its analogy will be proven in the diffusive experiments. Sparrow, Husar, and Goldstein (1970) find a conduction layer thickness of 0.1 to 0.2 cm for higher values of heat flux ($6 < \Delta T_{1/2} < 20$ C).

We remain mute on point (ii) but will discuss points (iii) and (iv) in the remainder of this section. Point (v) is an important one. Ideally, one does not want the boundary itself to play a role in the dynamics. Therefore, the plate surface should be smooth (no "thermal roughness elements") and uniform and the plate should have a large thermal capacity which would tend to keep the surface at constant temperature. We are not sure how close our nickel-plated

aluminum plates come to being ideal[19].

We have already seen that it is above the thermal boundary layer that the temperature records begin to be dominated by bursts. This is the beginning of a transition region in which the thermal bursts stir the fluid. A similar stirring must be done above the diffusive interface but in that case the region analogous to the thermal boundary layer is free. We will look in moderate detail at changes in burst records with both height above the bottom and with heat flux.

Plots of the observed number of bursts in a standard length of record against normalized burst magnitude are shown in Fig. 12 for Exp. 12 at various heights. The shortest record length used happened to be 43.5 minutes. This is taken to be a standard record length; longer records are analyzed and then the results normalized to this value. In this type of plot the value $T_b/\Delta T = 0.5$ should be considered a rigid upper bound since it is usual for ΔT to be divided symmetrically between the boundaries.

---

[19] The ideal plate would have no temperature variation but a record of a plate temperature for Exp. 12 ($\Delta T = 5.6$ C) shows a peak-to-peak variation of 0.44 C with a typical period of about 6 min. (This is in comparison to a period of 30 sec or less and an average temperature fluctuation of 0.61 C at 0.25 cm from the plate.) Since the plate thermistors are merely snugly fit into a drilled hole in the plates there is a good chance that much of the variation is due to water temperature changes which are lagged by the thermistor's glass encapsulation.

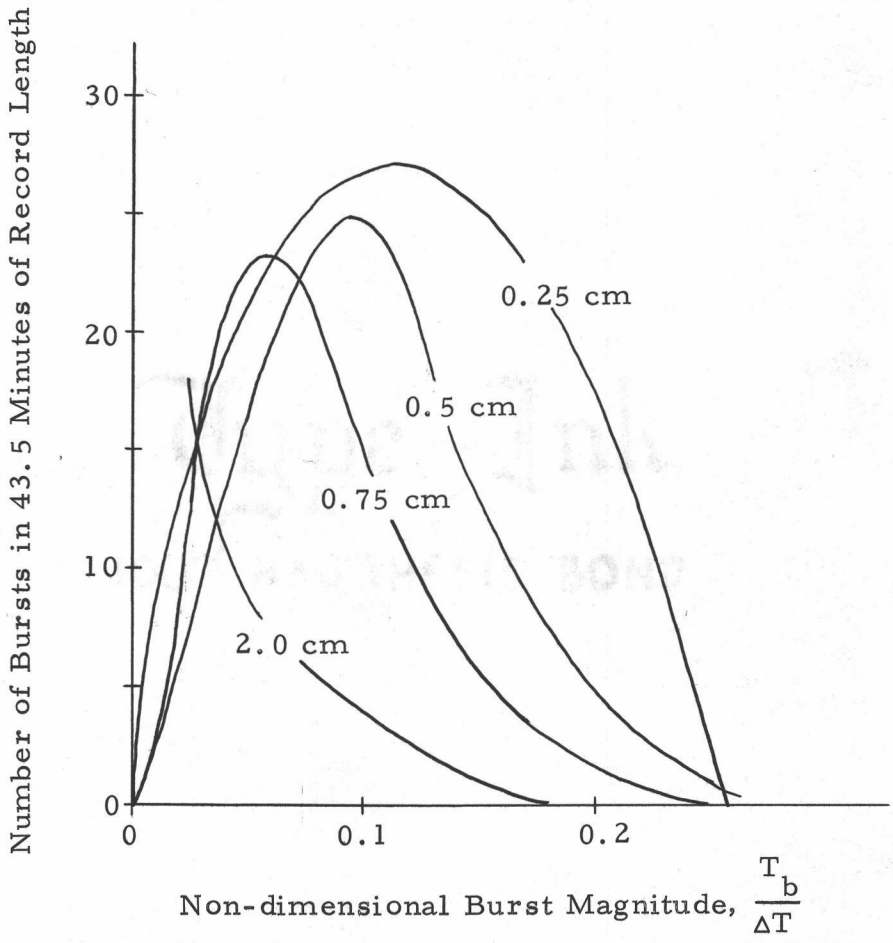

Figure 12. Number of bursts vs. burst magnitude at various distances from the bottom plate. (From Exp. 12)

The analyzed records for Exp. 12 show the following:

Height from the bottom (cm)	Number of observed bursts of all magnitudes in the standard record length of 43.5 min.
0.25	143
0.50	88
0.75	70
1.00	63
2.00	59

Obviously, all the thermals generated at the edge of the thermal boundary layer and recorded at $z = 0.25$ cm are not of sufficient magnitude to rise to $z = 0.5$ cm and higher.

Figure 12 shows that the total production of temperature fluctuations is greatest for $z \leq 0.25$ cm and falls off as z increases. Note also that the peak of the curve moves to the left as z increases. This movement should be expected, for in the case $z = \infty$ we expect no fluctuations of any magnitude and so all the area under the curve should be concentrated at $T_b/\Delta T = 0$. The curves, if normalized, would be probability density functions for T_b. Elder (1967) reports several probability density functions of temperature for different heights for an experiment using oil (fluid depth, 10 cm) at $R = 2.4 \times 10^8$. He observes nearly Gaussian densities within the sublayer and interior. Where the transport of heat is due to buoyant elements, the densities show "considerable skewness". This agrees qualitatively with our results.

Various theories exist which describe mean temperature

profiles in transition layers. One theory based on similarity predicts

$$\overline{T'}(z) \propto z^{-1/3}$$

We have computed $\overline{T}_b(z)$; an excellent fit for the range $0.25 \leqq z \leqq 2.0$ cm is

$$\overline{T}_b(z) \propto z^{-0.37}$$

Figure 13 reproduces the curve for $z = 0.5$ cm from Fig. 12 and compares it with the results from three experiments of lower heat flux. Experiments 3 and 4 can be seen from Table V to be almost equivalent and yet the curves in Fig. 13 do not look very much alike. In fact, there seems to be much more activity in Exp. 3. This probably means that the record lengths (2 to 3 hours or about 150 bursts) are not long enough. As a result the peaks may not have statistical significance. Notice however, that the curves for Exps. 3, 4, and 5 are bimodal and that as R increases, there is a smaller percentage of large magnitude bursts and that perhaps the bimodal character collapses.

If it is true that for a given height $T_b/\Delta T$ tends to be smaller as the heat flux increases then τ_b, the period between bursts, should decrease with increasing heat flux. That this is true can be seen from the tabulation below (see also Sparrow et al., 1970):

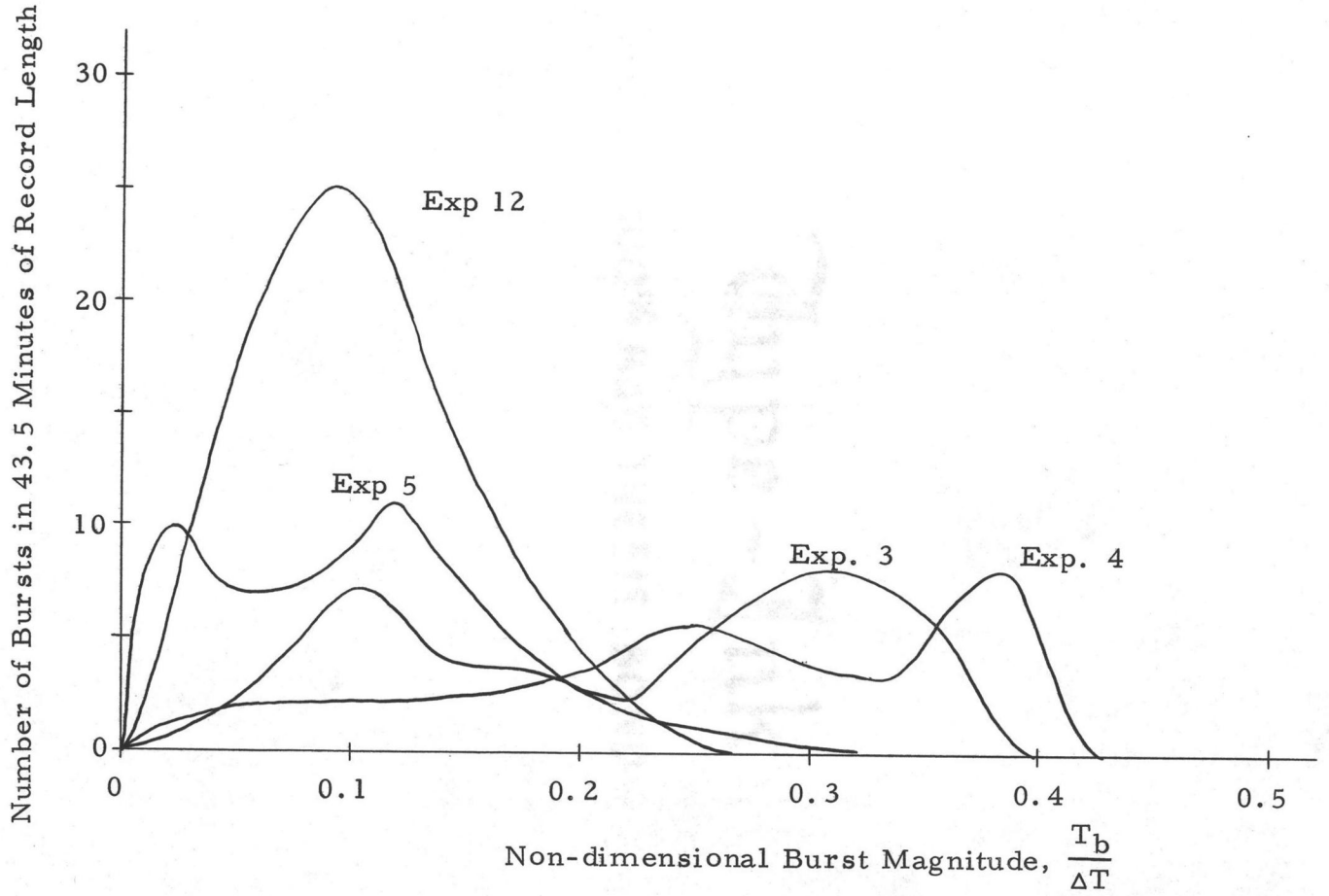

Figure 13. Number of bursts vs. burst magnitude at 0.25 cm from the bottom plate. (From Exps. 3, 4, 5, and 12)

Exp.	z (cm)	T_b^p (°C)	$T_b^p/\Delta T$	Period
2	0.5	0.16	.29	1 to 10 min
4	0.5	0.50	.33	15 sec to 8 min
5	0.5	0.55	.34	12 sec to 4 min
7	0.3	1.0	.25	10 sec to 2 min
12	0.5	1.42	.25	1 sec to 2 min

In the above, T_b^p is the peak or largest burst in a particular record. Notice that there is no significant variation in $T_b^p/\Delta T$ whereas there seemed to be a variation in $T_b/\Delta T$ with heat flux. More data will have to be examined before ascribing any significance to this. Clearly, τ_b decreases as the heat flux increases. These values were merely picked off temperature records visually and reported to give an indication of the variation in ranges encountered. A closer examination of the variation of τ_b is given in Fig. 14.

An estimation of a lower limit for $\bar{\tau}_b$ can be obtained from Lindberg (1970) because we can always expect $\bar{\tau}_b$ to be greater than

$$t^* = \frac{\pi L^2}{16\kappa} \left(\frac{2200}{R}\right)^{2/3},$$

where t^* is a characteristic time between bursts in the thermal boundary layer. For Exp. 12, this formula yields the value $t^* = 0.18$ sec. The lowest observed value of $\bar{\tau}_b$ is about 1 sec at $z = 0.25$ cm, above the boundary layer. The calculated t^* is seen to be a reasonable value.

Would it be possible to determine the heat flux in a system

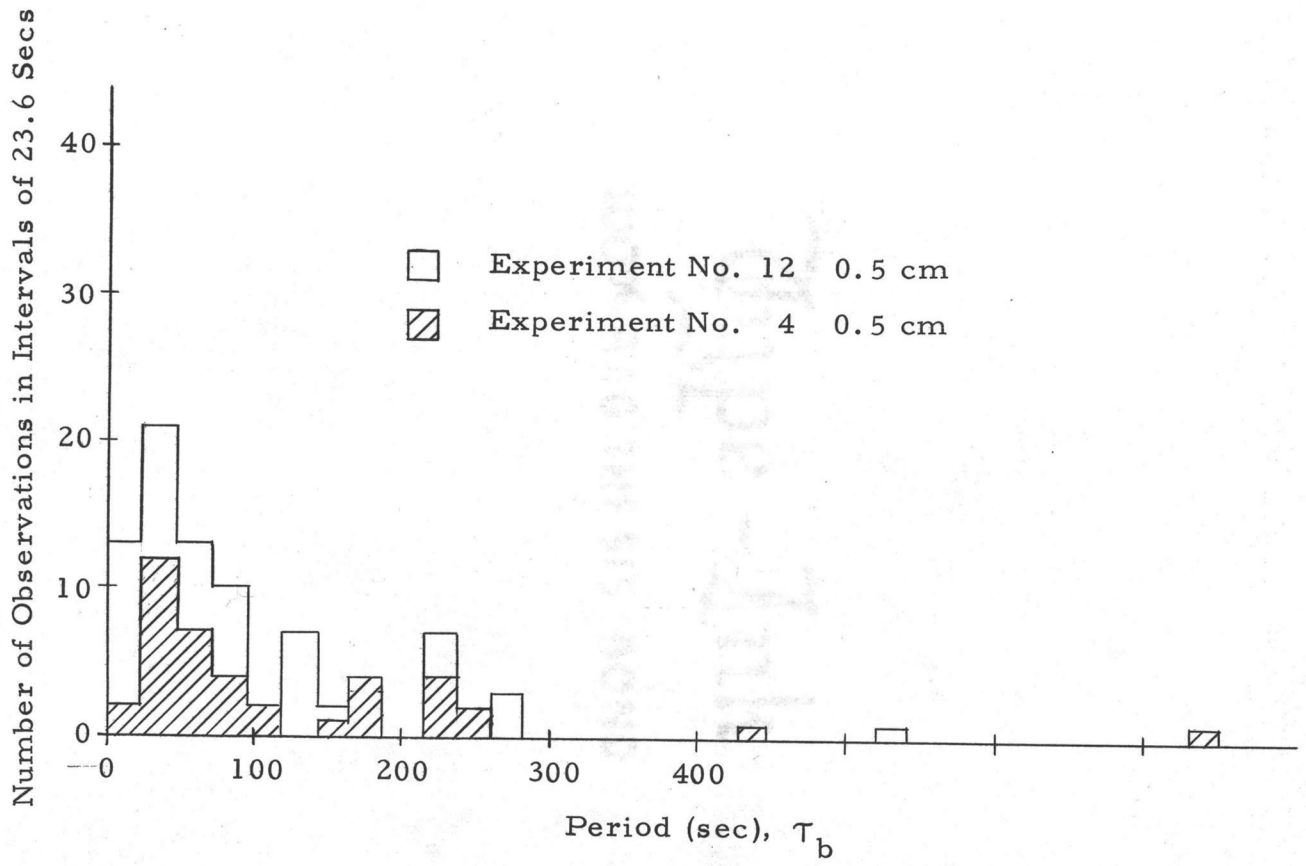

Figure 14. Histograms of number of bursts vs. burst period. The bursts included as observations for this plot are those of magnitude greater than the median value. The record lengths examined are only roughly equal: 105 min for Exp. 12; 132 min for Exp. 4.

knowing only T(t) at a single coordinate value? If the record is long enough the answer is probably yes, independent of the value of z, for it should be possible to determine the statistics with the required confidence; for z near a boundary or near a zone of temperature variance production, perhaps a shorter record will suffice. Our burst records are of the latter type. Can H be predicted from T_b and τ_b based on our limited analyses, without knowledge of the burst mass or planform? A rough formulation might be

$$H = a\rho c_p \tilde{T}_b z \frac{1}{\tilde{\tau}_b}$$

where $\tilde{T}_b$ and $\tilde{\tau}_b$ are some kind of representative values (means for example), a is a dimensionless proportionality factor, and z is the observation height. Choosing z = 0.5 cm we calculate a = 6.1 and a = 11.3 for Exps. 3 and 12 respectively. These values are actually fairly close considering the quality of treatment of the raw data and more importantly, the factor of 6 difference in heat flux between Exps. 3 and 12. For the time being, let us adopt

$$H = 9\ \tilde{T}_b z \frac{1}{\tilde{\tau}_b} \tag{44}$$

as a predictive relationship for the heat flux.

Bursts continue to dominate the temperature records at 3, 4, 5 cm and higher. As the center of the tank is approached the records lose this characteristic along with the associated intermittency. At

the center, one expects effects due to both boundaries; this is manifested in the records as variation about a mean value. From some preliminary spectral analysis, one finds that while there may be spectral maxima near the plate, spectra of temperature records from near the center are flat and the auto-correlation function drops quickly to zero and fluctuates randomly within the interval ± 0.1. Such behavior is characteristic of a white noise process. Again, this result compares well with an analogous spectrum from Elder (1967).

A final question concerns the uniformity of temperature in the interior of the fluid. Means were obtained from long temperature records at heights of 5, 10, 20, 30, and 40 cm for the experiment with the best possibility of having a mean stratification, namely Exp. 12. It is concluded from these records that the mean gradient at the center of the tank is less than 0.009 C/cm. If this gradient were a permanent feature it would account for less than 5% of the observed heat flux.

Thermohaline convection experiments

Three high-Rayleigh-number, steady-state heat-flux experiments were conducted using sodium chloride solution ($\overline{S}$ = 29.70‰) as the working fluid. Their purpose was to determine if any changes could be detected in the heat transfer law and if there were a change, why it occurred.

The experiments are summarized in Table VI and the experimental points are compared with the work of the last section in Fig. 15. The values for ΔT were obtained by doubling the difference between T and one plate temperature as only one plate temperature was recorded for these three experiments. Had this been done in the thermal experiments instead of measuring ΔT directly, the results would not have changed significantly.

As can be seen by comparing Tables V and VI or by a glance at Fig. 15, the efficiency of the heat transfer is significantly increased in the thermohaline system over the thermal system. It seems odd that this should be the case and one immediately becomes suspicious of the procedure mentioned above. However, a reason can be suggested for this behavior.

The Soret effect acts to destabilize the thermal boundary layers for the mean temperatures used in the experiments. The magnitude of this effect can be calculated by using the results of Caldwell (1973).

Table VI. Summary of the thermohaline convection experiments.

Exp. No.	$H \times 10^3$ (cal/cm^{2}sec)	Mean T (°C)	ΔT (°C)	Pr	Nu	$R \times 10^{-9}$
1	3.56	22.24	1.3	7.18	115	6.82
2	9.62	21.32	2.7	7.35	152	13.5
3	14.3	21.65	3.22	7.29	185	16.4

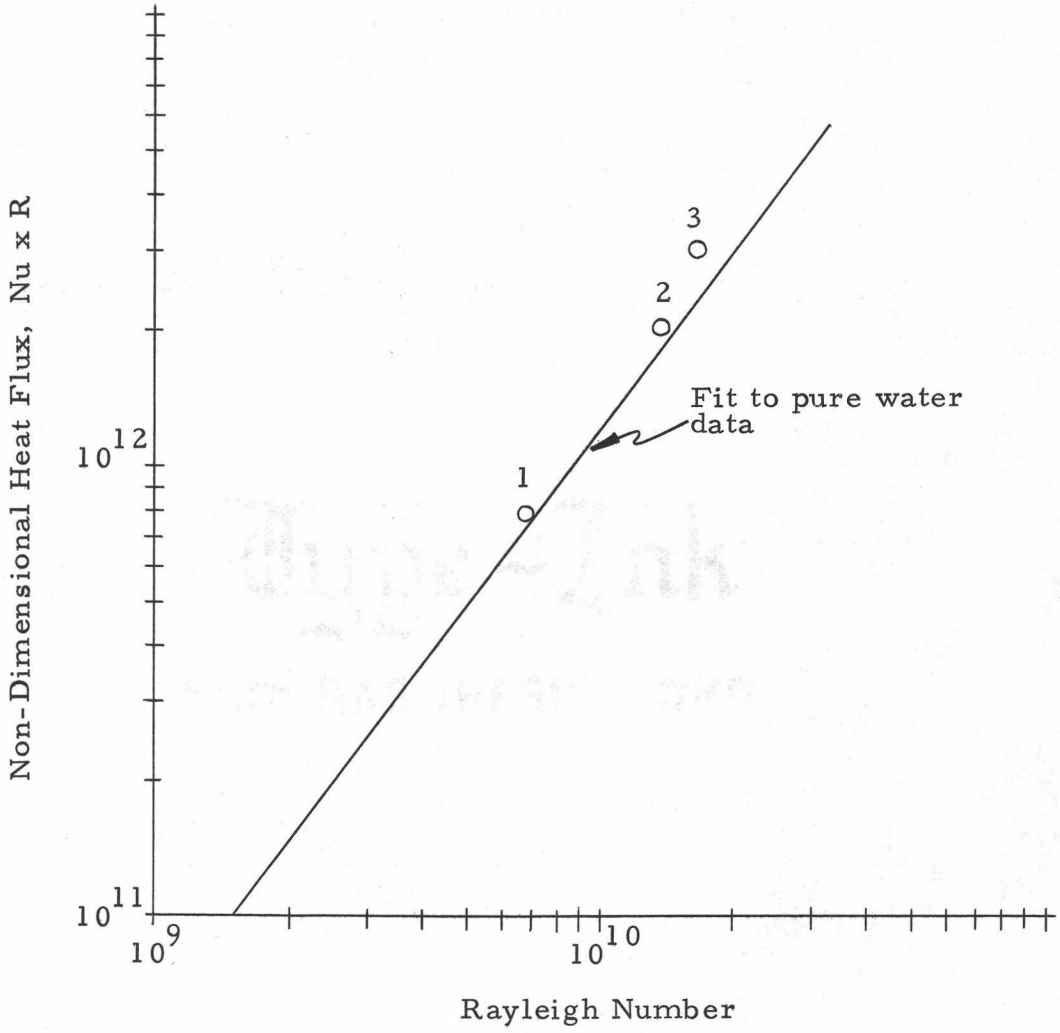

Figure 15. Experimental points for three thermohaline experiments compared with results from the thermal convection experiments on a Nu R vs. R diagram.

Using a Soret coefficient of 0.00088 C^{-1} we can calculate the salinity drop in a thermal boundary layer (ΔT = 1 C, say) to be about 0.027‰ in a destabilizing sense. This would cause an increase of about 8% in positive and negative buoyancy at the lower and upper boundary layers respectively and would explain why, for a given heat flux, the Rayleigh numbers are lower for these experiments than for the pure water results. A crude attempt to obtain samples of water from the boundary layer was made. The determined salinities were not different from $\overline{S}$.

Short temperature records were obtained at several heights for one of the thermohaline experiments. Generally, they appear quite similar to corresponding records from the thermal experiments. It was noticed though, that the record at 10 cm contained bursts of noticeably larger magnitude than the thermal counterpart. This implies a difference between the thermal and thermohaline boundary layers and supports the Soret-destabilization discussed above. No detailed analysis was made however, and the tentative conclusion that Soret effects may be active at boundaries in turbulent convection must await further experimentation.

Bursts in the diffusive experiments

In the thermal and thermohaline experiments, buoyant thermals stir the fluid and as a result the bulk of the solution is very well

mixed. The uniformity of layers in the diffusive experiments demands a stirring mechanism. Is this mechanism also the thermal burst phenomenon?

Other investigators have reported the nature of convective elements which leave an interface. Turner (1968b) reports that large eddies, produced by grids, can sweep up sheets of interfacial fluid which can then be completely or partially mixed into the layer depending upon the component diffusivity. Stern and Turner (1969, p. 500), for the case of a diffusive interface using salt and sugar solutions, report: "Vertical exchange was then observed to take place in the form of fluid sheets which formed intermittently at convergence zones on a paper-thin interface." Recently, Shirtcliffe (1973), for the same situation, says that plumes of fluid leave the interface in narrow regions. Can elements similar to the above be detected in our work?

Basically, our records of temperature at a fixed point in the tank look somewhat like the records of the previous sections, that is, a baseline value is evident, reflecting a mean layer temperature, and temperature fluctuations in one direction from the baseline exist. Figures 16 and 17 (a) show features above the upper edge of the interface. Assuming bursts to exist, Eq. (44) can be used to guess the heat flux. The number obtained is at least 100 times greater than the observed heat flux. A record from Exp. 24 (not shown) at $R\rho \approx 6$ and again from 2 cm above the edge of the interface, shows about one

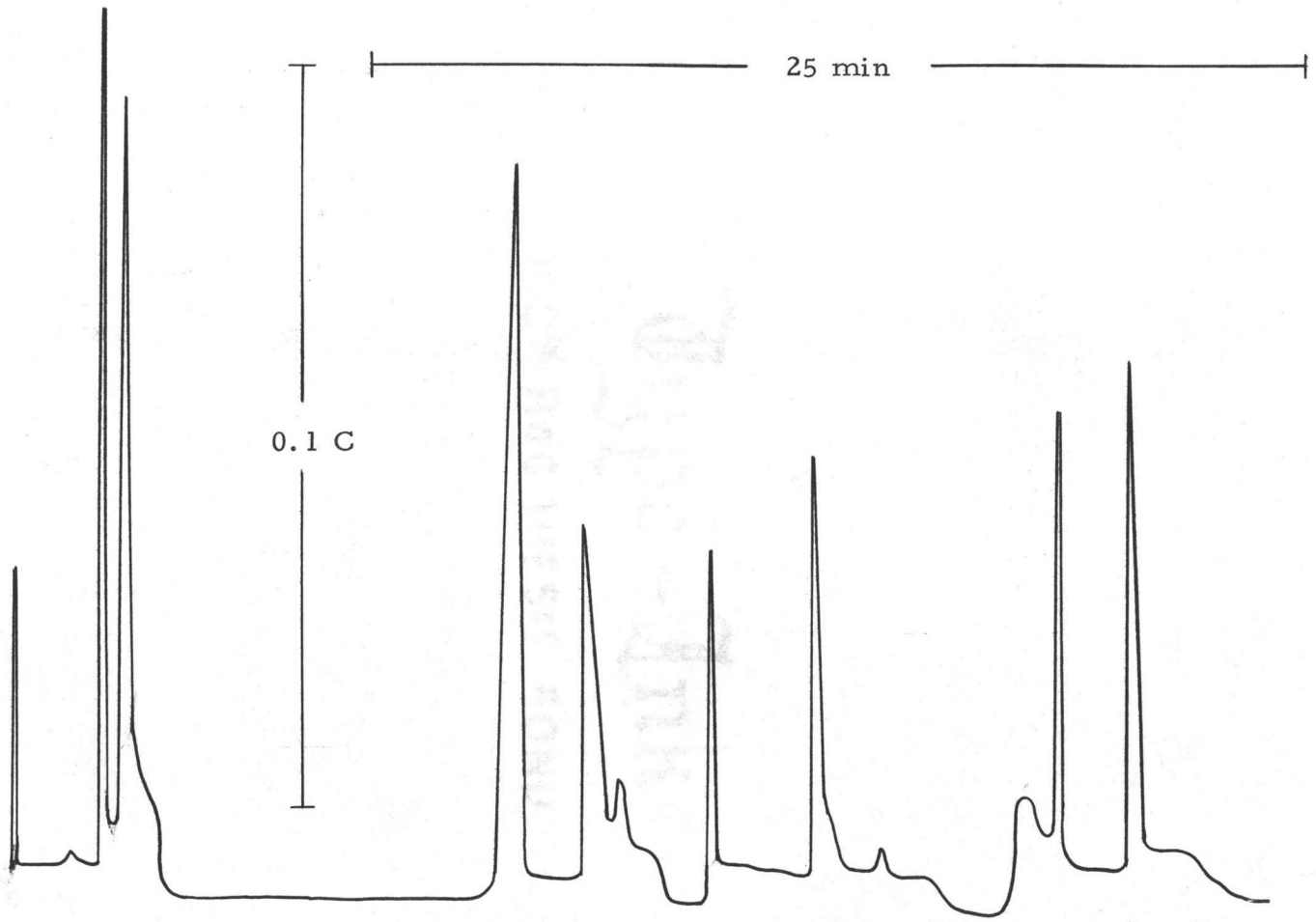

Figure 16. Temperature record 3 cm above the mean position of the center of the difusive interface. Interface motion is about 0.4 cm per day. The slope of the baseline reflects changes in the mean layer temperatures. (From Exp. 23: $R\rho = 4.1$; $\Delta T = 0.88$ C; and $d_T = 2$ cm)

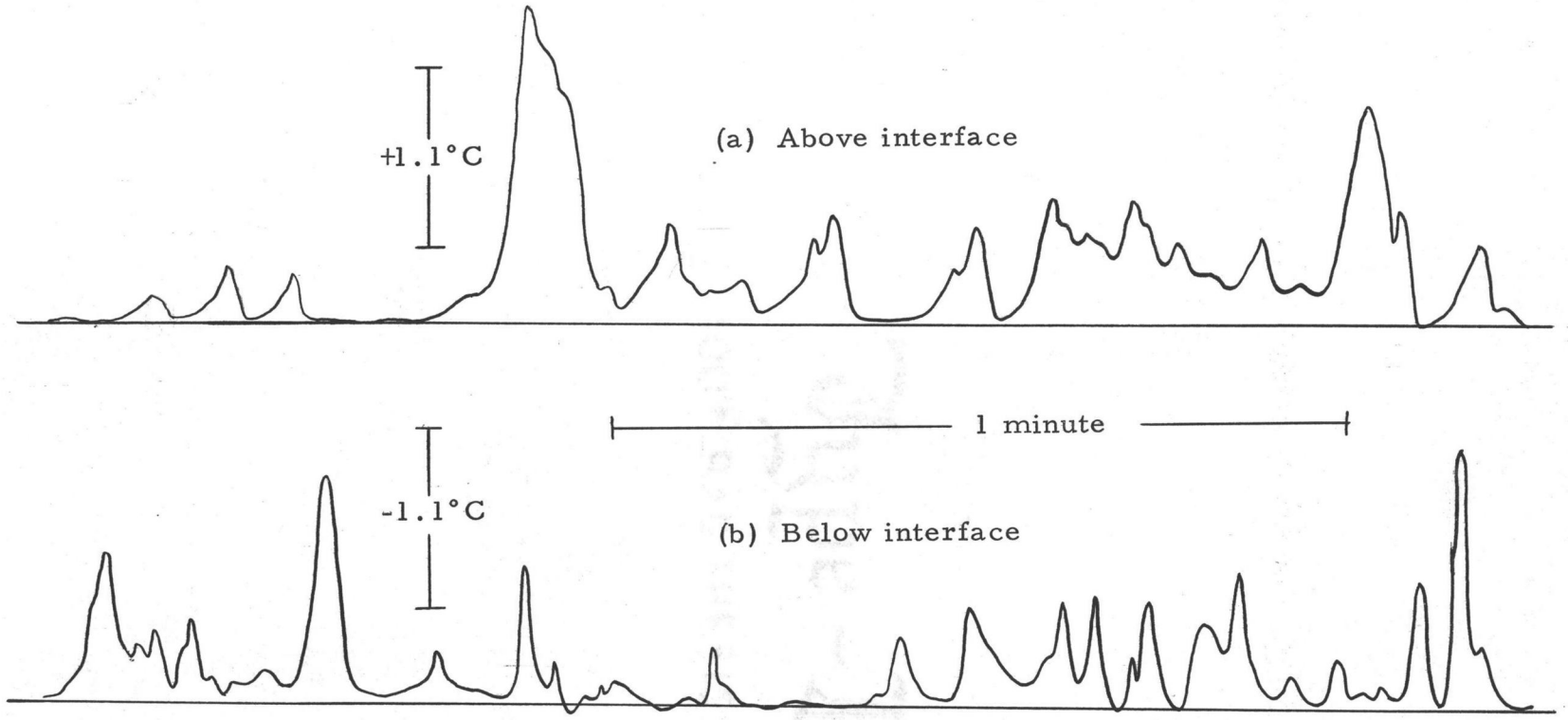

Figure 17. Temperature records at about 0.4 cm above (a) and below (b) a diffusive interface. The straight lines represent the mean temperature of the layers. The slope of these baselines reflect changes in the mean temperature of the layers. The records are not simultaneous. The buoyancy frequency of the interface at the time of these measurements is on the order of 0.33 cycles per second. (From Exp. 12: $R\rho = 2.7$; $\Delta T = 4.5$ C)

0.025 C feature every 20 minutes or so. Use of Eq. (44) would indicate a heat flux of twice the measured value. Shown in Fig. 18 is the usual plot (the upper bound on $T'/\Delta T$ is now unity) of the number of features against the magnitude of the feature for a 24 hour record of which Fig. 16 is a part. A comparison with the 2 cm curve in Fig. 12 is poor. All indications are that the observed temperature features are not all bursts which extend deep into the fluid layer as in the non-layered experiments. The feeling one gets from our work and the reports of others is that slightly buoyant elements are pulled from the interface but remain connected and quickly settle back to the interface giving rise to interfacial wave-like motions.

Figure 17 shows two short records from above and below an interface. The temperature fluctuations seem to be more intense above the interface; this is to be expected because of the positive flux of buoyancy through the interface. Notice that there is no temperature fluctuation recorded above (below) the interface of such a magnitude that it could have originated from the lower (upper) layer. This leads one to the conclusion that the temperature features originate in the transition region of the layer in which they are found.

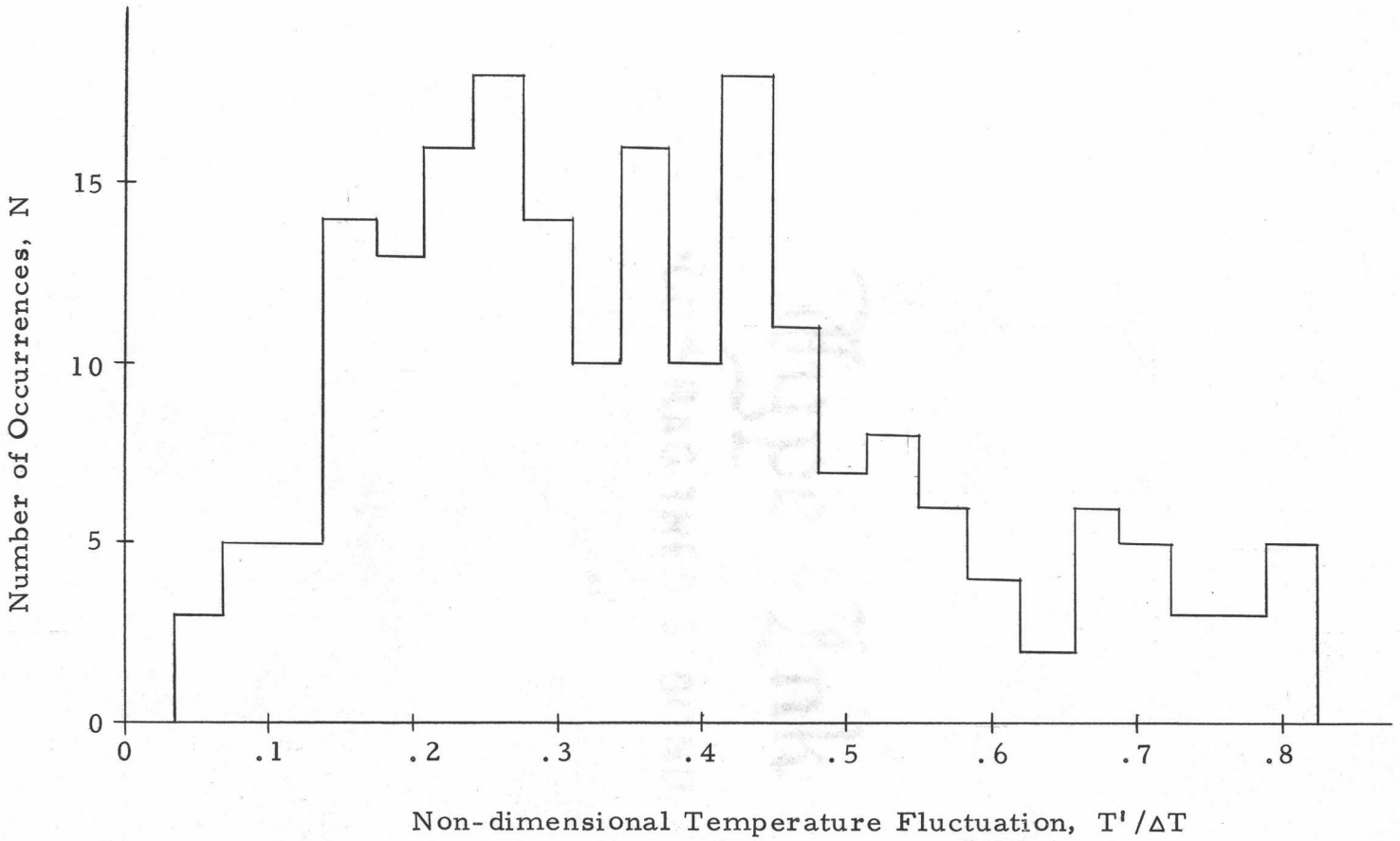

Figure 18. Histogram of number of temperature features vs. non-dimensional temperature. Length of record: 23 hours. (From Exp. 23: $\Delta T = 0.88$ C; $R\rho = 4.1$)

VI. NATURE OF DIFFUSIVE CONVECTION

Pilot experiments

A number of pilot experiments were conducted by the present author during August 1971 to gain familiarity with the diffusive mechanism and to test the suitability of solutions to some technical problems which arose in planning for more formal experiments. One experiment was performed to see if layers could form from diffusive convection by cooling a salinity gradient from above while also heating from below. The results from this particular experiment are interesting and rather new in themselves and are reported in Appendix C along with a comparison with a result of Turner (1968a) and some general observations on layered convection.

Uniformity of the layers

Generally speaking, the layers are well mixed. When profiling, no variation is found until the interface is nearly reached. At a distance of approximately 2 cm from the mean position of the top of the interface "warm spots" are sometimes encountered. These are intermittent but have a lifetime longer than the thermal bursts in non-layered experiments which leads one to speculate that they are large amplitude wavy disturbances on the interface.

Other features sometimes encountered are bumps of reverse

gradient located near the edges of the interface (see also Appendix C). These are on the order of five percent of ΔT. They remind one of small (1%) bumps found on the edges of unstable layers in the numerical model of steady thermohaline convection of Elder (1969). In the latter case however, there is a possibility that they are merely an artifact of the method of numerical solution.

Interface thickness

The thickness d_T is obtained from temperature profiles. The measurement of the temperature profile proceeded in one of two ways: (1) lowering the probe by hand in discrete steps through the interface and making a null measurement at each depth (discrete sampling) or (2) driving the probe at a known speed (generally 0.2 cm/sec) through the interface and producing a trace proportional to temperature on a chart recorder (continuous sampling). Continuous sampling produced linear traces through the interface with transition zones in temperature and salinity. Often the identical thickness was obtained on consecutive profiles but more usually they would differ by as much as 10%. Comparisons between the two methods shows the discrete profiles underestimate d_T and d_S by about 10%. An example of a discrete profile is shown in Fig. 19. This example comes from an experiment set up primarily to study the evolution of the interface as equilibrium is approached. Though the profile shown

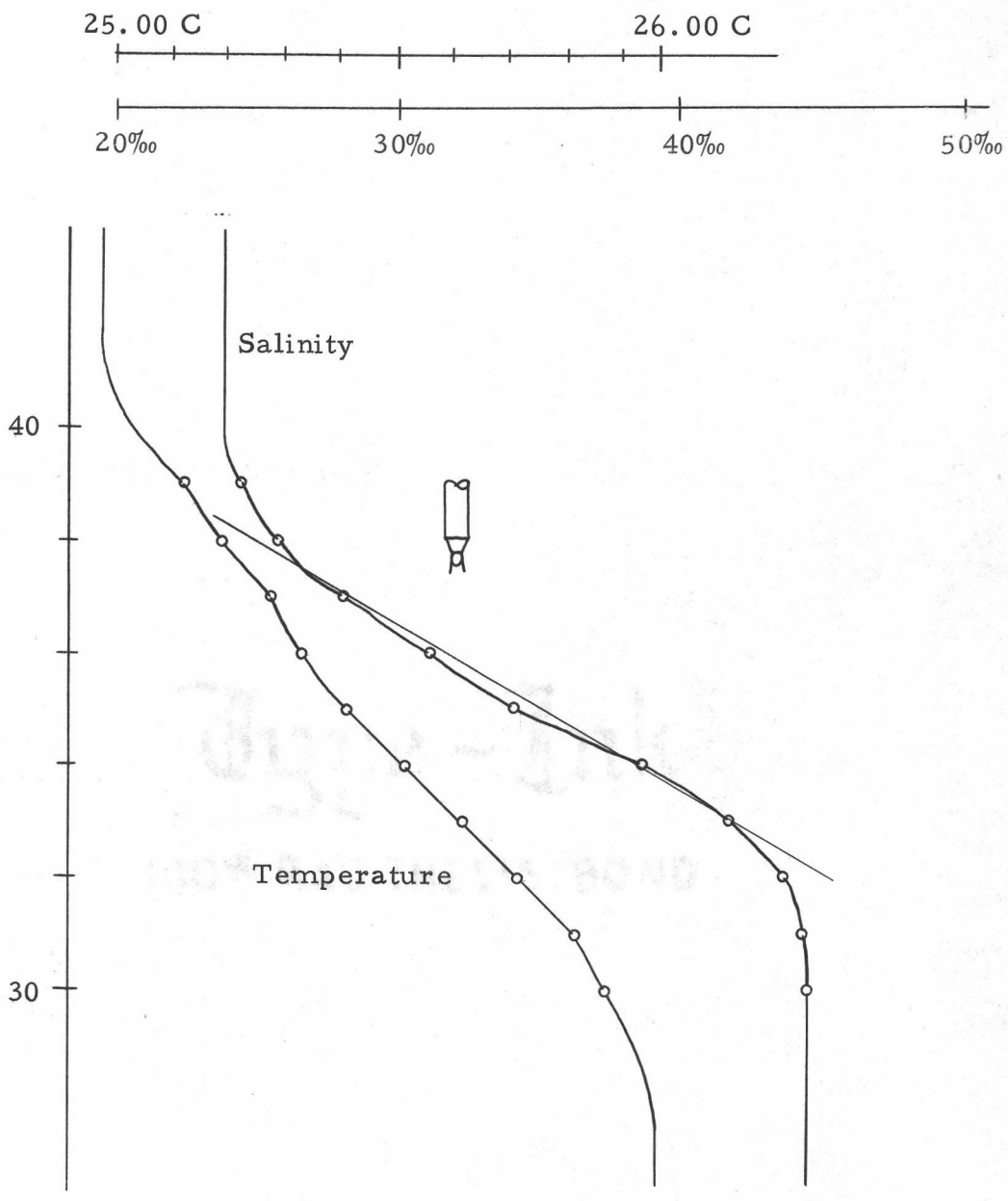

Figure 19. Discrete profile of the interfacial double boundary layer. The linearized thicknesses are d_T = 11.15 cm and d_S = 6.3 cm. The slight depressions from linearity are not seen during continuous profiling. The tip of the conductivity probe is also shown. (From Exp. 16, Run 8I; $R\rho \approx 51$)

is of a non-equilibrium interface at very high $R\rho$, the relative nature of the two curves is maintained throughout the approach but can be measured with less certainty since the ratio of probe length to interface thickness increases. Notice that even at very high stability, d_S is only about half d_T. Note also that the temperature trace is linear in the transition region of salinity. This must be a consequence of the great difference in the diffusivities. For another example of the double structure of the interface see Fig. D-2 in Appendix D.

What can we say about the expected value of d_T given an interface in equilibrium with prescribed values of ΔT and ΔS? Using our heat flux results in the form

$$H = A(\Delta T)^{4/3}(0.35)(R\rho-2)^{-0.6}, \text{ for } R\rho \geq 3 \tag{45}$$

and assuming

$$H = k_T \Delta T/d_T \tag{46}$$

leads to the functional relationship

$$d_T = f(H, R\rho)$$

The function f is shown in Fig. 20 along with the observed variation of d_T with H and $R\rho$. Agreement must be considered fair for the contours d_T = 1, 2, and 3 cm. Since most of the measured values were obtained from discrete profiling, the ten percent correction would result in closer agreement. The nature of the dependence of d_T on ΔT

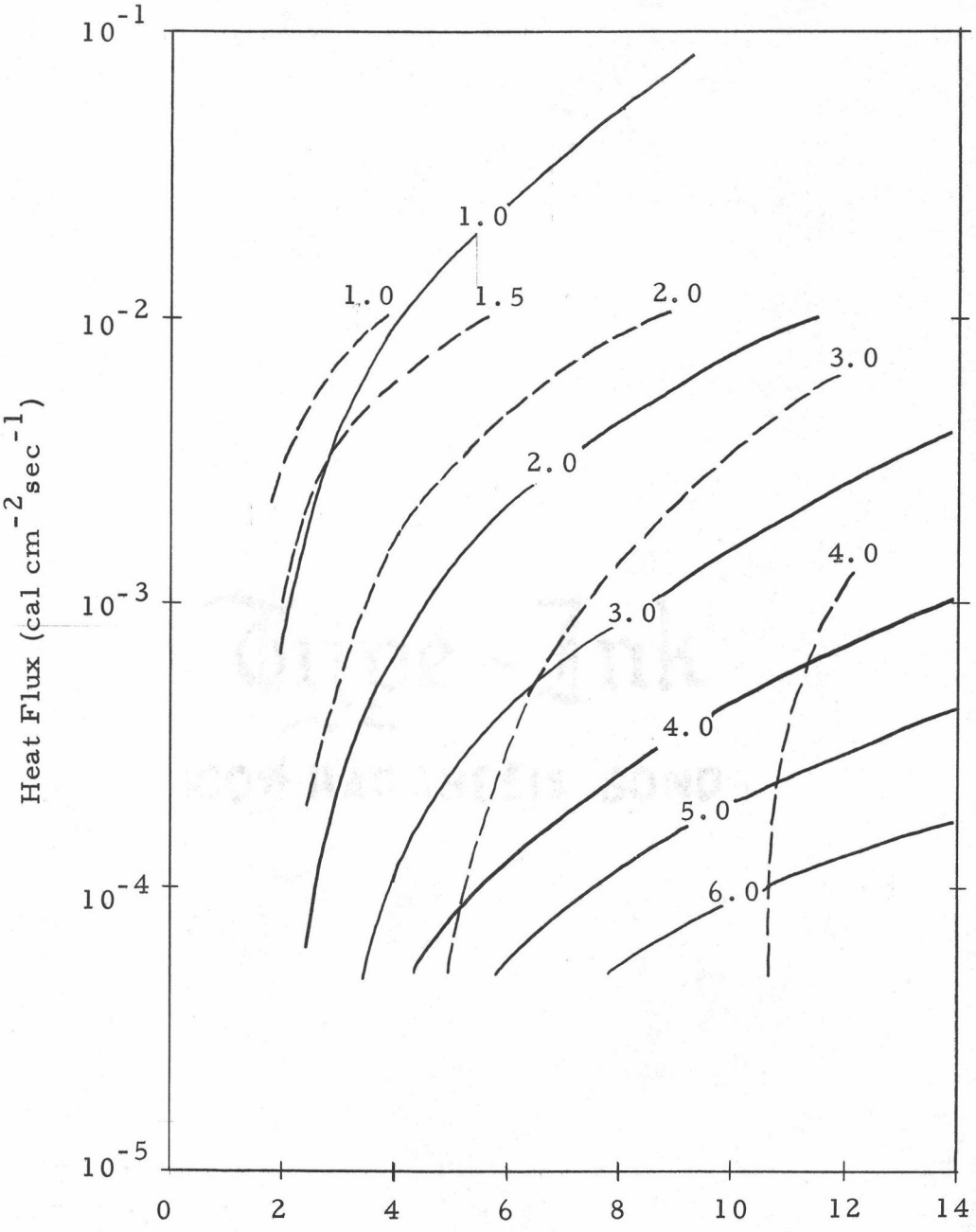

Figure 20. Variation of interface thickness with heat flux and stability number. The solid curves are obtained from Eqs. (45) and (46). The dashed curves are drawn on the basis of 24 measurements of d_T.

(or H) and Rρ supports an analogous observation by Stern and Turner (1969, p. 510) who report "...that a 'salt finger' interface, however it has been formed, will have an equilibrium thickness which is determined mainly by the salinity difference across it (with a weaker dependence on the temperature difference)." The reason for the large discrepancies at low heat flux is not known but may be the arbitrariness of the initial layer thicknesses.

The question which naturally arises at this point is: "What does the analogous plot for d_S look like?". Assuming Rf = 0.15 and Fs = $k_S \Delta S/d_S$ and again using Eq. (45) the variation of d_S with H and Rρ can be determined. It is sufficient to give the result at one value of heat flux. For H = 1.0×10^{-5} cal cm^{-2} sec^{-1} (and A = 0.00317) we have:

ΔT	ΔS	R_ρ	d_T	d_S	d_T/d_S
.0293	.0320	3.0	4.10	.88	4.667
.0400	.0583	4.0	5.60	1.60	3.500
.0480	.0875	5.0	6.72	2.40	2.800
.0546	.1195	6.0	7.64	3.28	2.333
.0604	.1542	7.0	8.45	4.23	2.000
.0655	.1913	8.0	9.17	5.24	1.750
.0702	.2306	9.0	9.83	6.32	1.556
.0746	.2721	10.0	10.44	7.46	1.400
.0786	.3157	11.0	11.01	8.65	1.273
.0825	.3611	12.0	11.55	9.90	1.167
.0861	.4083	13.0	12.05	11.19	1.077
.0895	.4573	14.0	12.53	12.53	1.000

Note that $d_T/d_S \rightarrow 1$ as Rρ increases. This behavior is just opposite to that hypothesized in Chapter III. Also, the ratio d_T/d_S, for a given

$R\rho$, is independent of heat flux.

Is it reasonable that d_T/d_S doesn't change with heating rate? Results in the next chapter indicate that Rf increases with decreasing heating rate. The consequence of this, assuming the conductive model of the interface, is an increase in d_T/d_S. An increase in the ratio d_T/d_S should be expected as the heat flux decreases for the following reason: in the limit of smaller and smaller heat flux, the mixing in the layers should weaken proportionately and the sweeping away of interfacial fluid should occur very intermittently; thus, the interface should grow, at least in spots, with the constraint due to Fickian diffusion,

$$\frac{dT}{dz} \Big/ \frac{dS}{dz} \sim \tau^{1/2}$$

which implies

$$\frac{d_T}{d_S} = \frac{1}{\sqrt{\tau}} \approx 10 .$$

Interfacial oscillations

A record of excursions of interfacial fluid past the thermistor is shown in Fig. 21. Many of the oscillations in the temperature trace have about a 3 sec. period; the other dominant period is roughly twice this or 6 sec. There are two time scales against which to compare these values. The first is the simple buoyancy or Brunt-Väisälä frequency. Using an estimate of d_T of 0.6 cm the buoyancy frequency

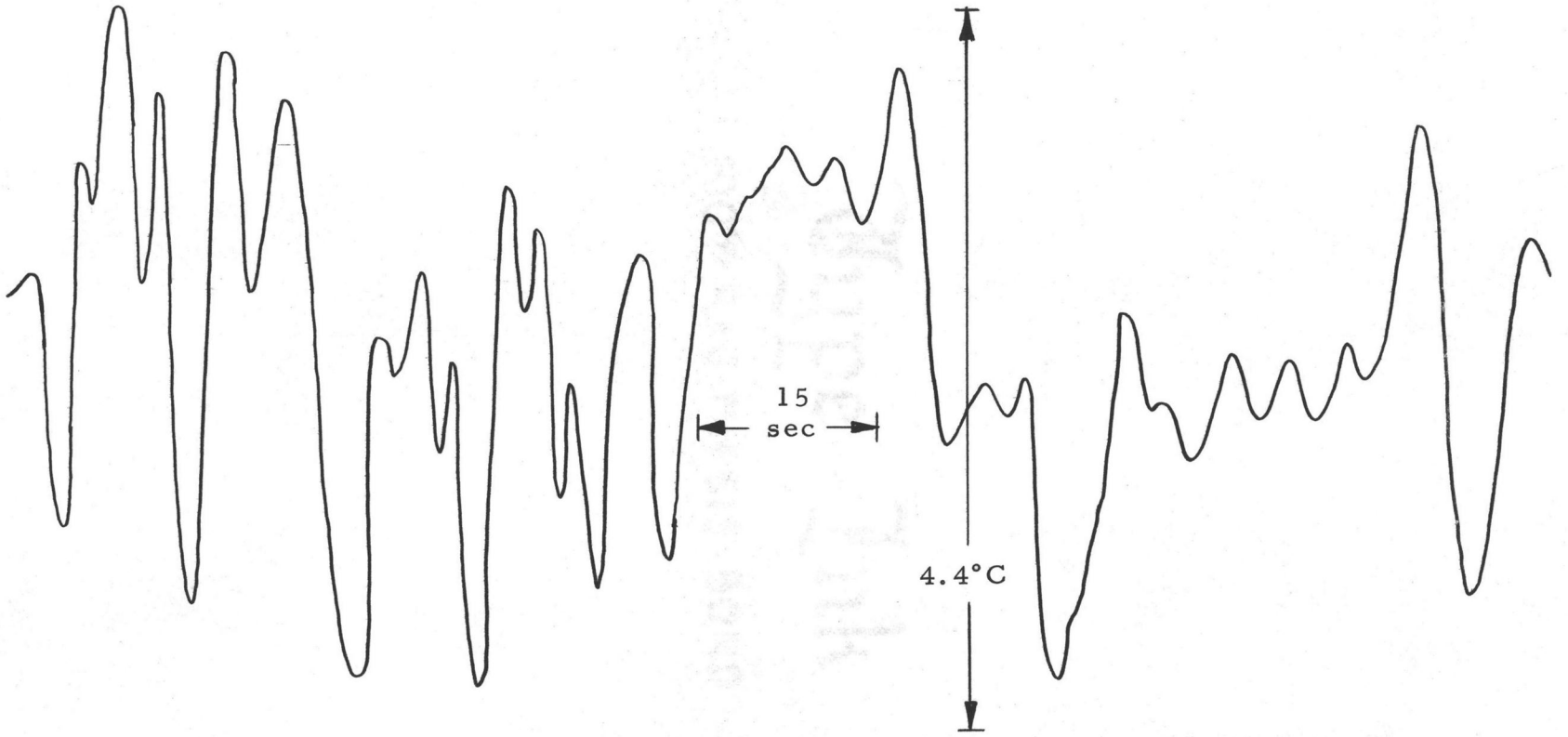

Figure 21. Temperature record with thermistor roughly midway in a diffusive interface. A signal above the mean represents a colder temperature. (From Exp. 12: $R\rho = 2.7$; $\Delta T = 4.5$ C; $\Delta S = 7‰$ and $\Delta\rho = 0.0029$)

is calculated to be 0.33 Hz, corresponding to a buoyancy period of 3.0 sec. The second time scale arises from overstable oscillations within the interface and is obtained by substituting $p = ip_i$ in Eq. (16) and solving for p_i. In dimensional units the result is[20]

$$f = \frac{1}{2\pi} \sqrt{g\beta \frac{\Delta S}{d_T} \left(\frac{\kappa}{\nu} + \kappa \right)}$$

in our notation where f [=] cy/sec. For the record in Fig. 21, f = 0.17 Hz or 1/f = 5.9 sec. Is it possible that both time scales are represented in the temperature record by the 3 sec and 6 sec periods?

Notice finally, that for the two minute record of Fig. 21, the interface never moves completely above or below the thermistor. Therefore, the vertical motion of the interface is less than ± 0.3 cm at a stability number of 2.7. Again, one is to conclude that most of the activity is connected with the transition zones on either side of the interface.

---

[20] Further, it is assumed that $a^2 >> n^2$ in Eq. (16). The validity of this assumption cannot be tested here because there are no observations of the horizontal wavenumber.

VII. TRANSPORTS THROUGH A DIFFUSIVE INTERFACE

Interfacial heat flux

A major result is the plot of heat flux vs. stability number shown in Fig. 22. Except for some illustrative points from Exp. 18, we believe all data points represent equilibrium conditions. Our suggested fit agrees well with Huppert's formula (Eq. (35) for $3 < R\rho < 5$. At very high $R\rho$ however, the discrepancy between the two approaches an order of magnitude. Therefore, Huppert's formula cannot be extrapolated for use, without error, above $R\rho \approx 7$. It is possible, in addition, that at very low $R\rho$ Huppert's formula underestimates the heat flux. We cannot be more certain of this because of the scarcity of data points for $R\rho < 2$. The difficulty in obtaining data for small $R\rho$ is partly inherent in the experiment, i.e., the system spends relatively little time at low stability. This is illustrated in Appendix E. The time factor is especially limiting when the time-consuming process of taking discrete samples is used.

A smooth curve was drawn through our data points. For $R\rho \geq 3$, this curve was fit with an equation similar in form to Eq. (34), but the origin was shifted to $R\rho = 2$ to account for the (assumed) change in transport mechanism which seems to set in at about $R\rho = 2$. The resulting equation:

Figure 22. Non-dimensional heat flux through a diffusive interface vs. the stability number of the interface. The symbols are defined in Table IV. A visual best fit is shown with a continuous solid line. The equation of this line for $R\rho \geqq 3$ is given. The arrows show the progression of experimental points with time for Exp. 22 (∇) and Exp. 18 (X). Some early (pre-equilibrium) data points for 18 are shown to indicate the deviation from the heat flux curve. The time between X's is about six hours. Huppert's equation, $H/H_{sp} = 3.8\ R\rho^{-2}$, is shown as a solid line over $1 < R\rho < 7$ and dashed for $R\rho > 7$. A fit to an interpretation of Broughton's data is shown as a continuous dashed curve.

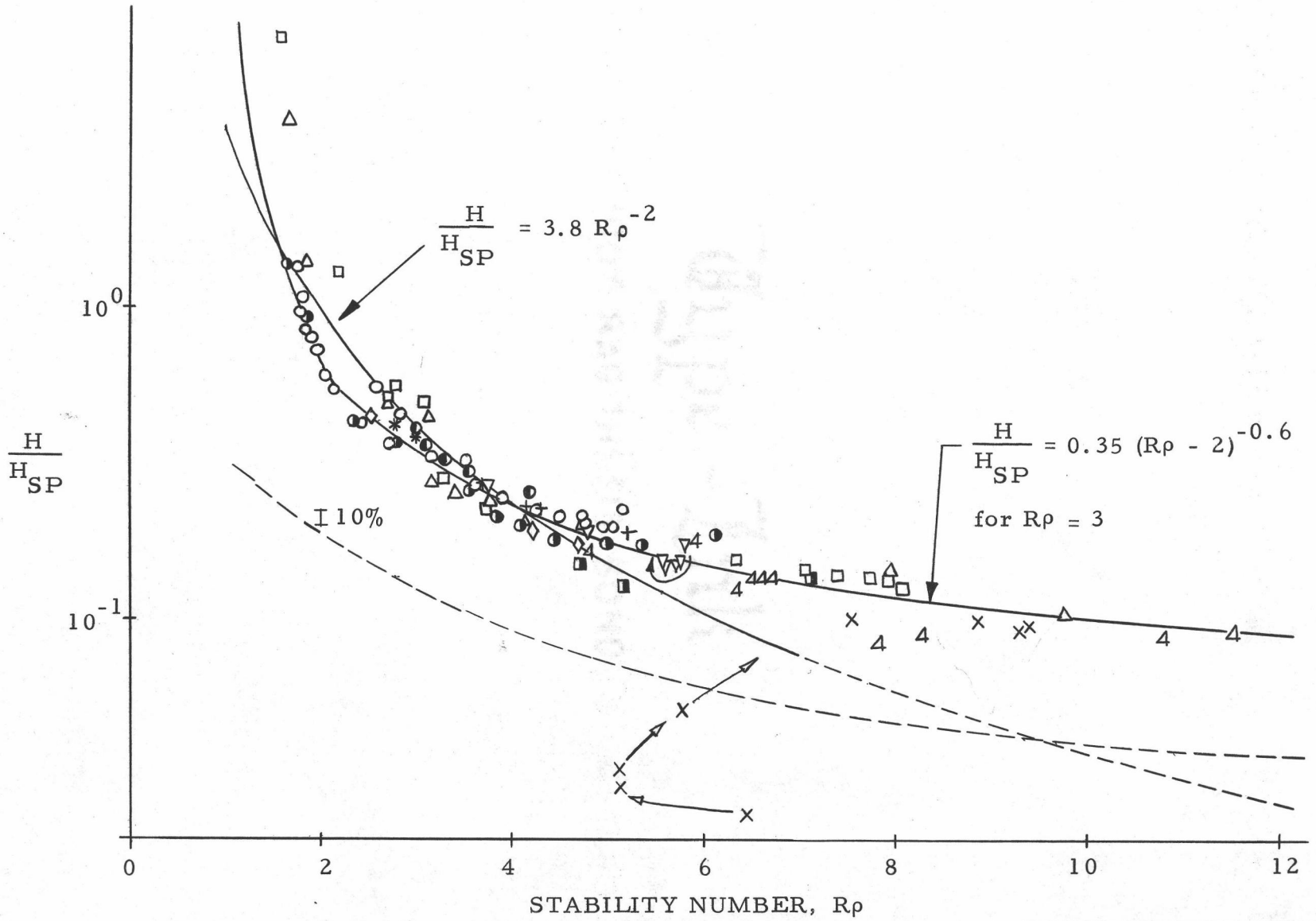
$\frac{H}{H_{SP}} = 3.8\ R\rho^{-2}$
$\frac{H}{H_{SP}} = 0.35\ (R\rho - 2)^{-0.6}$
for $R\rho = 3$
10%
10^0
10^{-1}
$\frac{H}{H_{SP}}$
0
2
4
6
8
10
12
STABILITY NUMBER, $R\rho$

$$\frac{H'}{H_{sp}} = 0.35\,(R\rho - 2)^{-0.6} \qquad (47)$$

fits the curve well for $R\rho \geq 3$ with a maximum deviation of less than 5%.

Broughton's data falls below our curve. Since we can obtain data points anywhere below our curve by taking measurements before the interface comes to equilibrium (e.g., Exp. 18), we suggest that Broughton did not allow enough time before taking measurements.

Flux ratio

In Fig. 23 results from two experiments are compared with Turner's 1965 discovery of a constant and variable regime for Rf. The heat flux for Exp. 20 is about half that used by Turner; that for Exp. 9 is a factor of ten lower. Each data point is based on difference calculations using results from two experimental runs. The time between points for Exp. 9 is several hours; for Exp. 20, twelve hours.

Both experiments show fairly good agreement with Turner's result of 0.15 for the constant regime. The salt flux in Exp. 20 was determined by sampling from the top layer only; the salinity of the bottom layer was determined from salt conservation equations assuming an infinitely thin interface. This approximation leads to a determination of ΔS which may be in some error; this may explain why the low stability data points for Exp. 20 appear to deviate from

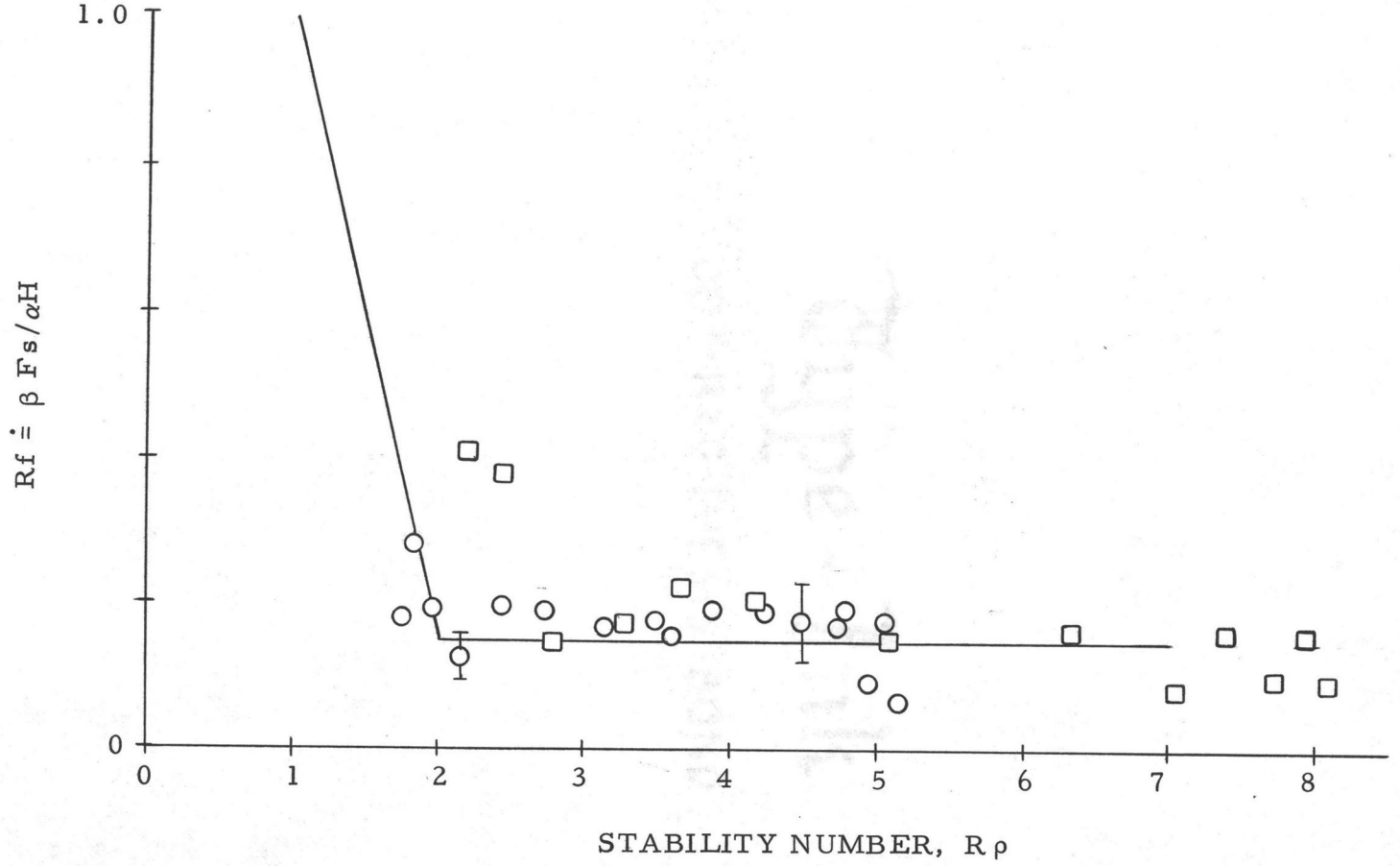

Figure 23. Plot of the flux ratio vs. stability number. The results of two experiments are shown. The time between points for Exp. 9 (O) is several hours; for Exp. 20 (□), twelve hours. The error bars are derived mainly from the difference in estimates of the salt flux between the top and bottom layers. The solid line is from Turner (1965).

Turner's curve in the variable regime (Fig. 23) and from our best fit in Fig. 22. Experiment 9 appears to enter the variable regime at $R\rho \approx 2$. There is some evidence of a decrease in Rf with an increase in $R\rho$ in the "constant regime". The final decay of Exp. 9 was unfortunately missed.

It will be noticed that values of Rf in Table IV for Exps. 10, 12, and 15 are greater than 0.15 and yet H is not far different from that used by Turner (1965). Notice however that the error bars are large enough to include the value 0.15. The lower estimate of Rf is based on estimates of Fs from the upper layer; the upper estimate on the lower layer. Temperatures of the lower layers for these experiments went quite high (over 40 C). The calibration of the conductivity probe was not known sufficiently well at these temperatures; as a result, we have more confidence in estimates of Fs from the cooler upper layer. Therefore, the lower estimates of Rf should be given higher confidence and these numbers do compare well with Turner's results. Excluding these three experiments because of the above uncertainty Fig. 24 summarizes our results on the variation of Rf for the constant regime with heat flux. Exclusive of the values for Exp. 24, Rf is seen to lie in the range $0.16 < Rf < 0.25$ for two orders of magnitude of heat flux. Although there does appear to be an increasing trend with decreasing heat flux, the jump to $Rf = 0.42$ for the lowest heat flux used was certainly unanticipated.

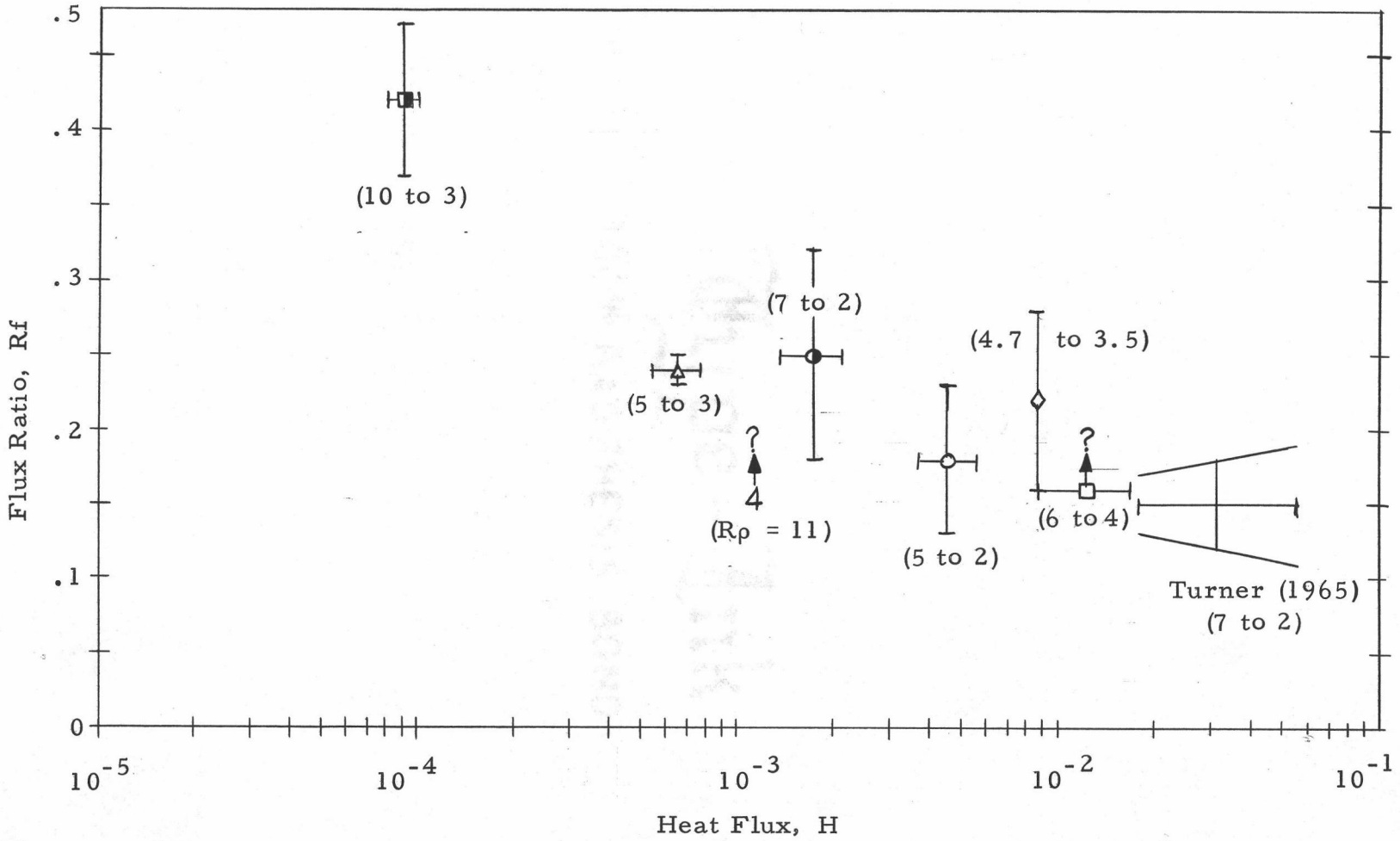

Figure 24. Plot of the flux ratio vs. interfacial heat flux. The extent of the error in salt flux associated with the points for Exps. 4 (4) and 20 (□) is unknown. For a discussion of Exp. 4 see Appendix D. Turner's data with approximate errors is shown as a trapezoid on the far right of the figure. The numbers in parentheses give the range of Rρ for which Rf was calculated.

Entrainment velocity

For all experiments, some interfacial migration was measured; this movement increased rapidly at low $R\rho$. When the boundaries were symmetric, the interface could move in either direction. In experiments with boundary conditions similar to those of Turner (1965), the interface always moved away from the heated plate. Let us look at some specific examples:

Exp.	Case	U_e (10^{-3} cm/sec)	$\Delta\rho$ (10^{-3} gm/cm^3)	$R\rho$
12	1	5	6.6	3.8
	2	12	4.9	3.05
	3	27	2.8	2.6
7	1	- .83	0.45	2.34
	2	- 2.5	0.26	2.03
	3	- 6.7	0.16	1.84
	4	-37.	0.09	1.63
23[21]	1	- 1	0.01	1.7

The quantity U_e is a measure of entrainment or interfacial mass flux. Observationally, it is defined as the rate of change of the height of the center of the interface. It can be seen from the above tabulation that for experiments with Turner-type boundary conditions (e.g., Exp. 12) $U_e > 0$. For Exp. 12 note that U_e depends, in a first

---

[21] See Appendix E for the calculation of U_e.

approximation, inversely on $\Delta\rho$ in agreement with Turner (1968b).

Experiments 7 and 23 are compared at equal values of $R\rho$ below:

Exp.	U_e	$\Delta\rho$	$R\rho$	ΔT
7	-37×10^{-3}	0.09	1.6	0.68 C
23	-1×10^{-3}	0.01	1.7	0.13 C

Notice that U_e changes by a factor of 37 and the product $\Delta\rho\Delta T$ by a factor of 45 between the two experiments. This suggests that $\Delta\rho$ and ΔT are equally important in determining U_e.

In the stability analysis of Huppert (1971), the effect convection may have in moving the interface is neglected as compared to transfer through the interface. This assumes essentially that the relative change in the height of the interface is very small compared to the change in a layer temperature over a given time interval, that is, that

$$\frac{\delta h}{h} / \frac{\delta T}{T} << 1.$$

This assumption is not supported at low stability by our work. For example, consider Exp. 23 at a stability number of 1.7. Compute changes in the thickness and temperature of the upper layer for a time interval of one second: δh is numerically equal to U_e ($= -1 \times 10^{-3}$); h, the layer depth, is about 30 cm; δT is about 4×10^{-6} °C sec^{-1} (see Appendix E); and we can let T = 20 C. Substituting, we

obtain,

$$\frac{\frac{\delta h}{h}}{\frac{\delta T}{T}} = \frac{\frac{1 \times 10^{-3}}{30}}{\frac{4 \times 10^{-6}}{20}} \approx 150 >> 1.$$

VIII. CONCLUSIONS AND SUGGESTIONS FOR FUTURE WORK

(1) On the plot of heat flux against interface stability, our results deviate from the graph of the equation suggested by Huppert (1971). Small discrepancies exist at low stability, where entrainment was an important consideration in the data analysis; at high stability, $R\rho = 15$, we predict an order of magnitude greater heat flux than is obtained from an extrapolation of Huppert's equation. We suggest the equation

$$\frac{H}{H_{sp}} = 0.35(R\rho - 2)^{-0.6}$$

for use in the range $3 \leqq R\rho \leqq 15$. Overall, our results must be considered in general agreement with those of Turner (1965) even though we have investigated a larger range of $R\rho$ and initial conditions and have used steady state heat fluxes covering almost three orders of magnitude.

(2) Migration of the interface is found in all the experiments (in either direction in the steady-state experiments). The rate of migration depended strongly on $R\rho$ and slightly less on $\Delta\rho$. Maximum entrainment velocities of 0.037 cm sec^{-1} were measured for $R\rho = 1.63$. Huppert (1971) theoretically analyzed the stability of a pair of stationary interfaces. We have found entrainment to be such an important feature that it is suggested the stability analysis be redone with a relaxation of the stationary assumption.

(3) Our measurements of the flux ratio ($Rf = \beta Fs/\alpha H$) confirm that $Rf = 0.15$ is a good value for the constant regime at a heat flux of at least 1×10^{-3} (cgs) but for a lower flux the salt flux appears to increase at the expense of the heat flux; Rf increases to about 0.4 at $H = 9 \times 10^{-5}$ (cgs) (much lower than used by Turner, 1965).

(4) The diffusive interface is shown to have a double boundary layer structure. The measured salinity boundary layer thickness is never less than half the thermal boundary layer thickness, d_T. Both T and S vary linearly through most of the interface with transition regions connecting them to the layers.

(5) Significant variation of d_T is found with H and $R\rho$, the change with H being more striking. This is analogous to a result in the salt-finger case of Stern and Turner (1969) who find that the equilibrium thickness is mainly controlled by ΔS. For an oceanic heat flux of 10^{-5} we can expect d_T to range from 2 cm at $R\rho \approx 2$ to 4 or 5 cm at $R\rho \approx 10$ on the basis of our work. (This does not agree so well with theoretical predictions of thicker interfaces.) This is approximately the range of thicknesses encountered in the ocean by Neshyba, Neal, and Denner (1971) and Osborn (1973) and in an Antarctic lake by Hoare (1966; 1968) and Shirtcliffe and Calhaem (1968). Thus, a typical d_T would be 5 cm and not on the order of millimeters as recently suggested by Munk and Woods (1973).

(6) The major oscillations seen near the interface (with a single thermistor) are caused by bodily movements of the interface in the vertical. The period of oscillations in a temperature record obtained by holding a thermistor in the interface is typically one to two buoyancy (Brunt-Väisälä) periods.

(7) The thermal burst phenomenon is the major transport mechanism for heat from a solid boundary in experiments with no internal layers.

(8) In the diffusive experiments, although some kind of buoyant release from the transition region may occur it is extremely vertically limited and does not appear to be quite as effective a transfer mechanism as for the thermal, non-layered experiments.

Some very important questions remain to be answered. These are listed below:

(1) Probably foremost in mind is: "Can a layered system be created via the double diffusive mechanism and be maintained so that the vertical heat and salt fluxes are constant; or does the condition of marginal stability at a growing interface (Turner, 1968a) preclude this possibility?"

(2) "Can a layered system set up by another mechanism be maintained in steady state?" These results would be compared with Huppert's theory which may need modification as a result of the present work.

(3) "If steady state is possible, what amplitude disturbances will destroy it?" This has obvious oceanographic motivation, since natural layers would be bombarded by shear instabilities and perturbations caused by time-dependent boundary conditions.

(4) "Are the number of layers formed or the individual layer thicknesses unique, given prescribed heat and salt fluxes?" The answer to this question would be useful to descriptive oceanographers.

(5) From a more theoretical viewpoint, "Is layered convection experimentally connectable with other convective regimes and flow patterns?" For example, do steady and time dependent laminar motions exist in layered convection for low R?

Very important related work which is, as yet, unpublished is a paper by Piacsek and Toomre (1972) in which a numerical time-dependent model yields layered structure for the diffusive regime. Also, much-needed visual observations on the diffusive interface may be forthcoming in work by Shirtcliffe (1972).

IX. BIBLIOGRAPHY

Accerboni, E. and F. Mosetti (1967) A physical relationship among salinity, temperature, and electrical conductivity of sea water. Bollettino di Geofisica Teorica ed Applicata, 9(34): 87-96.

Baines, P. G. and A. E. Gill (1969) On thermohaline convection with linear gradients. J. Fluid Mech. 37: 289-306.

Blumsack, S. (1967) Formation of layers in a stably stratified fluid. G. F. D. Notes, vol. 2, pp. 1-16. Refer. no. 67-54, Woods Hole Ocean. Inst., Massachusetts.

Boger, D. V. and J. W. Westwater (1967) Effect of buoyancy on the melting and freezing process. Trans. ASME 89 (Series C): 81-89.

Broughton, J. M. (1972) Experiments on steady layered convection in a a doubly-diffusive system. Master's thesis. Fort Collins, Colorado State University. 83 p.

Broughton, J. M. and R. I. Loehrke (1972) Experiments on natural convection in a layered doubly-diffusive system. p. 29-59. (Colorado State University. Dept. of Mechanical Engineering. Tech. Report No. 2 on Office of Naval Research Project NR 083-250).

Busse, F. H. and J. A. Whitehead (1971) Instabilities of convective rolls in a high Prandtl number fluid. J. Fluid Mech. 47: 305-320.

Caldwell, D. R. (1970) Non-linear effects in a Rayleigh-Bénard experiment. J. Fluid Mech. 42: 161-175.

Caldwell, D. R. (1973) Thermal and Fickian diffusion of sodium chloride in a solution of oceanic concentration. Deep Sea Res. 20: 1029-1039.

Caldwell, D. R. (1974a) Experimental studies on the onset of thermohaline convection. J. Fluid Mech. (in press).

Caldwell, D. R. (1974b) The thermal conductivity of seawater. Deep Sea Res. (in press).

Chandrasekhar, S. (1947) Thermal convection. Daedalus, 86: 323-339.

Chen, C. F., D. G. Briggs and R. A. Wirtz (1971) Stability of thermal convection in a salinity gradient due to lateral heating. Int. J. Heat and Mass Transfer, 14: 57-65.

Chiu, Y.-C. and R. M. Fuoss (1968) Conductance of the alkali halides. XII. Sodium and potassium chlorides in water at 25°. J. Phys. Chem. 72: 4123-4129.

Chu, T. Y. and R. J. Goldstein (1973) Turbulent convection in a horizontal layer of water. J. Fluid Mech. 60: 141-159.

Elder, J. W. (1967) Thermal turbulence and its role in the Earth's mantle. In: Mantles of the Earth and terrestrial planets, ed. by S. K. Runcorn, New York, John Wiley and Sons, 1967. p. 525-547.

Elder, J. W. (1969) Numerical experiments with thermohaline convection. Phys. of Fluids, 12, Suppl. 11: 194-197.

Fabuss, B. M. and A. Korosi (1968) Properties of sea water and solutions containing sodium chloride, potassium chloride, sodium sulfate, and magnesium sulfate. (Monsanto Research Corp., Everett, Mass., for the Office of Saline Water on Contract No. 14-01-0001-466 of the U. S. Department of the Interior).

Federico, I. D. and F. P. Foraboschi (1966) A contribution to the study of free convection in a fluid layer heated from below. Int. J. Heat and Mass Transfer, 9: 1351-1360.

Fisher, F. H., R. B. Williams and O. E. Dial (1970) Analytic equation of state for water and sea water. S.I.O. Report No. MPL-U-99. 1/67.

Globe, S. and D. Dropkin (1959) Natural convection heat transfer in liquids confined by two horizontal plates and heated from below. Trans. ASME, J. Heat Transfer, 81: 156-165.

Gregg (1973) The microstructure of the ocean. Sci. Amer. 228: 65-77.

Herring, J. R. (1963) Investigation of problems in thermal convection. J. Atmos. Science, 20: 325-338.

Herring, J. R. (1964) Investigation of problems in thermal convection: rigid boundaries. J. Atmos. Sci. 21: 277-290.

Hoare, R. A. (1966) Problems of heat transfer in Lake Vanda, a density stratified Antarctic Lake. Nature, 210: 787-789.

Hoare, R. A. (1968) Thermohaline convection in Lake Vanda, Antarctica. J. Geophysical Research, 73: 607-612.

Houk, D. and T. Green (1973) Descent rates of suspension fingers. Deep Sea Res. 20: 757-761.

Howard, L. N. (1963) Heat transport by turbulent convection. J. Fluid Mech. 17: 405-432.

Howard, L. N. (1969) (Cited in: Lindberg, W. R., 1970).

Huppert, H. E. (1971) On the stability of a series of double-diffusive layers. Deep Sea Res. 18: 1005-1021.

Huppert, H. E. (1972) Double-diffusive convection. G.F.D. Notes, vol. I, p. 43-56. Refer. No. 72-79, Woods Hole Oceanogr. Inst., Massachusetts.

Hurle, D. T. J. and E. Jakeman (1971) Soret-driven thermosolutal convection. J. Fluid Mech. 47: 667-687.

Korosi, A. and B. M. Fabuss (1968) Thermophysical properties of saline water. 53 p. (Monsanto Research Corp., Everett, Mass. for the Office of Saline Water on Contract No. 14-01-0001-466 of the U. S. Department of the Interior).

Kraicknan, R. H. (1962) Turbulent thermal convection at arbitrary Prandtl number. Phys. Fluids, 5: 1374-1389.

Krishnamurti, R. (1970) On the transition to turbulent convection. J. Fluid Mech. 42: 295-320.

Krishnamurti, R. (1973) Some further studies on the transition to turbulent convection. J. Fluid Mech. 60: 285-303.

Lieber, P. and L. Rintel (1963) Convective instability of a horizontal layer of fluid with maintained concentration of diffusive substance and temperature on the boundaries. Report No. MD-6, Inst. Engr. Res., Berkeley, University of California. (Cited in: Lindberg, W. R., 1970).

Lindberg, W. R. (1970) Theoretical aspects of thermohaline convection. Doctoral dissertation. Fort Collins, Colorado State University. 194 p.

Linden, P. F. (1971) Salt fingers in the presence of grid-generated turbulence. J. Fluid Mech. 49: 611-624.

Loehrke, R. I., T. R. Mancini, and R. D. Haberstroh (1973) Experimental studies on a captive thermocline. (Abstracted in Trans. Am. Geophys. Union 54: 322-323, April, 1973.)

Malkus, W. V. R. (1954) Discrete transitions in turbulent convection. Proc. Royal Soc. (Series A) 225: 185-195.

Mendenhall, C. E. and M. Mason (1923) The stratified subsidence of fine particles (and) theory of settling of fine particles. Proc. Nat. Acad. Sci. 9: 199-202 and 202-207.

Miller, R. C. (1968) A thermally convecting fluid heated non-uniformly from below. Doctoral dissertation. Department of Geology and Geophysics, Massachusetts Institute of Technology.

Mull, W. and H. Reiker (1930) Gesundh. -- Ing. Beihefte, 1, 28. (Cited in: Lindberg, W. R. Theoretical aspects of thermohaline convection. Doctoral dissertation. Fort Collins, Colorado State University, 1970. p. 41.)

Munk, W. H. and J. D. Woods (1973) Remote sensing of the ocean. Boundary Layer Meteor. 5: 201-210.

Musman, S. (1968) Penetrative convection. J. Fluid Mech. 31: 343-360.

Neshyba, S., V. T. Neal and W. Denner (1969) The significance of temperature stratification in the Arctic. In: Proceedings of the Sixth U. S. Navy Symposium on Military Oceanography, Seattle, Washington, 1969. p. 457-471.

Neshyba, S., V. T. Neal and W. Denner (1971) Temperature and conductivity measurements under Ice Island T-3. J. Geophys. Res. 76: 8107-8120.

Nield, D. A. (1967) The thermohaline Rayleigh-Jeffreys problem. J. Fluid Mech. 29: 545-558.

Osborn, T. R. (1973) Temperature microstructure in Powell Lake. J. Phys. Oceanogr. 3: 302-307.

O'Toole, J. L. and P. L. Silveston (1961) Correlations of convective heat transfer in confined horizontal layers. Chem. Engr. Prog. Symp. Series, 32: 81-86.

Pears, C. D., W. T. Engelke, and J. D. Thornburgh (1964) The thermophysical properties of plastic materials from -50° F to over 700° F. 259 p. (Tech. Doc. Report No. ML-TDR-64-87 (part 1) prepared by Southern Research Institute, Birmingham, Alabama, under Air Force Contr. No. AF 33(657)-8594).

Piacsek, S. A. and J. Toomre (1972) Thermohaline convection by finite-difference and modal techniques. (Abstracted in: EOS Trans. Amer. Geophys. Union, 53(4): 425).

Pickard, G. L. (1966) Descriptive physical oceanography. Pergamon Press, New York. 200 p.

Reinders, R. D. and R. D. Haberstroh (1972) Conducting-sheet model for convection through a density-stratified interface. p. 2-16. (Colorado State University. Department of Mechanical Engineering. Tech. Report No. 2 on Office of Naval Research Project NR 083-250).

Rossby, H. T. (1969) A study of Bénard convection with and without rotation. J. Fluid Mech. 36: 309-335.

Sani, R. L. (1965) On finite amplitude roll cell disturbances in a fluid layer subjected to a heat and mass transfer. Am. Inst. Chem. Eng. J. 11: 971-980.

Schmidt, E. and P. L. Silveston (1959) Natural convection in horizontal liquid layers. Chem. Eng. Progr. Sym. (Series 29), 55: 163-169.

Schmidt, R. J. and O. A. Saunders (1938) On the motion of a fluid heated from below. Proc. Royal Soc. (Series A), 165: 216-228.

Seitz, R. C. (1973) Observations of intermediate and small scale turbulent water motion in a stratified estuary (Parts I and II). (Chesapeake Bay Institute, Johns Hopkins University. Refer. no. 73-2. Tech. Report 79).

Shirtcliffe, T. G. L. (1967) Thermosolutal convection: observation of an overstable mode. Nature, 213: 489-490.

Shirtcliffe, T. G. L. (1969a) An experimental investigation of thermosolutal convection at marginal stability. J. Fluid Mech. 35: 677-688.

Shirtcliffe, T. G. L. (1969b) The development of layered thermosolutal convection. Int. J. Heat and Mass Transfer, 12: 215-222.

Shirtcliffe, T. G. L. (1972) Colour Schlieren observations of double-diffusive interfaces. J. Fluid Mech. (in press). (Cited in: Turner, 1973).

Shirtcliffe, T. G. L. (1973) Transport and profile measurements of the diffusive interface in double diffusive convection with similar diffusivities. J. Fluid Mech. 57: 27-43.

Shirtcliffe, T. G. L. and I. M. Calhaem (1968) Measurements of temperature and electrical conductivity in Lake Vanda, Victoria Land, Antarctica. N. Z. J. Geol. Geophys. 11: 976-981.

Somerscales, E. F. C. and I. W. Gazda (1969) Thermal convection in high Prandtl number liquids at high Rayleigh numbers. Int. J. Heat and Mass Transfer, 12: 1491-1511.

Sparrow, E. M., R. B. Husar, and R. J. Goldstein (1970) Observations and other characteristics of thermals. J. Fluid Mech. 41: 793-800.

Spiegel, E. A. (1971) Convection in stars I. Basic Boussinesq convection. Ann. Rev. Astron. and Astrophys. 9: 323-352.

Spiegel, E. A. (1972) Convection in stars II. Special effects. Ann. Rev. Astron. and Astrophys. 10: 261-304.

Stern, M. E. (1960) The 'salt fountain' and thermohaline convection. Tellus, 12: 172-5.

Stern, M. E. and J. S. Turner (1969) Salt fingers and convecting layers. Deep Sea Res. 16: 497-511.

Stommel, H. (1947) Convection patterns in the atmosphere and ocean. Ann. New York Acad. Sci. 48: 705-844.

Stommel, H. (1962) Examples of mixing and self-stimulated convection on the S-T diagram. Okeanologiya, 2: 205-209.

Stommel, H., A. B. Arons, and D. Blanchard (1956) An oceanographical curiosity: the perpetual salt fountain. Deep Sea Res. 3: 152-153.

Thompson, P. D. (1962) A simple statistical theory of highly turbulent convection. (Cited in: Lindberg, 1970).

Thorpe, S. A., P. K. Hutt, and R. Soulsby (1969) The effect of horizontal gradients on thermohaline convection. J. Fluid Mech. 38: 375-400.

Townsend, A. A. (1959) Temperature fluctuations over a heated horizontal surface. J. Fluid Mech. 5: 209-241.

Turner, J. S. (1965) The coupled turbulent transports of salt and heat across a sharp density interface. Int. J. Heat and Mass Transfer, 8: 759-767.

Turner, J. S. (1967) Salt fingers across a density interface. Deep Sea Res. 14: 599-611.

Turner, J. S. (1968a) The behaviour of a stable salinity gradient heated from below. J. Fluid Mech. 33: 183-200.

Turner, J. S. (1968b) The influence of molecular diffusivity on turbulent entrainment across a density interface. J. Fluid Mech. 33: 639-656.

Turner, J. S. (1973) Buoyancy effects in fluids. Cambridge, Cambridge University Press. 367 p.

Turner, J. S. and E. B. Kraus (1967) A one-dimensional model of the seasonal thermocline. I. A laboratory experiment and its interpretation. Tellus, 19: 88-97.

Turner, J. S., T. G. L. Shirtcliffe, and P. G. Brewer (1970) Elemental variations of transport coefficients across density interfaces in multiple-diffusive systems. Nature, 228: 1083-1084.

Turner, J. S. and H. Stommel (1964) A new case of convection in the presence of combined vertical salinity and temperature gradients. Proc. U. S. Nat. Acad. Sci. 52: 49-53.

Veronis, G. (1965) On finite amplitude instability in thermohaline convection. J. Mar. Res. 23: 1-17.

Veronis, G. (1968) Effect of a stabilizing gradient of solute on thermal convection. J. Fluid Mech. 34: 315-336.

Vertgeim, B. A. (1955) Prikl. Mat. Mekh. 19: 745-750. (Cited in: Nield, D. A. The thermohaline Rayleigh-Jeffreys problem. J. Fluid Mech. 29, 1967).

Walin, G. (1964) Note on the stability of water stratified by both salt and heat. Tellus, 16: 389-393.

Weinberger, H. (1963) The physics of a solar pond. Solar energy, 8: 45-56.

Whitehead, J. A. (1971) Cellular convection. Am. Scientist, 59: 444-451.

Wirtz, R. A., D. Briggs, and C. F. Chen (1972) Physical and numerical experiments on layered convection in a density-stratified fluid. Geophys. Fluid Dyn. 3: 265-288.

APPENDICES

APPENDIX A: Notation Guide

Each of the symbols listed below has a unique definition which is consistently used throughout the thesis. Definitions of symbols which change their meaning and/or are defined in the text are not necessarily repeated here.

English

$A \equiv ck_T \left(\frac{g\alpha}{\kappa\nu}\right)^{1/3}$, $(°C)^{-4/3}$.

C — a concentration, usually gm cm^{-3}.

c_p — specific heat at constant pressure, cal gm^{-1} $°C^{-1}$.

c_v — specific heat at constant volume, cal gm^{-1} $°C^{-1}$.

d_S (d_T) — linearized thickness of the solutal (thermal) interface, cm.

Fs — salt flux, gms of salt cm^{-2} sec^{-1}.

g — gravitational acceleration.

H — heat flux, cal cm^{-2} sec^{-1}.

IE — internal energy.

J_C — flux of C-stuff, gms of C-stuff cm^{-2} sec^{-1}.

k_S — molecular transport coefficient for salt, cm^2 sec^{-1}.

K_S — turbulent transfer coefficient for salt through the diffusive interface, cm sec^{-1}.

k_T — molecular transport coefficient for heat, cal cm^{-1} $°C^{-1}$ sec^{-1}.

K_T — turbulent transfer coefficient for heat through the diffusive interface, cal cm^{-2} sec^{-1} $°C^{-1}$.

L	thickness of fluid layer, cm.
PE	potential energy.
s_T	Soret coefficient, $^\circ C^{-1}$.
S	salinity, ‰, or salt concentration, gm cm^{-3}.
t	time, sec.
T	temperature, °C.
T_b	burst temperature, °C.
u, v, w	velocity components, cm sec^{-1}.
V	velocity vector, cm sec^{-1}.
z	vertical coordinate, positive upwards.

Greek

$\alpha \equiv -\frac{1}{\rho}\frac{\partial \rho}{\partial T}$	coefficient of thermal expansion, $^\circ C^{-1}$.
$\beta \equiv -\frac{1}{\rho}\frac{\partial \rho}{\partial S}$	coefficient of density change due to a change in S, $(‰)^{-1}$ or $cm^3\ gm^{-1}$.
$\Delta\rho(\Delta S)$	the density (salinity) difference between centers of layers in a diffusive experiment.
ΔT	the temperature difference between boundaries in a thermal or thermohaline experiment or between layer centers in a diffusive experiment.
κ	thermal diffusivity, $cm^2\ sec^{-1}$.
κ_S	salt diffusivity, $cm^2\ sec^{-1}$.
ν	kinematic viscosity, $cm^2\ sec^{-1}$.
ρ	solution density, gm cm^{-3}.
τ_b	period between bursts, sec.

Non-dimensional parameters

c	a numerical constant with the experimental value of about 0.085.
$Nu \equiv \frac{H}{k_T \frac{\partial T}{\partial z}}$	Nusselt number, the ratio of the actual heat flux to a heat flux due only to molecular conductivity.
$Pr \equiv \nu/\kappa$	Prandtl number, the ratio of viscous to thermal diffusion.
$R \equiv g\alpha\Delta TL^3/(\kappa\nu)$	the thermal Rayleigh number.
$R_{(d)}$	Rayleigh number based on the distance d.
Rf	the flux ratio.
$R \equiv \frac{\beta\Delta S}{\alpha\Delta T}$	the stability ratio: an overall ratio of stabilizing density difference to destabilizing difference.
$Rs \equiv g\alpha\Delta SL^3/(\kappa\nu)$	the solutal Rayleigh number.
$Sh \equiv \frac{Fs}{k_S \frac{\partial S}{\partial z}}$	Sherwood number
$\tau \equiv \frac{\kappa_S}{\kappa_T}$	component diffusivity ratio. Identical to the inverse Lewis number.
$\phi(\psi)$	the exponent (coefficient) in the Nusselt-stability number correlation.

Special symbols

‰	read as "parts per thousand". Its use in oceanography when referring to solids dissolved in sea water invokes a strict definition but here we take it to mean gm of salt per kgm of solution.

$\equiv$	read as "is defined by".
x'	a perturbation of a perturbed quantity.
$\overline{x}$	an average.
$\partial_x \equiv \frac{\partial(\ )}{\partial x}$	a partial derivative.
$[=]$	read as "is dimensionally equal to".

APPENDIX B: Conductivity Probe

The transducer was constructed at one end of a long 4 mm glass tube which could be lowered and raised vertically through the experimental fluid either manually or by use of an electrically operated drive mechanism. The electrodes are made from 0.010 inch diameter platinum wire of 3 mm length and spaced 2 mm apart. A small thermistor was put to one side of their center. A similar design was used by Prausnitz and Wilhelm (1956). An approximate, geometrical cell constant can be calculated as $A = 1.5\ cm^{-1}$.

The electrodes are platinized according to procedures outlined in Jones and Bollinger (1935) in order to reduce the polarization resistance (Jones and Bollinger, 1931). The sufficiency of platinization was judged by using a test described in Jones and Christian (1935). We found in this way that a deposition of platinum equivalent to a total charge of 10 coul/cm^2 of electrode area was adequate.

Conductance measurements were made by using the probe as one arm of a standard Wien bridge. A critical feature of the Wien bridge circuit is a parallel capacitor, needed to balance the electrical double layer capacitance introduced by the platinum-electrolyte interfaces. Our work was done at 10 KHz.

The probe was calibrated using the secondary standards of Bremner, Thompson, and Utterback (1939) and Chiu and Fuoss (1968).

In preparing the samples, we used doubly distilled water as solvent and J. T. Baker NaCl, C. P. grade as solute. Buoyancy corrections were not made as they were small compared to other errors. The NaCl was not dried.

Determinations of the cell constant of the probe were made by fitting the probe into a small flask filled with a known solution and immersing the flask in a temperature bath and measuring R. Samples of approximately 11‰, 20‰, and 27‰ were used at 10, 15, 20, 25, 30, and 35°C. To avoid possible error due to evaporation while filling the flask, additional repetitive determinations were made at room temperature with samples of 10‰, 20‰ and 30‰.

For a precision of ± 0.01‰ in salinity, the conductance must be known to ± 0.02%. At the highest salinities our error in resistance measurement was ± 0.2%. Sample preparation error due to weighing leads to an error in specific conductance of ± 0.1%. The temperature of the sample as measured with the thermistor was known to ± 0.005°C which implies an error in specific conductance of ± 0.01%. From the relationship among cell constant, specific conductance, and measured resistance, the uncertainty in A is ± 0.3%. This assumes the neglect of drying the NaCl and non-purity of the NaCl introduced errors which do not appear when comparing relative determinations of A.

The measured values of the cell constant depend significantly on temperature and salinity. The calibration curves are shown in Fig. B-1.

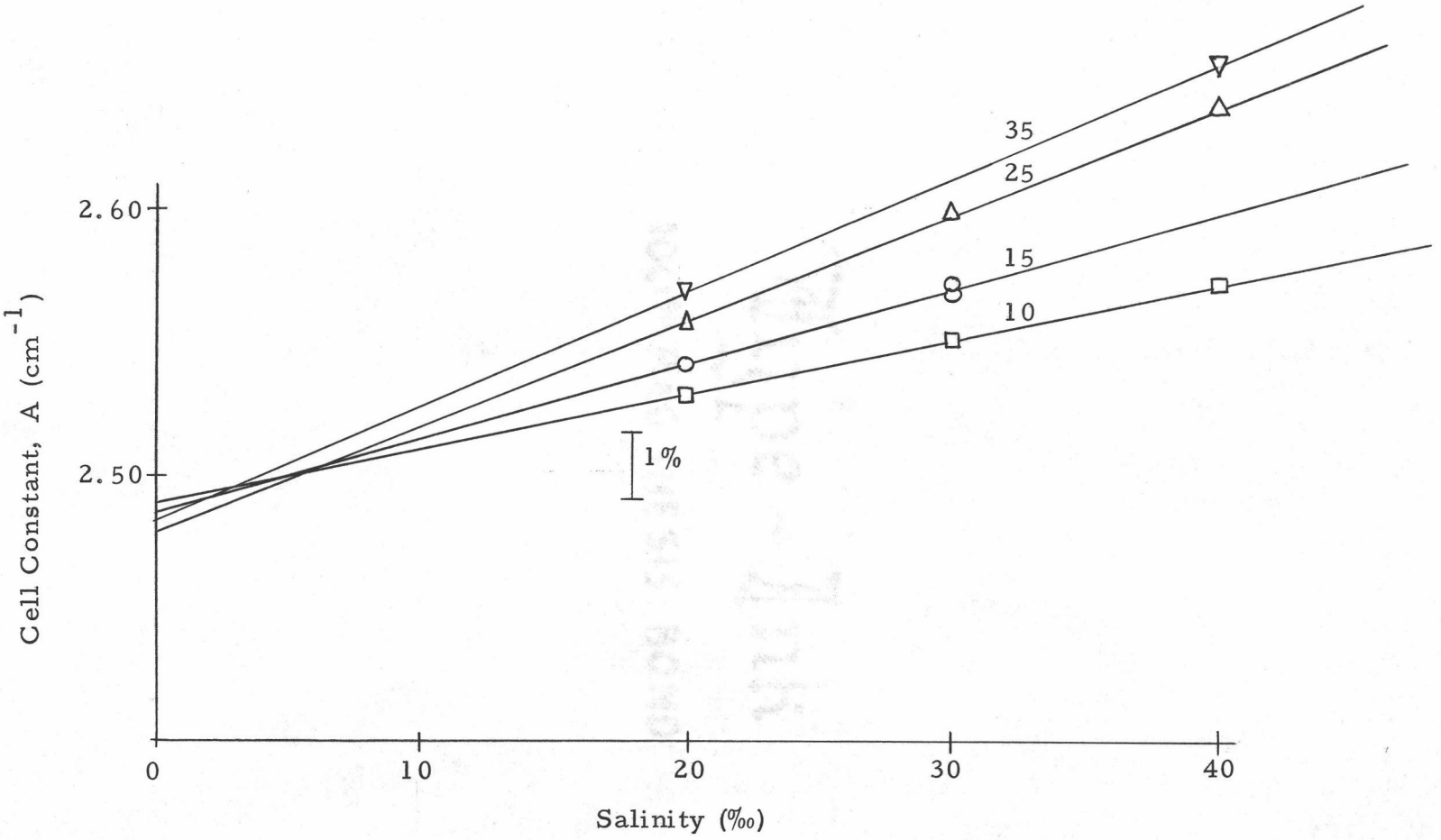

Figure B-1. Variation of the cell constant with temperature and salinity.

These curves were used in the determination of salinity for diffusive experiments prior to Exp. 19. The cell constant for zero salinity is A = 2.483. This value changed by about 4% in three months' use of the probe. When not in use, the probe was immersed in distilled water.

References

Bremner, R. W., T. G. Thompson and C. L. Utterback (1939) Electrical conductances of pure and mixed salt solutions in the temperature range 0 to 25°. J. Am. Chem. Soc. 61: 1219-1223.

Chiu, Y.-C. and R. M. Fuoss (1968) Conductance of the alkali halides. XII. Sodium and potassium chlorides in water at 25°. J. Phys. Chem. 72: 4123-4129.

Jones, G. and G. M. Bollinger (1931) The measurement of the conductance of electrolytes. III. The design of cells. J. Am. Chem. Soc. 53: 411-451.

Jones, G. and D. M Bollinger (1935) The measurement of the conductance of electrolytes. VII. On platinization. J. Am. Chem. Soc. 57: 280-284.

Jones, G. and S. M. Christian (1935) The measurement of the conductance of electrolytes. VI. Galvanic polarization by alternating current. J. Am. Chem. Soc. 57: 272-280.

Prausnitz, J. M. and R. H. Wilhelm (1956) Turbulent concentration fluctuations through electrical conductivity measurements. Rev. Sci. Instr. 27: 941-944.

APPENDIX C: Pilot Experiments

We briefly describe here a simple convection tank, make some general observations on layered convection, and report the results of a "layering" experiment conducted in August 1971.

The tank is made from a 24 cm diameter cylinder of 0.005 in. cellulose acetate glued to a thin sheet of aluminum which rests on a heating pad, insulated on the bottom and around the sides. The heating pad provides 0.022 cal cm^{-2} sec^{-1}. The sidewalls can be insulated with 5 cm of styrofoam; when they are not insulated, they provide a good optical window. In either case, they practically eliminate vertical sidewall heat conduction. The depth of the working fluid layer is variable; 20 cm is a convenient depth.

Temperature measurements were made by lowering a thermistor by hand and nulling a bridge circuit. Occasionally a null could not be obtained because of thermal fluctuations but often the limits of the fluctuations could be delineated. These cases are indicated on the graphs which follow. An individual run of about 30 measurements would take from four to five minutes to complete. No conductivity measurements were made.

Some general observations can be made at this time. In experiments without sidewall insulation, one can study the formation of the layers and interfaces. When dye or aluminum flake tracers are not

used, the interfaces can still be detected by the variation in the index of refraction of the fluid through the interface. Though the interfaces must form sequentially in time, observationally it often seems that one notices two or three interfaces where just moments before there were none. Needless to say, visual detection is extremely subjective. When viewed from the side of the tank, the interface first appears as a very thin plane covering the tank cross-section. It is so thin (c. 1 mm) in fact, that one sometimes thinks he is seeing only an optical effect caused by a distortion in the container wall. Soon after formation, waves or undulations appear and the interface thickens. A typical thickness is about 1 cm for the heat flux given above and moderate salinity gradients. Eventually (and presumably at low stability number) the surface becomes irregular but the motions on it still look like waves. When the waves reach the sidewall they often reflect and collide with other waves. The initial layer thickness is not much more than the final interface thickness, i.e., about 1 cm. These relatively thin interfaces interact and merge to form thicker layers which have longer lifetimes.

When a dye with small diffusivity is slowly introduced into the fluid, from a capillary tube for example, a number of interesting effects can be seen. If the dye descends through a region in which no interfaces have been detected visually, the vertical dye streak will often zig-zag from side to side. The wavelength is on the order of

twice an initial layer thickness (c.f. Turner and Stommel, 1964, Fig. 2a). Thus, it seems some laminar horizontal motion precedes layer formation. Can this be a sidewall effect? If so, then the possibility exists that the initial layer thicknesses are set by sidewall-induced convection (c.f. Turner, 1973). Convective motions in a newly formed layer are slow and laminar. This is to be compared with the vigorous stirring in the lowest layer where a dye blob will be completely mixed in 10-30 seconds by rms velocities of the order of 1 cm/sec. If dye is placed near an interface, it is swept out along the interface. Therefore, the edge of the interface is a zone of shear. No simultaneous observations of this motion were made on both sides of an interface and so we cannot confirm the observation of Turner and Stommel that the motion of opposite sides is thermally and not frictionally driven.

A particular example of a layered experiment will now be described. The (roughly linear) initial salinity gradient is 1.5‰ cm^{-1}. The heating rate from below is 22×10^{-3} cal/cm^2 sec; an average value through the interfaces, as calculated from Runs 8 and 9, is about 9.4×10^{-3} cal/cm^2 sec. The upper boundary is an acrylic plate with an ice-water mixture above it. The temperature of the ice-water is between 6 and 8 C. Notice that two different boundary conditions are used: constant heat flux (bottom) and constant temperature (top). It is only at steady state conditions that the two conditions

produce equivalent effects. The pertinent experimental details are continued below:

Fill of tank complete; withdraw filling float. Fluid temperature is about 32 C.	$17^{\underline{44}}$
Upper boundary is in place; fill with ice-water mixture. Turn heat on.	$20^{\underline{05}}$

Run Number	Begin to profile:
2	$20^{\underline{37}}$
4	$21^{\underline{11}}$
6	$21^{\underline{47}}$
7	$22^{\underline{06}}$
8	$22^{\underline{24}}$
9	$22^{\underline{48}}$

The temperature profiles are shown in Figs. C-1 (a) and (b).

The rapid growth of the top layer prior to Run 2 is due to the large initial temperature gradient under the acrylic boundary. The temperature difference between the boundary and the fluid layer can only decrease after the initial shock. Therefore, the convection in the top layer weakens with time and the growth rate consequently decreases. Thus, between Runs 2 and 7, the thickness of this layer increases by only 0.5 cm. The situation at the bottom is quite different. There, the thermal boundary layer and the associated convection increase in intensity with time until a local steady state is reached. The point is, there is a constant driving from the bottom but a driving of decreasing intensity at the top. When the fluid near the top

Figure C-1 (a) and (b). Temperature profiles from a pilot experiment. The profiles do not extend completely to the boundaries. The error bars (⊢——⊣) denote the extent of thermal fluctuations which prevent a null from being read. The profile from Run 7 is drawn in both (a) and (b) for convenience and is dashed for this reason.

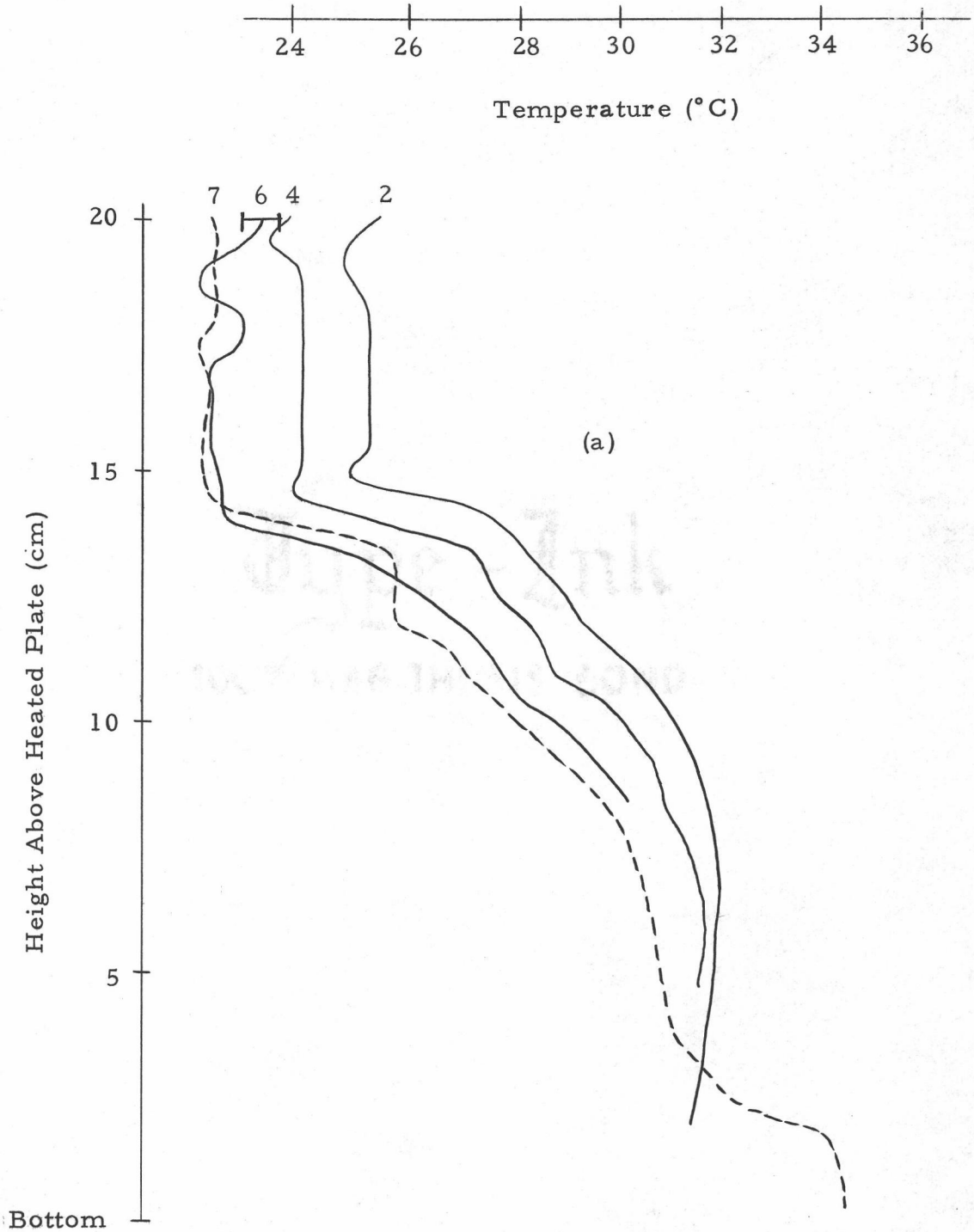
24
26
28
30
32
34
36
Temperature (°C)
7
6
4
2
20
15
10
5
Bottom
Height Above Heated Plate (cm)
(a)

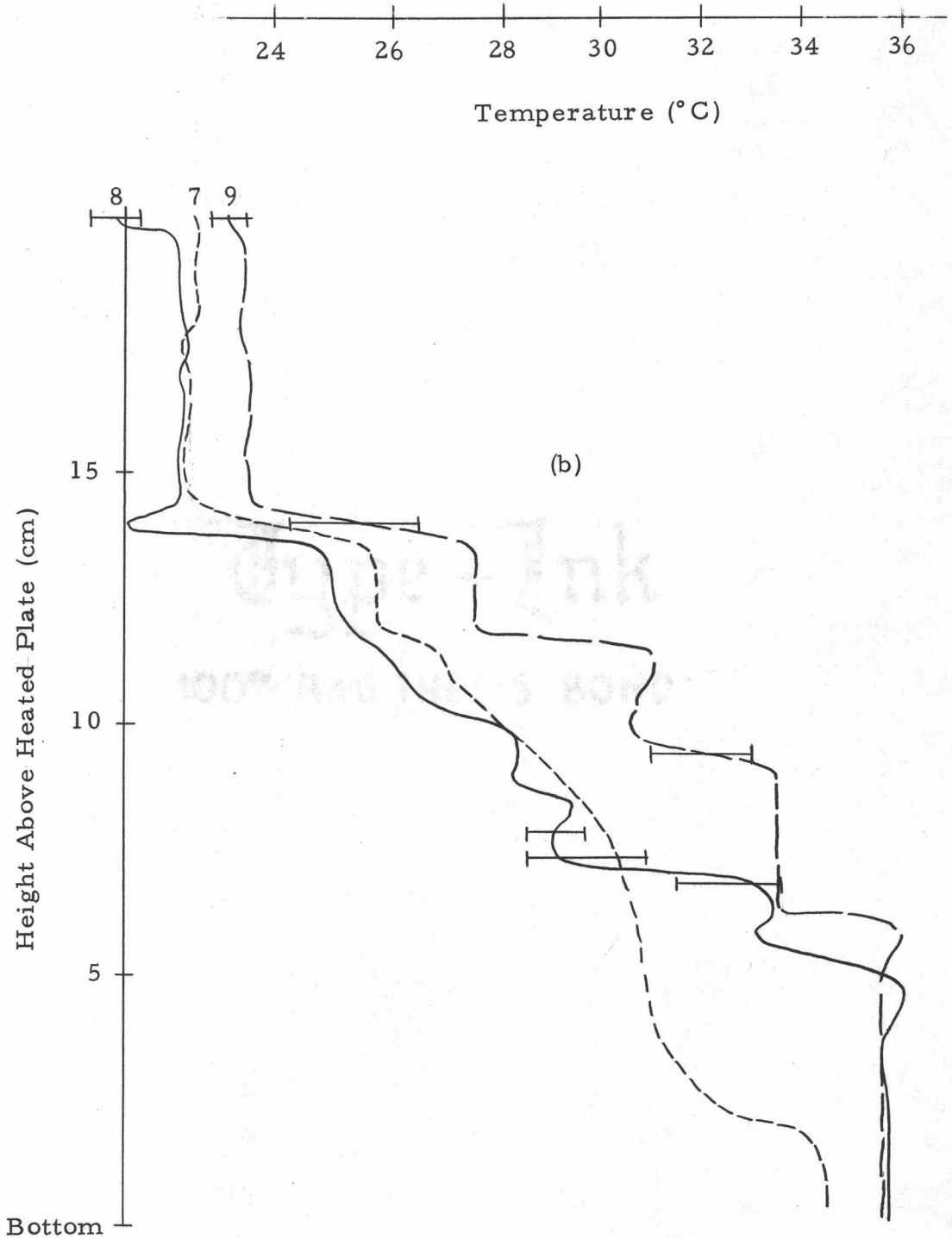
24
26
28
30
32
34
36
Temperature (°C)
8
7
9
(b)
15
10
5
Bottom
Height Above Heated Plate (cm)

feels the effects from the heating the boundary layer under the upper plate can reassert itself. The difference in thermal capacity between the two boundaries due to the nature of the materials used might also have some effect on the growth rates.

The expected increase in the thickness of the layer formed at the bottom can be calculated from (Turner, 1968a):

$$h(t) = (H^*/S^*)^{1/2} t^{1/2}$$

where H^* is a dimensional buoyancy flux and $(S^*)^{1/2}$ is the Brunt-Väisälä or buoyancy frequency (see below). Turner found that the proportionality factor for his experiments was equal to 0.89. We compare the observed growth from Runs 7-9 with the formula $h(t) = 0.89\, t^{1/2}$. The results are:

Time (sec)	h(t), observed (cm)	h(t), calculated (cm)
0	0.0 (1.8)	0.0
1080	3.1 (4.9)	2.9
2520	4.3 (6.1)	4.5

where the numbers in parentheses are heights from the tank bottom. The agreement is good as should be expected since the experimental conditions are nearly the same as Turner's.

We can also calculate a value for $(H^*/S^*)^{1/2}$:

$$H^* \equiv -g\alpha H/\rho c_p \doteq -g\alpha H \doteq -(980)(3\times10^{-4})(9.4\times10^{-3}) = 2.75\times10^{-3}$$

$$S^* \equiv -\frac{1}{2} g \beta \left(\frac{dS}{dz}\right) \doteq -\frac{1}{2} (980)(0.74)(1.5 \times 10^{-3}) = 0.54$$

and so

$$\left(\frac{H^*}{S^*}\right)^{1/2} = 0.71 \text{ cm sec}^{-1/2} .$$

This value is a minimum however, since a maximum value of S* has been used (any nonlinearity in the initial salinity profile would reduce S*). Since we never directly measure the salinity gradient to check our formula based on the filling procedure, and because of the uncertainty in H, we should say the agreement between 0.71 and 0.89 is reasonable.

The novel feature of this experiment can be seen in the profile for Run 7. The second layer from the top must clearly have been formed by cooling from above. It is not clear whether some of the other layers are also produced this way.

Interesting also are the reverse-slope regions which occasionally border an interface. These can be seen especially well in the profile for Run 8. Assuming these are transient features, we can interpret them as being caused by the presence of some fluid from the opposite side of the layer. The anomalous fluid must change its T-S characteristics if it is to remain or absorb or release heat if it is to return to its origin. Temperature inversions at the edges of salt-finger interfaces have been observed by Linden (1971).

APPENDIX D: Failure of the steady state experiments

It was originally proposed that steady state experiments be conducted in which constant heat and salt fluxes would be maintained at the upper and lower boundaries of the experimental apparatus (the tank used in the work for this thesis was designed with this in mind). The experimental region of the tank would be layered, either artificially or by the double diffusive mechanism itself, and it was expected that the system would adjust to allow the heat and salt fluxes across horizontal planes to become statistically stationary in time. We had envisioned the attainment of this final steady state from various initial conditions to be most interesting.

The difficult part about an experiment of this kind is providing salt fluxes at the boundaries in the correct way. What was thought to be a convenient means of doing this proved to be unsuccessful. It will be briefly described here nonetheless as some modification may yet be suitable for future experiments if they are deemed desirable. Also, one run from an experiment of this kind will be described and some calculations performed.

The essence of a multi-layered steady state experiment is shown in Fig. D-1. Three layers are shown bounded by permeable membranes (we used filter paper). The membranes separate layers 1 and 3 from cold, flowing, fresh tap water and stirred, hot brine

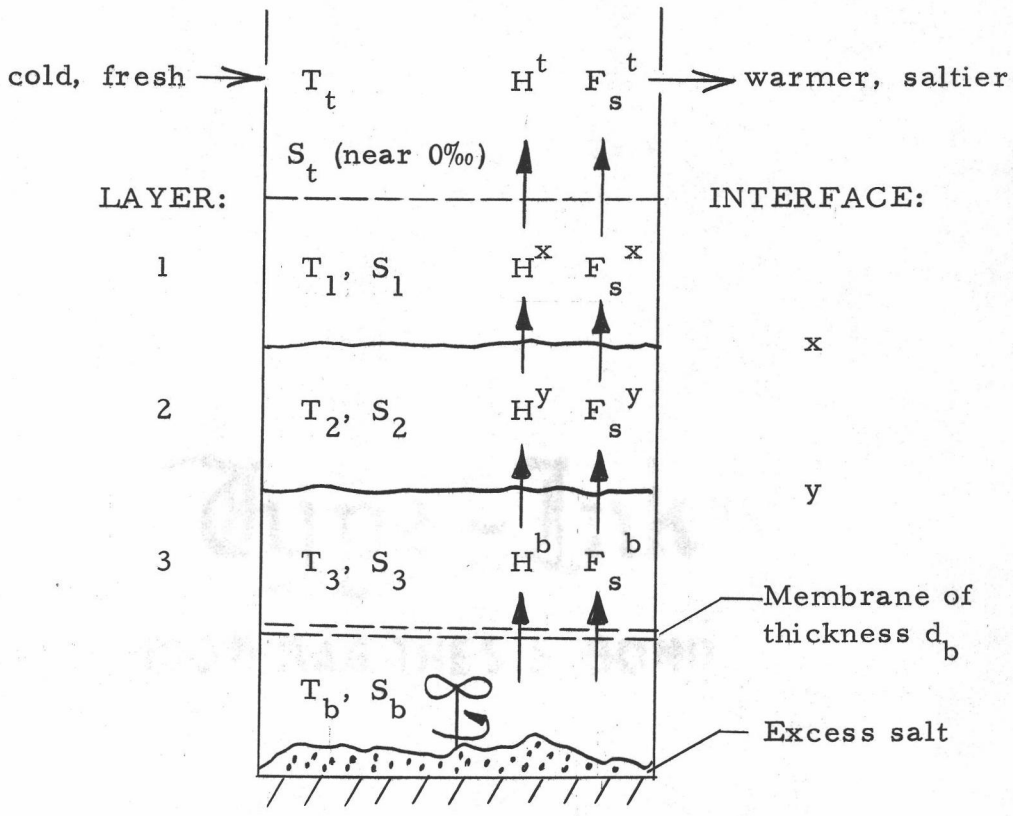

Figure D-1. A model of a three layer steady state thermohaline experiment (see text).

respectively. The (constant) concentrations of these two reservoirs are shown. The fluxes through interfaces and membranes are indicated by arrows.

Our basic assumption was a predictable law for F_s^b. Assume for instance the linear law

$$F_s^b = C \frac{S_b - S_3}{d_b} \qquad \text{(D-1)}$$

where C depends on the type of membrane (porosity of the filter paper) and d_b is the effective membrane thickness (proportional to the number of sheets of filter paper used). Now S_b is fixed at the saturation value at T_b (about 260‰). The parameters in Eq. (D-1) are chosen so that F_s^b is a reasonable value. After the heating rate from below and T_t are prescribed the H^i (i = t, x, y) adjust. With a longer time constant, the S_i (i = 1, 2, 3) adjust so that the salt fluxes are all equal.

Since conductivity data is available for sodium chloride solutions of concentrations in the range 0‰ to about 60‰ we choose S_1, S_2, S_3 to be in this range. The problem experimentally is that the difference, $S_b - S_3$, across the bottom membrane is overwhelming and it is not long into a run when one detects the presence of a growing, saline, boundary zone of thickness d(t) forming about (under, through, and above) the membrane. The mechanical mixing by the stirrer from below and by the weak convection in layer 3 is just not sufficient for annihilation of the boundary zone. Eq. (D-1) is effectively replaced by

$$F_s^b = B(t) \cdot (S_b - S_3) \qquad (D\text{-}2)$$

where B(t) depends in some way on d(t). The flux F_s^b is now a function of time and hence, the interfacial fluxes are also; the experiment cannot attain a steady state. Any attempt to prevent the boundary zone formation at the bottom by increasing S_3 and thus decreasing $S_b - S_3$ would of course result in the same problem at the top. The other solution which comes to mind is working with a larger range in conductance, for example, S_1 = 65‰, S_2 = 130‰, and S_3 = 195‰, i.e., ΔS = 65‰ between centers of layers. This remedy is undesirable because each interface would have such great differences across it that the physics of the transfers might be substantially different from naturally occurring cases.

The only real solution is to maintain the bounding reservoirs at constant property values by a suitable pumping network. This however, involves a huge network of pumps, reservoirs, salt-balancing tanks, heat exchangers, etc. Such an extensive set up was beyond our intentions and available laboratory space. A larger group of workers at Colorado State University (for example, Haberstroh, Loehrke, Reinders, Plumb, and Broughton, 1972) was, unknown to us at first, already making first attempts at such work. They should be able to produce, in the future, some significant results in steady, thermohaline convection.

We will now look at one run from an attempted steady experiment and although the heat and salt fluxes turn out to not both be steady some interesting results can still be obtained. For this particular run (Run 13) $R\rho = 11.53$; this is high enough to allow calculation of H and Fs directly from the profiles themselves with a good deal of certainty. The profiles are shown in Fig. D-2.

Examination of Fig. D-2 shows the two boundary layers which are attached to the filter paper boundaries; it can be seen that they are quite thick. The profiles in these regions and in the interfacial zone are linear and so the transports are probably molecular. The interface appears to be in equilibrium because there is little change in its thickness from the previous run (Run 12); because the boundary temperatures have stayed relatively constant over the 22 hours between runs 12 and 13; and because of the good agreement among the calculated heat fluxes through the three linear regions (see below).

Using the notation introduced previously we calculate the heat fluxes. We obtain

$$H^t = 1.05 \times 10^{-3} \text{ and } H^b = 1.06 \times 10^{-3} \text{ cal/cm}^2 \text{ sec}$$

and for the interface x,

$$H^x = -k_T \nabla T = -1.4 \times 10^{-3} \frac{2.7^\circ C}{3.5 \text{ cm}} = 1.08 \times 10^{-3} \text{ cal/cm}^2 \text{ sec} .$$

We take the interfacial heat flux to be $H = (1.07 \pm .02) \times 10^{-3}$.

Figure D-2. Temperature (□) and salinity (○) profiles for diffusive experiment 4, run 13. R_ρ = 11.53. Note the changes in the S axis and the breaks in the z axis. The filter paper boundaries are at z = 48.8 cm and at z = -3 cm.

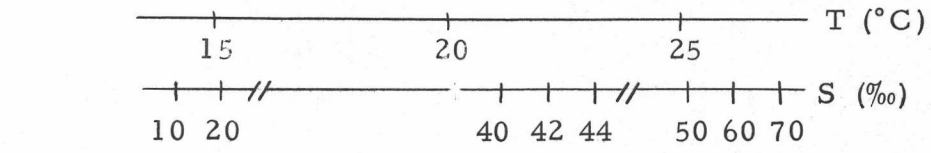
T (°C)
15
20
25
S (‰)
10 20
40 42 44
50 60 70

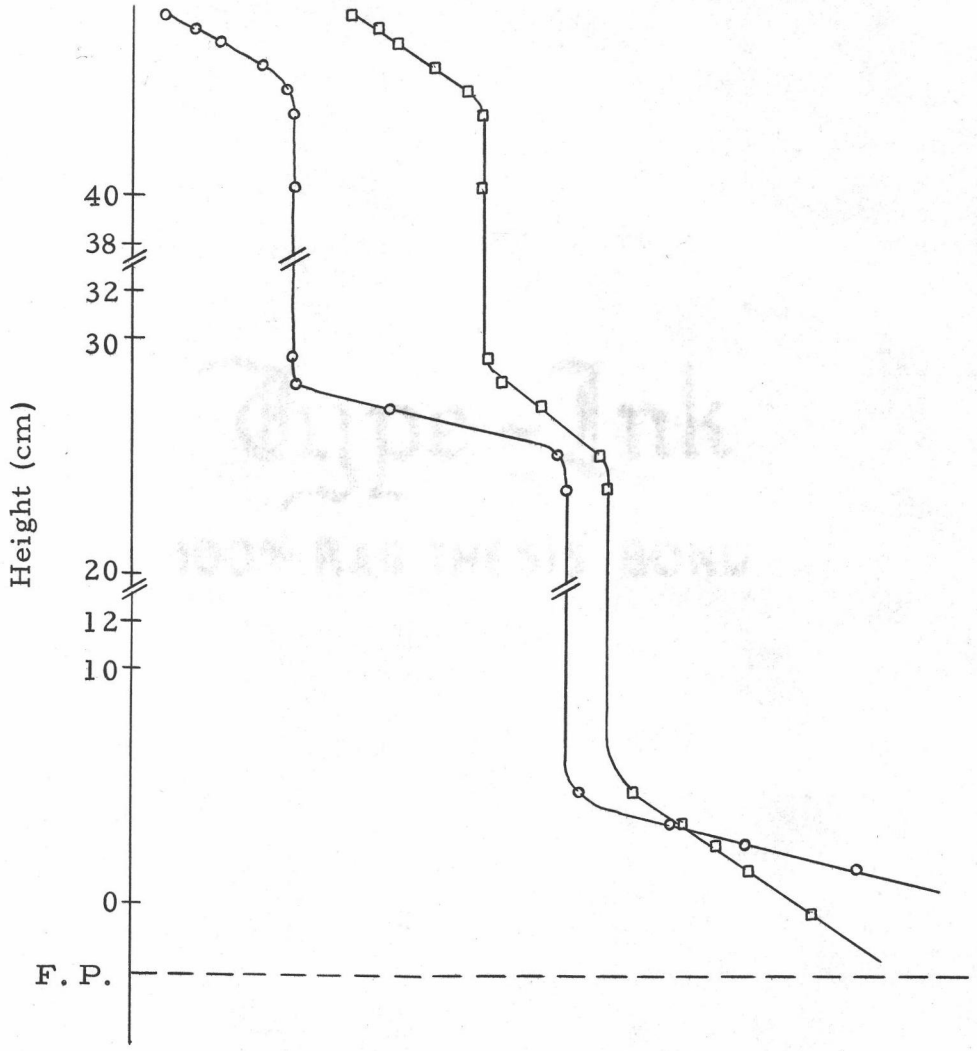
Height (cm)
40
38
32
30
20
12
10
0
F. P.

From the salinity profiles we calculate

$$F_s^t = 14 \times 10^{-8} \text{ and } F_s^b = 35 \times 10^{-8} \text{ gm salt/cm}^2 \text{ sec}$$

and for the interface,

$$F_s^x = -10^{-3} \bar{\rho} k_S \nabla(S‰) = -10^{-3}(1.02)(1.5 \times 10^{-5})\left(\frac{4.14‰}{1 \text{ cm}}\right)$$

$$= (6.2 \pm 0.1) \times 10^{-8} \text{ gm salt/cm}^2 \text{ sec}$$

Apparently, the salt fluxes have not yet adjusted so as to be comparable. As mentioned before, the bottom salt flux is overwhelming and as a result the bottom boundary layer grows with time (for Run 12 it was 0.75 cm thinner). The growth continues, forcing R_ρ to increase (R_ρ for Run 12 was 10.8) and decreasing the heat flux (for Run 12, $H = 1.12 \times 10^{-3}$ cal/cm^2 sec). There is no appreciable change in the thickness of the upper boundary layer, as is to be expected. Notice that the boundary layers do provide a means of obtaining H (and Fs in a steady experiment).

Since H and Fs are known, Rf can be calculated:

$$Rf \doteq \beta Fs/\alpha H = (0.74)(6.2 \times 10^{-8})/(2.73 \times 10^{-4})(1.07 \times 10^{-3})$$

$$= 0.155 \pm 0.005.$$

This value agrees very well with the mean values 0.15 obtained by Turner (1965). However, this result is significantly different from

the experimental values Rf = 0.25 (Exp. 7) and Rf = 0.24 (Exp. 23). Assuming the latter values are correct, how do we explain the value Rf = 0.155 for Exp. 4? We cannot, except to say Exp. 4 was conducted under very different conditions from Exps. 7 or 23. As a result, the diffusive salt flux differs by at least a factor of two from the boundary fluxes; therefore, the salt flux is not an equilibrium value. If the boundary values were substituted for Fs, Rf would increase to more than 0.30.

References

Haberstroh, R. D., R. I. Loehrke, R. D. Reinders, O. A. Plumb, and J. M. Broughton (1972) Three experiments in natural convection. 59 p. (Colorado State University. Department of Mechanical Engineering. Tech. Report No. 2 on Office of Naval Research Project NR 083-250).

APPENDIX E: A comparison with a numerical simulation

What follows is a comparison between Exp. 23 and a numerical simulation using approximately the same conditions. The numerical simulation assumes: (1) the fluxes are given by Eqs. (36) and (37), (2) constant fluid properties, (3) no vertical migration of the interface, (4) identical heat fluxes into and out of the system beginning at $t = 0$, and (5) the experiment ceases when S becomes negative.

The time $t = 0$ for Exp. 23 is chosen when the interface is first at equilibrium. This is recognized a posteriori by the first simultaneous decrease in ΔT, ΔS, $\Delta\rho$, $R\rho$, and d_T.

The initial conditions for the simulation and the initial conditions for the experiment at the time of fill are identical: $\Delta T = 0$ C, $\overline{T} = 20$ C, $\Delta S = 1.5$‰, and $\overline{S} = 33$‰. Some results are shown in Figs. E-1 (a) and (b).

A comparison Fig. E-1 (a) and (b) reveals: (1) the curves have the same general appearance but the experiments terminate at different times. The difference in duration is mostly due to the increased salt flux present in Exp. 23 and this supports the (higher) measured value of Rf (0.24). (2) $R\rho$ drops quickly from some high value as ΔT is established across the interface; (3) all the curves are roughly linear changing to (4) nonlinear at $R\rho \approx 2$ at which point it looks like the system collapses exponentially. (5) (the time spent

Figure E-1. Plots of ΔT, ΔS, $\Delta \rho$, and $R\rho$ against time for (a) a numerical simulation of a diffusive experiment ($H = 5 \times 10^{-4}$) and (b) diffusive experiment 23. The coordinates are identical for both (a) and (b): the left-hand scale is for $R\rho$; the right-hand scale is for $\Delta T \times 10$, $\Delta S \times 10$, and $\Delta \rho \times 10^4$. The units are ΔT(°C), ΔS(‰), and $\Delta \rho$ (gm/cm^3). In (b) the circles represent nine data points for the ten runs. Smooth curves are shown for variables other than $R\rho$. The inset in (b) shows sections of the temperature profiles from the final two runs.

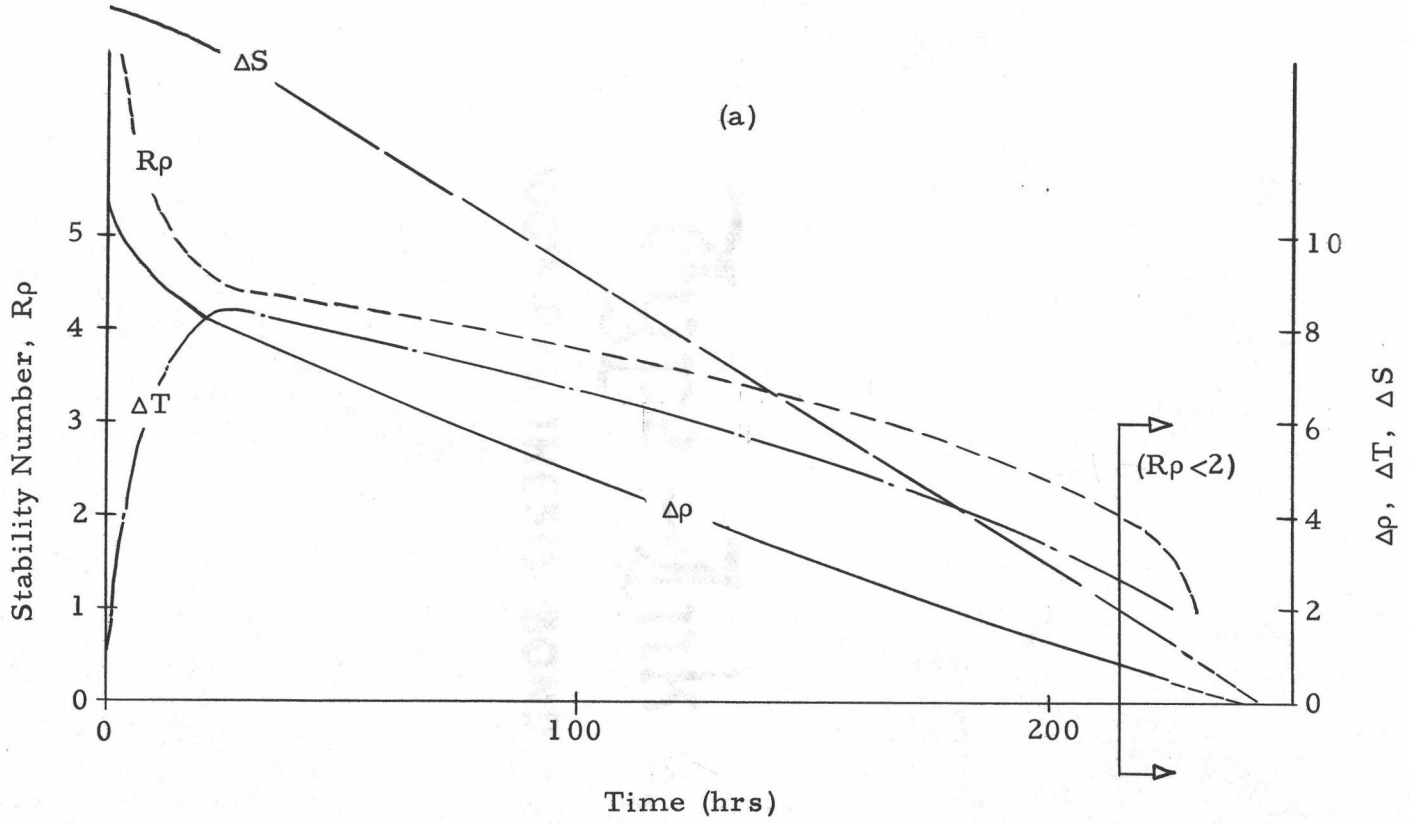
(a)
ΔS
Rρ
ΔT
Δρ
(Rρ<2)
Stability Number, Rρ
Δρ, ΔT, ΔS
Time (hrs)
0
1
2
3
4
5
0
2
4
6
8
10
0
100
200

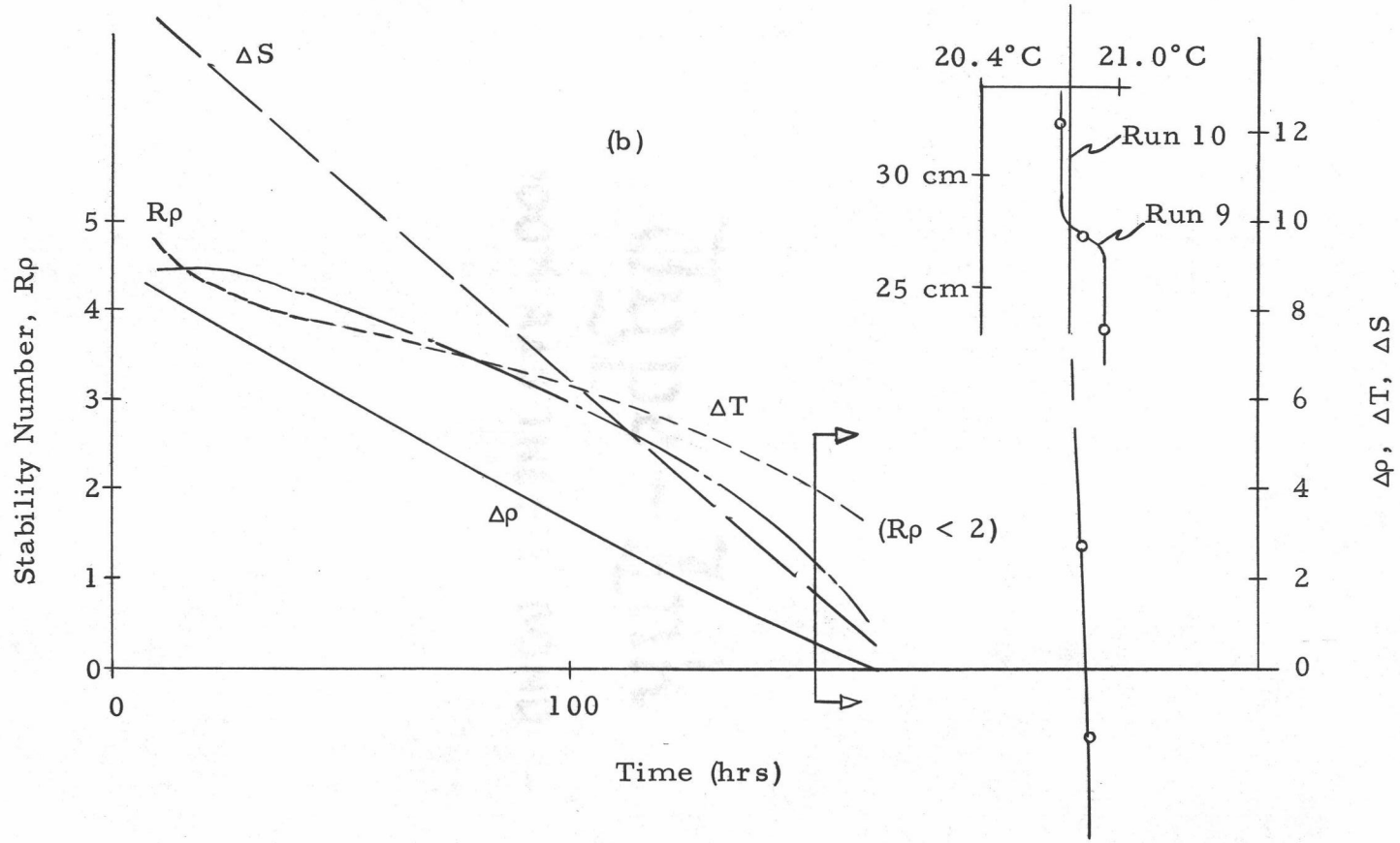
(b)
ΔS
Rρ
ΔT
Δρ
(Rρ < 2)
20.4°C
21.0°C
30 cm
25 cm
Run 10
Run 9
Stability Number, Rρ
Δρ, ΔT, ΔS
Time (hrs)
0
100
0
1
2
3
4
5
0
2
4
6
8
10
12

by the system at $R\rho < 2$)/(total time of the experiment) = 7% and 6.7% for the model and the experiment respectively. This is a relatively short time considering $2 < R\rho < 4.5$ for 93% of the time.

In Exp. 23 the center of the interface remained at the same height until Run 9 ($t = 163.5$, $R\rho = 1.7$) at which time it was found to be 1 cm lower than at the previous recording: an entrainment velocity of greater than 1.4×10^{-5} cm/sec in the negative direction. This speed is not too different from the value calculated on the basis of an interfacial mass flux (Chapter III) but the velocity is in the wrong direction! Therefore, this movement is due to unequal mixing in the layers.

The position of the interface is obvious for Run 9 (see the inset in Fig. E-1 (b)); but where is the interface for Run 10? Applying the usual rule to find d_T we would choose $z = 16.5$ to be the center of the interface. The time between Runs 9 and 10 is Δt = 2 hr 50 min. The entrainment velocity then is (16.5 cm -27.4 cm)/Δt = -1×10^{-3} cm/sec. This is a big velocity, of the same order as an upwelling speed in the ocean.